Miocene calc-alkaline volcanism in southern Jackson Hole, Wyoming : evidence of subduction-related volcanism

by David Congdon Adams

A thesis submitted in partial fulfillment of the requirements for the degree of Master of Science in Earth Sciences
Montana State University

Abstract:
Late Miocene lava flows in southern Jackson Hole are distinctly intermediate, calc-alkaline in composition in contrast to the bimodal basalt-rhyolite assemblages characteristic of most Neogene volcanic rocks in the Yellowstone Plateau-Snake River Plain region. Despite limited stratigraphic continuity between units, geochemical and petrographic analysis reveals strongly unifying and distinctive features. Silica variation diagrams are remarkably coherent, suggesting a co-genetic, if not co-magmatic, origin. As a whole, these rocks are significantly lower in K and Fe and higher in Ca and especially Mg than rocks of similar silica content from the Snake River Plain and Yellowstone. The basaltic andesites in particular are characterized by abundant olivine phenocrysts (Po 80-90) and extremely high Ni (200 ppm) and Cr (550 ppm) values. Within the suite, basaltic andesites and andesites (54-58% SiO_2, with olivine and augite) differ from dacites (60-62% SiO_2, aphyric or hornblende-rich) which differ from rhyodacites (66-69% SiO_2, with hypersthene and rounded andesine) and rhyolites and obsidian (73-75% SiO_2). Both geochemical and petrographic features suggest involvement of varying degrees of crustal contamination and/or magma mixing, especially in the more silicic rocks.

Low $^{143}Nd/^{144}Nd$ ratios in this suite clearly distinguish it from the Yellowstone-Snake River Plain volcanics and suggest the absence of asthenospheric input, precluding melt generation due to convective heat transfer. A possible melting mechanism is suggested by the high Ba/Nb values of these rocks, a feature considered diagnostic of involvement of subducted slab-derived hydrous flux in melt generation. It is proposed that a fragment of subducted slab detached as the Cascade subduction zone was disrupted by the inception of the Yellowstone mantle plume was buoyed and transported eastward, where its descent and dehydration beneath western Wyoming produced calc-alkaline magmas by solidus depression in the lithospheric mantle and lower crust.

MIOCENE CALC-ALKALINE VOLCANISM IN SOUTHERN JACKSON HOLE, WYOMING: EVIDENCE OF SUBDUCTION-RELATED VOLCANISM

by

David Congdon Adams

A thesis submitted in partial fulfillment
of the requirements for the degree

of

Master of Science

in

Earth Sciences

MONTANA STATE UNIVERSITY-BOZEMAN
Bozeman, Montana

May 1997

APPROVAL

of a thesis submitted by

David Congdon Adams

This thesis has been read by each member of the thesis committee and has been found to be satisfactory regarding content, English usage, format, citations, bibliographic style, and consistency, and is ready for submission to the College of Graduate Studies.

Dr. David R. Lageson D.R. Lageson 4-17-97
Date

Approved for the Department of Earth Sciences

Dr. W. Andrew Marcus W. Andrew Marcus 4-17-97
Date

Approved for the College of Graduate Studies

Dr. Robert L. Brown R L Brown 4/20/97
Date

STATEMENT OF PERMISSION TO USE

In presenting this thesis in partial fulfilment of the requirements for a master's degree at Montana State University-Bozeman, I agree that the Library shall make it available to borrowers under rules of the Library.

If I have indicated my intention to copyright this thesis by including a copyright notice page, copying is allowable only for scholarly purposes, consistent with "fair use" as prescribed by the U.S. Copyright Law. Requests for permission for extended quotation from or reproduction of this thesis in whole or in parts may be granted only by the copyright holder.

Signature 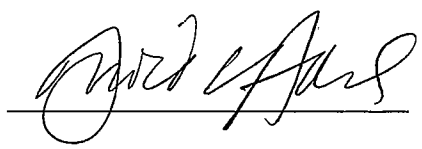

Date 4-15-97

TABLE OF CONTENTS

LIST OF TABLES

LIST OF FIGURES

ABSTRACT

Late Miocene lava flows in southern Jackson Hole are distinctly intermediate, calc-alkaline in composition in contrast to the bimodal basalt-rhyolite assemblages characteristic of most Neogene volcanic rocks in the Yellowstone Plateau-Snake River Plain region. Despite limited stratigraphic continuity between units, geochemical and petrographic analysis reveals strongly unifying and distinctive features. Silica variation diagrams are remarkably coherent, suggesting a co-genetic, if not co-magmatic, origin. As a whole, these rocks are significantly lower in K and Fe and higher in Ca and especially Mg than rocks of similar silica content from the Snake River Plain and Yellowstone. The basaltic andesites in particular are characterized by abundant olivine phenocrysts (Fo 80-90) and extremely high Ni (200 ppm) and Cr (550 ppm) values. Within the suite, basaltic andesites and andesites (54-58% SiO2, with olivine and augite) differ from dacites (60-62% SiO2, aphyric or hornblende-rich) which differ from rhyodacites (66-69% SiO2, with hypersthene and rounded andesine) and rhyolites and obsidian (73-75% SiO2). Both geochemical and petrographic features suggest involvement of varying degrees of crustal contamination and/or magma mixing, especially in the more silicic rocks.

Low $^{143}Nd/^{144}Nd$ ratios in this suite clearly distinguish it from the Yellowstone-Snake River Plain volcanics and suggest the absence of asthenospheric input, precluding melt generation due to convective heat transfer. A possible melting mechanism is suggested by the high Ba/Nb values of these rocks, a feature considered diagnostic of involvement of subducted slab-derived hydrous flux in melt generation. It is proposed that a fragment of subducted slab detached as the Cascade subduction zone was disrupted by the inception of the Yellowstone mantle plume was buoyed and transported eastward, where its descent and dehydration beneath western Wyoming produced calc-alkaline magmas by solidus depression in the lithospheric mantle and lower crust.

CHAPTER 1

INTRODUCTION

Overview

Cenozoic volcanism in the interior regions of the western United States has been extensive and has exhibited a wide range in geochemical character (Lipman, 1992; Luedke and Smith, 1978a-e). In their seminal papers, Christiansen and Lipman(1972) and Lipman et al. (1972) identified two general tectono-magmatic associations: an early calc-alkaline, predominantly andesitic episode attributed to shallow subduction of the Farallon Plate and a later period of basaltic, bimodal, or "fundamentally basaltic" volcanism associated with regional extension. They also noticed broad spatial trends in the timing of the transition from one association to the other, attributed to the gradual replacement of the coastal subduction zone with a transform boundary. However, owing to the fairly ambiguous nature of the geochemical nature of the later group, this transition is not always clear, especially in the northern portions of the region, where subduction presently continues off the Oregon and Washington coasts. Many volcanic fields elsewhere in the western United States also do not fit neatly into either category (e.g. the Jemez in New Mexico (Perry et al., 1987)).

Christiansen and Lipman (1972) purposely refrained from proposing a petrogenetic explanation for these tectonic-geochemical relationships and never implied any paleostress

aspects to the earlier subduction-related trend. Subsequent workers, however, have assumed a "compressional" tectonic character for subduction environments and claim to identify the timing of a shift from "compressional" to extensional tectonism in particular locales (Barnosky, 1984; McDowell and Fritz,1995). It is not clear that Lipman and Christiansen intended a paleostress interpretation for this geochemical transition, and they also acknowledged the difficulty in applying these concepts to individual areas as opposed to regions.

Stress in volcanic arcs can range from tensional in the backarc to compressional in the arc and forearc. Present-day stress fields in the Pacific Northwest also show a dominant component of dextral shear oblique to the arc axis (Zoback and Zoback, 1989). Indeed, the arc and forearc regions of any subduction environment may experience extension if the rate of slab rollback exceeds that of plate convergence (Royden, 1993).

The association of compressional paleostress with intermediate volcanism stems from early theories in which basaltic melts would be trapped in crustal magma chambers, as contraction closed available conduits. In such chambers, differentiation and crustal assimilation produces andesitic magmas. Extensional paleostrain would allow basaltic melts to pass unaffected through the crust (Hildreth, 1981; Norman and Leeman, 1989). Subsequent experimental work on andesites (Green 1973,1982; Eggler, 1972,1974; Eggler and Burnham, 1973) has suggested that certain conditions of partial melting (such as high water content) are perhaps more important than fractionation in the genesis of andesitic volcanism, especially as regards arc magmatism. In certain circumstances such

as the Mogollon-Datil volcanic field (Cather, 1990), such a relationship between stress and volcanism may be realistic. However, in no way should the mere presence of extensional tectonism be taken as evidence precluding the possibility of subduction-related volcanism as some authors seem to suggest (Hooper et al., 1995).

Continued work on Cenozoic andesitic volcanism in the western United States has shown that, in many areas, lavas of intermediate composition can be generated by magma mixing (McMillan and Dungan,1988; Gerlach and Grove, 1982) or crustal assimilation (Gans et al., 1989) without necessarily requiring subduction of oceanic crust and that shifts in gross geochemistry may be a normal part of open-system magmatic evolution. Significant amounts of basalt can also occur in areas such as the Cascades, where subduction is indisputably the dominant tectonic process (Leeman et al., 1990; McBirney et al., 1974). Studies of bimodal volcanism have emphasized the primary importance of upwelling of asthenospheric mantle in areas of both significant (Suneson and Lucchitta, 1983) and minimal extension (Leeman, 1982a).

It thus appears that intermediate composition volcanism need not indicate subduction and that basaltic or bimodal volcanism need not preclude it. Instead, detailed study of each particular case is required, especially given the tectonic complexity of the western United States and the heterogeneity of its lithosphere, both crust and mantle (Menzies et al., 1983; Menzies, 1989; Lum et al., 1989). As pointed out by Arculus and Johnson (1978), there has often been an overemphasis on generalized models thereby ignoring the valuable information to be gained from the unique aspects of individual case

histories. In this regard, it is also preferable that traditionally accepted geochemical subduction signatures (Gill, 1981) be critically examined to ascertain their applicability in this more or less intracontinental setting (Arculus, 1987).

Subduction Geochemistry

Crucial to Christiansen and Lipman's (1972) division of Cenozoic volcanism in the western United States, and the spatio-temporal trends displayed thereby, is not the distinction between extensional and compressional tectonism nor intermediate and basaltic or bimodal lavas. *Instead, it is the presence or absence of subduction-related volcanism.*

Following Christiansen and Lipman's 1972 paper, considerable work has been done on the geochemical aspects of subduction as expressed in arc magmas. Major and trace element contents in subduction-related volcanic rocks have been summarized by Jakes and White (1973), Ewart (1982), and Pearce (1982). Isotope systematics have been summarized by Hawkesworth (1982). Based on these features, various discriminant diagrams have been developed to distinguish arc magmas from those of other tectonic settings.

Primary among these features is the general depletion in subduction-related lavas of high field strength elements (HFSE, e.g., Ti, Hf, Nb, Ta) relative to large ion lithophile elements (LILE, e.g., Rb, Cs, Ba, K). These two groups show similarly incompatible

behavior in crystal fractionation processes; however, LILE partition much more readily into a hydrous phase (Pearce and Norry, 1979; Tatsumi et al., 1986). Some workers (Eggler, 1987) have found little or no LILE vs. HFSE fractionation in hydrous systems. However, Eggler's findings involve the derivation of fluid-crystal partitioning data from the combination of fluid-melt and melt-crystal partitioning data; whereas Tatsumi directly observed fluid-crystal partitioning in the dehydration of spiked synthetic serpentine. Gill (1981) asserted that "a Ba/Ta ratio greater than 450 (Ba/Nb > ~25) is the single most diagnostic characteristic of arc magma." Although HFSE depletion has also been attributed to the stabilization, in either the slab or mantle wedge, of a residual phase such as rutile (Ryerson and Watson, 1987) or fractionation of other minor mineral phases (Saunders et al., 1980), the most widely accepted explanation is the enrichment and melting of the overlying mantle wedge by a flux derived from a descending and dehydrating oceanic crustal slab (Hooper and Hawkesworth, 1993). The question remains of the relative content of hydrous fluid versus silicate melt in this slab-derived flux (Arculus, 1987). Ratios such as K/Ti (Kempton et al., 1991) and Nb/Ta (Stolz et al., 1996) have been used to determine the relative importance of these two metasomatic modes.

Although such features have been used to assign an arc setting to rocks as old as the Precambrian (Pearce and Cann, 1973), in Tertiary volcanics of the western United States, they are often briefly acknowledged and then dismissed usually due to excessive distance from and/or non-alignment with potential coastal subduction zones (Robyn, 1979;

Goles, 1986; Gans et al., 1989). In the case of many recent studies, consideration of the process of initial melt generation is essentially ignored in favor of concentrating on subsequent aspects of magma evolution.

What then would constitute sufficient evidence of subduction-related volcanism in the interior of the western United States? Ratios such as Ba/Nb, although compelling, can be of dubious significance in the more alkalic provinces, where, for reasons other than slab dehydration, LILE values can be extreme (Dudas, pers. comm.). More importantly, much of the lithospheric mantle underlying the western U.S. may have experienced one or more episodes of subduction-related metasomatism; thus the geochemical characteristics of subduction may be *inherited* rather than the result of contemporaneous slab dehydration.

It is clear that in addition to evidence of slab dewatering metasomatism, evidence of *melt generation* by hydrous flux depression of solidus temperatures must also be established. The other options for melting the lithosphere are adiabatic decompression due to rapid extension, heat input from the asthenosphere, or increase in burial depth due to tectonic crustal thickening. Decompression melting requires substantial rates of crustal extension (McKenzie and Bickle, 1988; White and McKenzie, 1989) that are seldom encountered outside of mid-ocean ridges or continental rift zones, where "passive" upwelling of asthenosphere can occur. Upwelling of asthenospheric mantle also occurs without major extensional tectonism in association with mantle plumes, or "hot spots", which melt the lithosphere by conductive and/or convective thermal input.

The question of the relative amount of incorporation of asthenospheric mantle material in melts generated in the Cenozoic in the western United States is a very important one, as it can provide constraints on the possible mechanisms of initial melting. In other words, in regions where the geochemical signature of the asthenospheric (i.e. convecting) mantle can be distinguished, the absence of said signature would tend to preclude melting mechanisms that require heat input by advection of hot asthenospheric material. Lachenbruch and Sass (1978) pointed out that "the ultimate source of high heat flow in the Basin and Range province must be upward convective transport in the asthenosphere." Under these conditions, McKenzie and Bickle (1988) have shown that the first point of intersection of the geotherm with solidus (i.e. melting) will always occur at the transition from the conductive to the adiabatic geotherm at the base of the thermal boundary (i.e. within the asthenosphere).

Some workers (Christiansen and McKee, 1978; Dudas, 1991; Hooper et al., 1995) have suggested that melting entirely within the lithosphere could be induced by extension, perhaps with some degree of conductive pre-heating from the asthenosphere. However, decompression is the vital component of this process; thus the lithosphere would need to undergo either extensive removal of crustal overburden (increasing heat loss due to steepening of the conductive geotherm) or diapiric upwelling. The latter would require, at the outset, a density contrast, presumably thermally induced, between the diapir and its surrounding material. As much of the material above the developing diapir would be of increasingly lower- density crustal nature, it is not clear how extension could trigger this

process. In any event, as outlined earlier, an asthenospheric melt would already be present due to extension-induced upwelling (McKenzie and Bickle, 1988); thus any lithospheric melting would more likely be the result of direct contact with intruding or underplating asthenospheric melts, most probably leading to some asthenospheric signature in the resulting magmas. This positive relationship between amount of extension and asthenospheric input has been noted in Rio Grande Rift lavas (Perry et al., 1987).

Leeman (1982b) has proposed a purely lithospheric source for the Snake River Plain tholeiitic basalts and the associated rhyolites in a setting involving minimal extension but dominated by high heat flow from an upwelling mantle plume (Leeman, 1982a). Once again, deriving sufficient heat from hot, convecting asthenospheric mantle to melt the lithosphere in such large volumes without asthenospheric admixture seems improbable. In fact, Menzies (1989) includes a small amount of OIB (ocean island basalt) type mantle as a component of these magmas, acknowledging the inevitability of some asthenospheric admixture during heat transfer. Based on low seismic velocities to depths of 250 km. and a high ^{3}He flux at Yellowstone, Hildreth et al. (1991) also suggested sublithospheric magma contributions.

The prevailing model for melt generation in volcanic arcs does not involve the asthenosphere as a source of heat; rather it is solidus depression due to slab-derived hydrous fluxes that initiates melting. Nonetheless, in the majority of arc settings, the nature of the mantle wedge in which the melting occurs is convecting, asthenospheric mantle. Only in situations in which the descending slab is directly overlain by lithospheric

mantle would the resulting melt contain no evidence of asthenospheric input. Some workers have suggested that a convecting mantle wedge is necessary in order to transport mantle metasomatized by shallow slab-derived fluxes to deeper, hotter levels appropriate for melting (Tatsumi, 1989). Indeed, areas in the Andean arc where shallow subduction is apparently taking place and where the slab is interpreted to be in direct contact with the lithosphere (Sacks, 1983) are distinctly non-volcanic. Nevertheless, this lack of volcanism could just as well be due to the lack of correct pressure and temperature conditions for slab dehydration or lithospheric melting as due to the absence of asthenospheric mantle per se.

In summary, in areas such as Yellowstone and the surrounding region where an asthenospheric signature can be determined with a reasonable amount of certainty, lavas lacking that signature strongly suggest the possibility of the involvement of slab-derived fluids in the melting of the lithosphere.

Regional Setting

Northwest Wyoming and the surrounding region has experienced a complex magmatic and tectonic history during the Cenozoic. Sevier and Laramide-style contractional tectonism spanned a period from the late Cretaceous to the Eocene, during which extensive calc-alkaline and alkalic volcanism produced the Challis, Absaroka, and Central Montana volcanic provinces. These provinces, and the Sevier and Laramide

orogenies themselves, have been attributed to the shallow subduction of the Farallon Plate beneath the western portion of the North American Plate (e.g. Lipman et al., 1972; Snyder et al., 1976). Other workers (Fitton et al., 1991; Hooper et al., 1995) have suggested that the geochemical subduction signature of these lavas is inherited from the metasomatized mantle of the accreted arc terranes which make up most of the western U.S., including portions of the Archaean Wyoming craton (Dudas, 1991).

Since the early Miocene the region has been dominated by a northeast-propagating system of explosive, rhyolitic volcanism followed by extrusion of basalt without any intermediate lavas (Pierce and Morgan, 1992). The present locus of explosive activity is in Yellowstone National Park and vicinity, where caldera-forming eruptions have occurred at 2.0, 1.3, and 0.6 Ma (Hildreth et al., 1991; Christiansen, 1995). To the west, the distribution of various widespread ash-fall tuffs suggest the presence of earlier calderas; in the vicinity of Rexburg, Idaho, 6.6 to 4.3 Ma (Morgan et al., 1984; Morgan and Hackett, 1988; Morgan, 1992); and in the general vicinity of Twin Falls, Idaho, ~10 to ~8 Ma (Leeman, 1982c). The system can be traced back as far as the McDermitt volcanic field (~16 Ma.) in the Owhyee Mountains in eastern Oregon (Pierce and Morgan, 1992).

Although the region has, during the Neogene, been experiencing a very general, eastward-propagating front of "Basin and Range" extension (Rodgers et al., 1990), it appears that the developing magmatic system has also confined the distribution of extensional tectonism to a parabolic or "bow wave" pattern (Anders et al., 1989; Anders and Sleep, 1992). In addition, a sequence of initial regional uplift followed by subsidence

can be seen associated with the eastward migration of explosive rhyolitic activity (Fritz and Sears, 1993; Smith and Braile, 1994).

The interpretations of the Snake River Plain-Yellowstone province and this eastward-propagating magmatic system are numerous, but only one substantially explains the tectonic, geochemical, and isotopic evidence. Interpreting the Plain as an eastward-propagating extensional rift (Myers and Hamilton, 1964) is contrary to overwhelming evidence of an extensional direction parallel to the axis of the Plain (Allmendinger, 1982; Kuntz et al., 1992). Reactivation of an ancient plain of weakness (Eaton et al., 1975; Mabey et al., 1978) or characterization as a "leaky transform" between regions of differing rates of extension (Christiansen and McKee, 1978) may explain the overall geometry of the province but fail even to begin to consider the localization or the nature of the region's magmatism.

Only a model involving a deep-seated upwelling of asthenospheric mantle or "mantle plume" fully treats the time-transgressive nature of the magmatism (Armstrong et al., 1975), its large volume and geochemical features (Leeman, 1982c), regional heat flow (Brott et al., 1981; Blackwell, 1989), the deep-mantle signature of the He^3/He^4 ratios (Craig et al., 1978; Kennedy et al., 1987), and regional uplift and subsidence (Fritz and Sears, 1993; Pierce and Morgan, 1992). For this reason, the subcrustal mechanism responsible for the Snake River Plain-Yellowstone volcanic province will herein be referred to as a mantle plume rather than some other, more coy and obfuscatory term.

Under the mantle plume model, a broad plume "head" produced a regional epeirogenic uplift and possibly affected volcanic activity as far east as Colorado (Leat et al., 1991). This plume head may have produced (Draper, 1991; Geist and Richards, 1993), strongly influenced (Hooper, 1990; Hooper and Hawkesworth, 1993), or had no effect on the Columbia River Basalts (Carlson and Hart, 1987; Hart and Carlson, 1987). The more narrowly focused plume "tail" subsequently produced the eastern Snake River Plain and Yellowstone Plateau as the North American plate drifted to the west-southwest over the essentially stationary plume (Pierce and Morgan, 1992). Basaltic melts derived from the ascending, superheated mantle caused extensive anatexis in the lower crust. These rhyolitic melts not only led to explosive, caldera-forming eruptions by the formation and catastrophic draining of upper crustal magma chambers, but they also served as a low-density cap blocking the ascent of the denser basalts (Leeman, 1982c; Anders and Sleep, 1992). Only around the periphery of the province or after the rhyolite had cooled sufficiently to allow brittle fracture, could the less viscous basalt exploit the resulting conduits and reach the surface (Hildreth et al., 1991; Kuntz, 1992). This bimodal magmatism, rhyolite followed by basalt with no intermediate compositions, dominates the province; although some "hybrid" ferrobasalts and ferrolatites (Leeman, 1982d) and evidence of basalt-rhyolite mixing (Wilcox, 1944) do exist.

In the area of southern Jackson Hole, Wyoming, approximately 70 km south of Yellowstone National Park, there exist, however, scattered outcrops of late-Miocene intermediate lava flows. Not only are these volcanics distinctly not bimodal, but, as will be

shown in subsequent chapters, their major and trace elements and isotopic ratios also indicate that they can in no way be derived from the magmas of the Yellowstone-Snake River Plain system. In addition, nowhere in the literature, to the author's knowledge, is there mention of a similar Neogene volcanic suite in the region. These lavas, herein referred to as the Jackson Hole volcanic complex (JHV), are apparently unique.

CHAPTER 2

STUDY AREA

Structural Overview

Jackson Hole, in northwestern Wyoming, is a north-trending, flat-bottomed valley approximately 12 km wide by 75 km long. (Figure 1) It is flanked on the east, from north to south, by the Pinyon Highlands, Leidy Peak Highlands, Gros Ventre Range, and Hoback Range. On the west it is flanked from north to south by the Teton Range and Snake River Range.

For most of its length, the valley is a half graben which constitutes the downdropped hanging-wall block of the east-dipping Teton normal fault. At its southern end, the half graben is reversed, with the master fault, the west-dipping Hoback normal fault, lying on the eastern side of the valley. The transition between the two half grabens coincides with two opposing WNW-trending thrust faults which mark the boundary between two major structural provinces. To the north, the Teton and Gros Ventre Ranges and the intervening valley occupy the hanging wall of the Cache Creek thrust, a thick-skinned, basement-cored, Laramide-style contractional fault. To the south, the Snake River and Hoback Ranges and intervening valley occupy the hanging walls of several

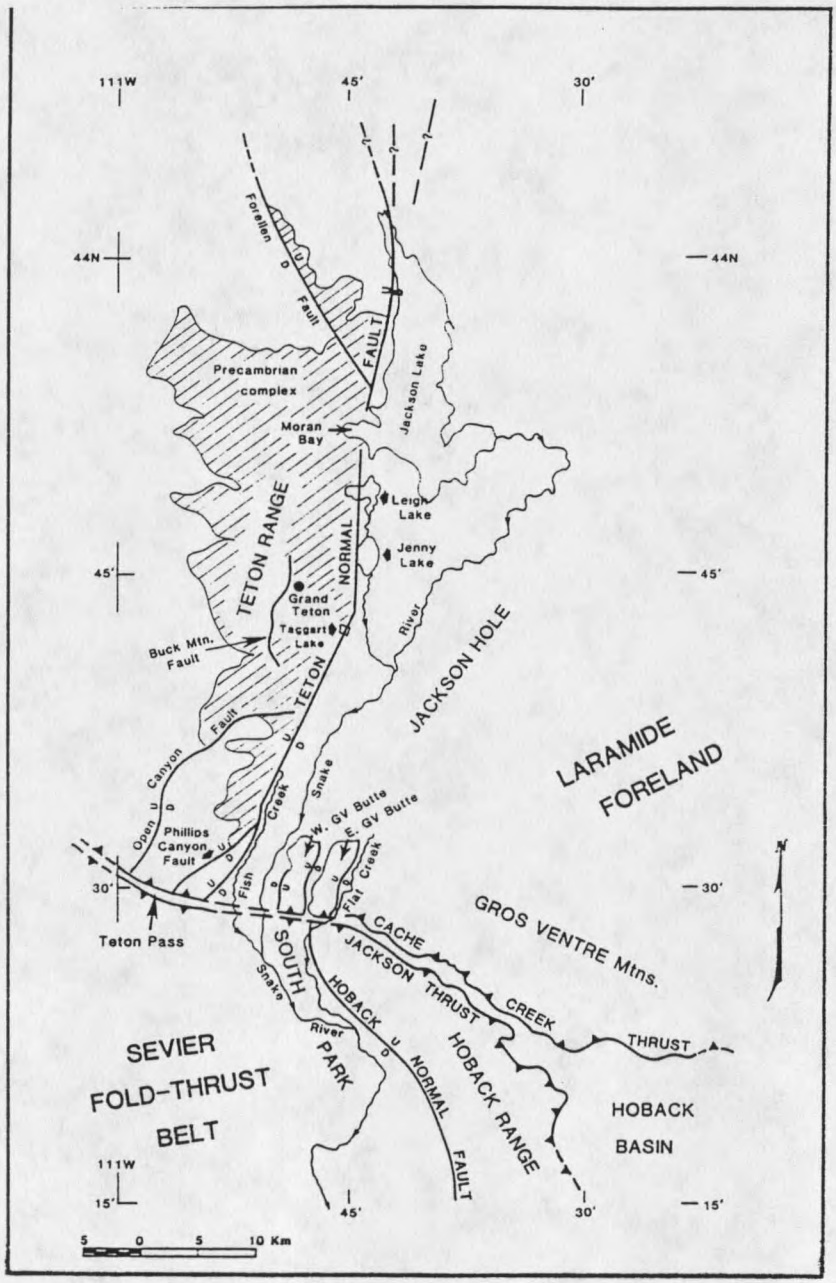

Figure 1. Structural index map of the Teton Range, reprinted from Lageson (1992).

imbricates of thin-skinned, Sevier-style thrusts, the Jackson-Prospect thrust being the northernmost. The episode of contractional tectonism that produced these structures lasted from late Cretaceous to perhaps early Eocene. The extensional tectonism which produced the Teton and Hoback faults and Jackson Hole itself commenced in the middle Miocene and continues to the present day (Byrd et al., 1994).

Considerable disagreement exists as to whether the Teton normal fault is confined to the Cache Creek thrust plate (i.e., soles into the Cache Creek decollement) or if it continues south of the province boundary (traced approximately by Wyoming Hwy. 22) into the region of the Sevier-style Snake River Range. It is of note that the Teton fault appears, as it approaches the edge of the Cache Creek thrust plate to the south, to shift from a single master fault, or fault zone, to a more distributed extensional system of normal faults. These faults, as mapped from west to east, are the Open Canyon fault, the Phillips Canyon fault, the Teton fault, and the faults bounding the east sides of the West and East Gros Ventre Buttes (Figure 1). Also present are several east-west faults, the Rendezvous Peak fault, the Warm Springs fault, and the Cache Creek fault, which may have served as transform structures accommodating differential extension in the area. It is this area of distributed extension that contains the bulk of the Jackson Hole volcanic complex.

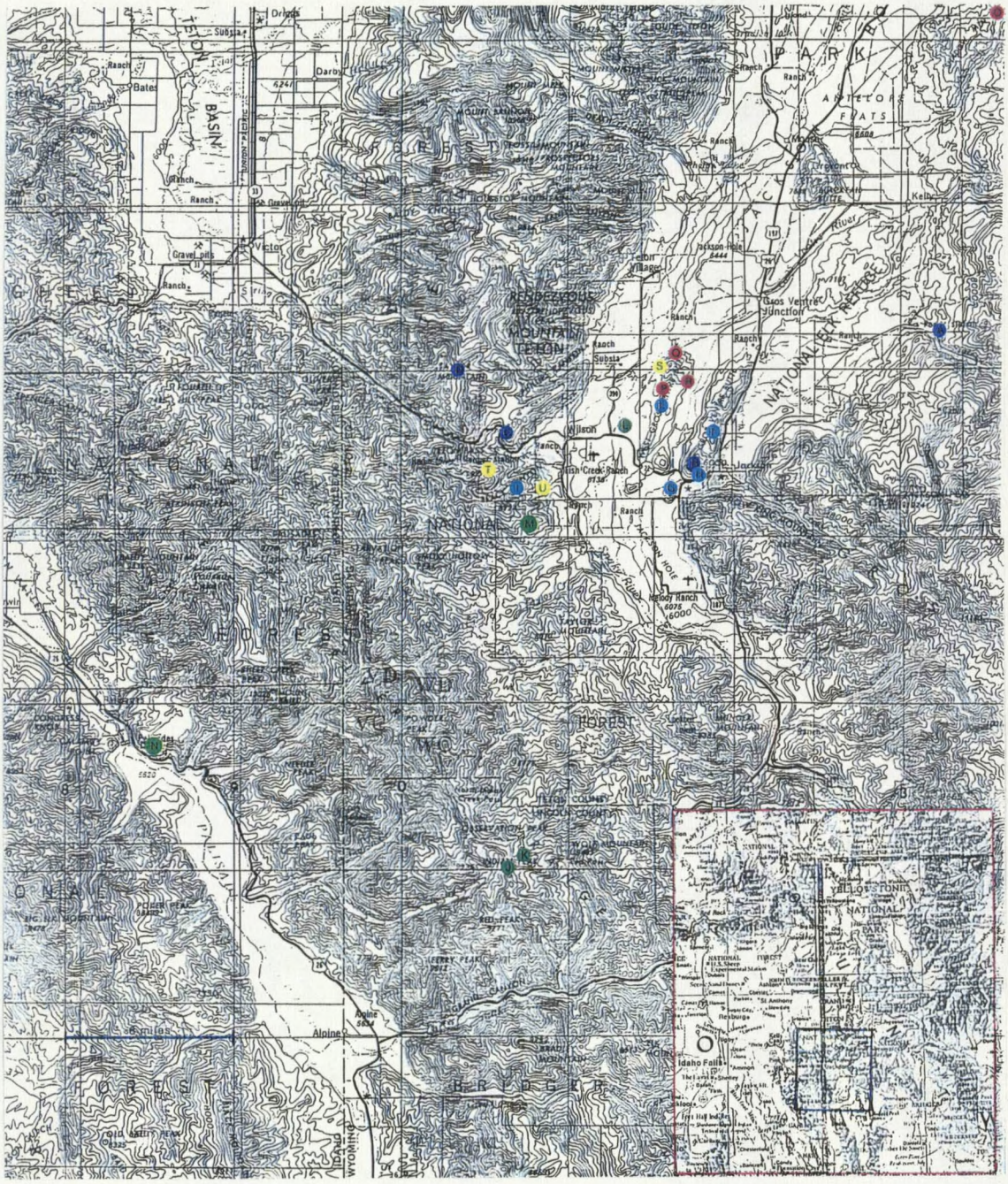

Figure 2. Map of study area, adapted from USGS Map NK 12-2, Western United States 1: 250000, Driggs, Idaho; Wyoming. Site labels correspond to samples listed in Tables 1-6.

Previous Work

Early work in southern Jackson Hole was done by Blackwelder (1915) and Fryxell (1930), with emphasis on the geomorphology of the area. Earlier studies on the structure of the Teton Range as a whole were performed by Horberg et al. (1949) and Edmund (1956). Geologic mapping in the vicinity of the study area was performed by Albee (1968; 1973), Schroeder (1969; 1972; 1974; 1976), Pampeyan et al. (1967), Love and Albee (1972), Love and Reed (1975),Oriel and Moore (1985), and Love et al. (1992). Interpretations of the geologic history of the area have been published by Love and Reed (1971) and Love et al. (1973). The Bureau of Reclamation has investigated local geology as part of seismotectonic studies in regard to construction on the Palisades Dam (Piety et al., 1986) and the Jackson Lake Dam (Gilbert et al., 1983). Other geophysical investigations in Jackson Hole have been carried out by Behrendt et al. (1968), Doser and Smith (1983), Smith et al. (1977), Smith et al. (1992), and Byrd et al. (1994). Structural studies have been conducted in the vicinity of Teton Pass by Zeller (1982), Vasko (1982), Lamerson (1983), and Dunn (1983); and further north in the Teton Range by Smith (1990), Smith et al. (1991), Lageson (1987; 1992), and Erslev and Rogers (1993). Geochronologic studies in the area have been performed by Evernden et al. (1964), Condie et al. (1969), Reed and Zartman (1973), Naeser et al. (1980), Armstrong et al. (1975) and Armstrong et al. (1980). Petrologic studies on the Precambrian rocks of the

area have been conducted by Horberg and Fryxell (1942), Bradley (1956), Miller et al. (1986), and Hildebrandt (1989).

Studies on Tertiary deposits in Jackson Hole have been done by Love (1956a, 1956b, 1956c, 1960, 1973, 1977), Love and Taylor (1962), Love and Montagne (1956), Lindsay (1972), Davis and Wilkinson (1983), Olsen and Schmitt (1987), Schmitt (1987), and Simons et al. (1988). Those with paleontological emphasis include Sohn (1956), Taylor (1956), C.W. Barnosky (1984), A.D. Barnosky (1985, 1986), Burbank and Barnosky (1990), and Whitlock (1992). Those with Quaternary emphasis include Glenn et al. (1983), Harrington (1985), Mahaney and Spence (1990), and Pierce and Good (1992). And those studies with significant mention of Cenozoic volcanic deposits include Scopel (1949, 1956), Houston (1956), Christiansen and Love (1978), Love et al. (1976), Love et al. (1978), Ritchie (1981), Love (1983), Barnosky (1984), Love (1986), and Perkins and Nash (1994).

Distribution of Volcanic Rocks

Volcanic deposits of various ages and various sources, both known and unknown, exist in the Jackson Hole area. Ash and breccias from Eocene Absaroka volcanic centers are abundant to the northeast of the valley and may extend southward in limited amounts. The Colter Formation, faunally dated as early to middle Miocene (Barnosky, 1984), lies primarily in the northern part of the valley but extends southward to the northern edge of the study area. Portions of this formation have been identified as pyroclastic surge

deposits; however, no evidence of an eruptive center, which should lie within 30 to 40 km, has been found.

The Teewinot Formation, faunally and K-Ar dated (Evernden et al., 1964) as middle Miocene (~10 Ma), lies to the immediate north of the study area. It consists of a substantial thickness of waterlain volcanic ash and freshwater limestone and marl. Recently, this ash has been correlated with that in the lacustrine middle Camp Davis Formation, which lies at the very southern end of the valley, and both have been re-dated (^{40}Ar-^{39}Ar, ~7Ma). The source of these ashes is uncertain but may be twofold. Trace element studies (Ritchie, 1981; Love, 1986) suggest that one source type bears a resemblance to many other regional ash deposits and may be related to activity on the Snake River Plain. The other source type resembles the trace element trend of the JHV.

Other evidence of Yellowstone-Snake River Plain (YSP) volcanism is common throughout the valley. The Conant Creek Tuff (~4.5 Ma) is exposed in the northern part of the valley, as is the extremely voluminous Huckleberry Ridge Tuff (~2.0 Ma). Pinkish tuff resembling the latter is common near Teton Pass in the western part of and in the Signal and Shadow Mountain areas to the north and northeast of the study area.

Outcrops of the JHV are found primarily in the area of Teton Pass and the East and West Gros Ventre Buttes. Samples from Teton Pass have K-Ar whole-rock age determinations of $8.06 \pm .08$ Ma (rhyolite), $8.48 \pm .08$ Ma (obsidian) (Naeser et al., 1980), and 8.1 ± 0.9 Ma (basaltic andesite) (Chevron USA written comm., 1985, in Love,

et al., 1992). As is typical of more silicic lavas, these flows are not laterally extensive, and flows of differing lithology are seldom in stratigraphic contact. In addition, Miocene to recent extension has further separated the various outcrops on isolated fault blocks. In fact, the close geochemical correlation between the basaltic andesite capping the East Gros Ventre Butte above the town of Jackson with the aforementioned dated basaltic andesite on Teton Pass provides the first real maximum age for extensional tectonism in the southern Teton Range. The previous estimate was based on the absence of coarse-grained (i.e. orogenically derived) sediments in the middle Miocene Teewinot Formation (Love et al, 1973).

The absence of clear stratigraphic relationships between the various outcrops makes morphological reconstuction of the original volcanic field difficult. Without extensive and highly precise dating, even the sequence of eruptive events is uncertain. Extensive glaciation has not only eroded much of the original volcanic material but has perhaps also buried a substantial portion of the complex beneath the abundant glacial outwash that covers the valley floor and the lower slopes of the surrounding ranges. The original volcanic field may have existed as a group of isolated to slightly overlapping silicic domes and more laterally extensive andesitic flows erupted onto a surface of moderate relief and appears to have been structurally controlled more by the reactivated (?) east-west trending Laramide thrust faults than by the north-south Teton fault system.

The full spatial extent of the JHV is yet to be established. As chemical analyses are performed on various previously unsampled volcanic outcrops in the region, many show a

much stronger affinity to the JHV (or possibly to the Absaroka volcanics) than to the lavas of the YSP system. To the southwest of the main study area, at Palisades Dam, the Andesite of Calamity Point (K-Ar, whole rock, 6.3 ± 0.2 Ma, Armstrong et al., 1980) is essentially identical to a dacite flow south of Teton Pass. A block and ash flow exposed near Shadow Mountain northeast of the main study area is chemically very similar to the dacite flow covering the northern ends of the Gros Ventre Buttes, but could also be a remnant of Eocene volcanism. The hornblende-rich andesites found to the southwest of West Gros Ventre Butte and to the south of the study area at Indian Peak bear even more resemblance to the Eocene Absaroka group, but extensive crustal contamination, as evinced by abundant xenoliths, probably precludes successful dating or isotope analysis.

Given their general similarity, it is quite possible that more representatives of the Miocene calc-alkaline volcanic episode exist undated and undetected in the Absaroka calc-alkaline volcanics to the northeast. Lavas dated as Pliocene (K-Ar, 3.6 ± 1.0 Ma, Blackstone, 1966) in the Crescent Mountain area of the southern Absaroka Range show a much closer chemical affinity to the Jackson Hole Volcanics than Yellowstone lavas. And many other Neogene flows in this area (e.g. the Crandall Creek volcanics, Lava Mountain, and Pilot Knob) remain to be chemically analyzed and/or accurately dated. The actual extent and volume of Neogene calc-alkaline volcanism here may likely never be determined. It is, nonetheless, safe to say that the JHV and related lavas are in this regard dwarfed by both the Absaroka and Yellowstone-Snake River Plain systems. But relative volume should never be taken as a measure of significance.

CHAPTER 3

MATERIALS AND METHODS

Samples of the least altered material possible were always collected directly from the outcrop. Portions of 25 samples were sent to the GeoAnalytical Laboratory at Washington State University, where they were ground in a tungsten-carbide swingmill and analyzed on a 2:1 lithium tetraborate: rock powder fused bead using an automatic Rigaku 3370 spectrometer (Hooper et al., 1993). For 10 samples, portions of the same rock powder were sent to James Wright at Rice University, Houston, Texas, for analysis of isotope ratios for Sr, Rb, Sm, Nd, and Pb. Standards used and analytical uncertainties are listed in Table 2 of Wright and Snoke (1993).

Blocks were cut from these and other samples and sent to Spectrum Petrographics in Winston, Oregon, for preparation of 71 thin sections, of which 11 received microprobe polish treatment. These latter slides were analyzed at the Imaging and Chemical Analysis Laboratory at Montana State University, Bozeman, Montana, using a JEOL scanning electron microscope equipped for X-ray analysis. Chemical analyses were plotted graphically using Igpet For Windows (version 1-6-95) developed by Terra Softa Inc., Somerset, New Jersey.

CHAPTER 4

RESULTS

Overview

The rocks of the Jackson Hole Volcanic Complex can be subdivided into six basic groups based primarily on SiO_2 content. Names are based roughly on the classification scheme of LeBas et al. (1986) (Figure 3). These are as follows:

1) basaltic andesites - SiO_2 52-55%; olivine, augite, plagioclase, ± enstatite;

2) low-silica andesites - SiO_2 56-59%; augite, plagioclase, ± olivine, ± enstatite-bronzite;

3) trachyandesites - SiO_2 53-61%; hornblende, plagioclase, augite; xenolith-rich (amphibolite and hornblendite);

4) high-silica andesites - SiO_2 62-64%; hypersthene, plagioclase, augite; or aphyric;

5) dacites - SiO_2 66-69%; plagioclase, hypersthene, ± biotite, ± augite;

6) rhyolites - SiO_2 73-75%; obsidian and aphyric (± plagioclase, ± biotite).

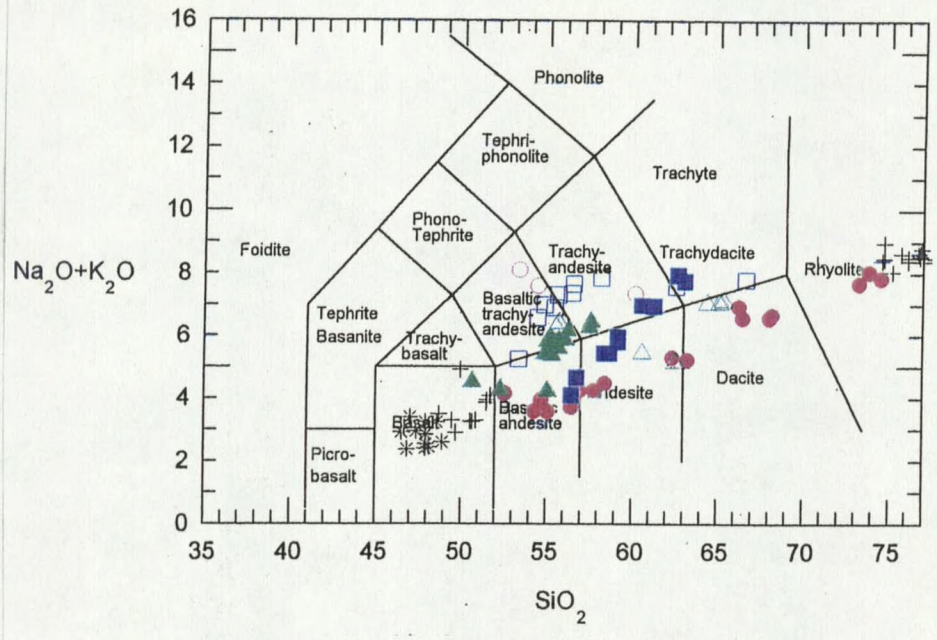

Figure 3. Total alkali vs. SiO_2 classification plot (LeBas et al., 1986) for the JHV and selected regional suites. Data from the Plio-Pleistocene Yellowstone Plateau Volcanic Field (YSP) (Hildreth et al., 1991) are plotted as black crosses (Yellowstone National Park) and asterisks (Island Park, Idaho). The Eocene Challis and Salmon Creek volcanics (SCV) (Norman and Mertzman, 1991) are plotted respectively as solid and hollow green triangles. The Cretaceous (most likely Eocene ?) Independence Peak volcanic rocks (Meens and Eggler, 1987) are plotted as solid (HABS-type) and empty (HATS-type) blue squares. The JHV are plotted as solid red circles with the intrusive andesites as hollow circles.

Locations and Field Characteristics

Basaltic Andesites

These flows are mainly found capping two fault blocks directly north of Teton Pass which are the hanging-wall blocks of the Open Canyon and Phillips Canyon faults, and the flows are clearly cut and displaced by at least the latter. Maximum thickness of

the flows is ~20 m., and they tend to be massive with only minimal flow foliation developed. They are directly underlain by limestones, shales, and cherts ranging from Mississippian to Permian in age. Samples were collected from the head of a Phillips Creek tributary near the pass between Mesquite and Coal Creeks (JH1) and from a large road cut on Hwy. 22 near Phillips Canyon (JH2). These lavas were not detected south of the highway (i.e. south of the Cache Creek thrust).

Basaltic andesite of almost identical chemical character is also found in an ~5 m thick outcrop capping the extreme southern end of the East Gros Ventre Butte, overlooking the town of Jackson (Sample JH5). This flow is highly foliated (~ subvertical) and grades abruptly downward into low-silica andesite with an intervening zone apparently consisting either of mixing of two viscous magmas or of mixed and remelted flow-top rubble from the former and basal breccia from the latter. The much harder basaltic andesite domains tend to weather out as knobs. Also present to the immediate northeast of this outcrop are abundant fragments of black and red scoria.

The close chemical similarity between JH5 and the Teton Pass samples suggests that they are parts of essentially the same flow or, at least, flows not greatly separated temporally. However, flows at the mouth of Flat Creek Canyon (Sample 81) to the northeast of the East Gros Ventre Butte show sufficient differences that, although most likely part of the same magmatic episode, these lavas may represent the products of a separate magma chamber from the basaltic andesites to west. The Flat Creek lavas have also been extensively contaminated by secondary calcite, making comparison of major

Sample	81cc A	JH5 B	JH2 C	JH1 D
SiO[2]	52.58	54.33	54.74	55.12
Al[2]O[3]	14.88	16.12	15.85	16.76
TiO[2]	1.548	0.594	0.632	0.633
FeO*	10.4	6.79	6.7	6.73
MnO	0.125	0.119	0.114	0.122
CaO	10.58	9.1	8.99	8.62
MgO	5.31	8.73	8.38	7.95
K[2]O	1.07	0.83	1	0.73
Na[2]O	3.07	2.75	2.93	2.84
P[2]O[5]	0.408	0.218	0.432	0.181
Mg*	47.6	69.6	69	67.8
Ni	161	204	208	180
Cr	286	551	522	540
Sc	27	18	22	28
V	171	137	126	132
Ba	881	662	1223	555
Rb	14	11	12	12
Sr	915	510	954	465
Zr	160	121	138	108
Y	20	18	21	18
Nb	12.6	7.1	7.6	8.9
Ga	22	19	14	18
Cu	53	32	37	36
Zn	99	71	69	75
Pb	5	6	12	5
La	54	41	69	25
Ce	124	67	115	55
Th	7	2	5	4
87Sr/86Sr		.706102(7)	.706460(9)	.706491(8)
143Nd/144		.511575(5)	.511483(5)	.511675(5)
208Pb/204		37.769	37.309	38.322
207Pb/204		15.476	15.377	15.466
206Pb/204		16.913	16.494	17.069

Major element values for 81cc adjusted for calcite contamination
Mg* = 100 Mg/(Mg + Fe) atomic

Table 1. Major and trace element contents and isotope ratios for basaltic andesite samples.

elements somewhat difficult and isotope analysis impossible, but leaving some trace elements arguably unaffected.

Low-silica Andesites

As mentioned previously, these lavas are found underlying basaltic andesites at the extreme southern end of East Gros Ventre Butte, where the flow attains a thickness of 25-30 m. Portions of this flow (Sample JH3) have subsequently been downdropped to the level of Broadway/ Highway 189 by the west-trending normal fault that bounds the south end of the butte. Parts of perhaps the same flow are found in a small outcrop to the southwest on Haystack Butte (Sample JH9) which is part of the Jackson thrust sheet.

Low-silica andesites are also found in the central portions of both East (Sample JH11) and West GrosVentre Buttes (Sample 617). These rocks have well-developed flow foliation in almost all exposures and occasional columnar jointing. A small outcrop approximately 4 km. southeast of Teton Pass (Sample 519) falls within this range of silica content and shares similar petrographic characteristics, but its trace element contents suggest it may not be closely related to the other low-silica andesites.

Sample	JH617 E	JH11 F	JH9 G	JH3 H	JH519 I
SiO[2]	56.48	56.66	56.96	57.81	58.44
Al[2]O[3]	16.99	17.34	17.33	17.55	16.81
TiO[2]	0.635	0.638	0.633	0.611	0.951
FeO*	6.85	6.44	6.13	5.95	6.67
MnO	0.108	0.108	0.098	0.102	0.116
CaO	8.35	8.26	8.09	8.15	7.1
MgO	6.37	5.74	5.51	5.35	4.33
K[2]O	0.92	1.03	0.99	1.01	1.05
Na[2]O	2.8	3.02	3.24	3.23	3.42
P[2]O[5]	0.132	0.17	0.213	0.202	0.404
Mg*	62.4	61.3	61.5	61.5	53.6
Ni	135	113	107	89	77
Cr	315	226	243	178	131
Sc	25	19	19	18	23
V	138	130	104	118	122
Ba	492	574	1101	699	1066
Rb	17	18	16	16	12
Sr	286	346	474	437	547
Zr	106	111	138	136	189
Y	20	21	23	20	31
Nb	4.9	8.2	9.9	9.2	16.2
Ga	19	17	16	18	16
Cu	47	45	37	30	14
Zn	69	72	70	66	94
Pb	5	8	11	9	3
La	17	13	32	30	48
Ce	59	64	76	68	69
Th	2	2	6	2	6
87Sr/86Sr		.706668(8)		.706245(9)	
143Nd/144		.511690(4)		.511579(5)	
208Pb/204		37.863		37.446	
207Pb/204		15.409		15.409	
206Pb/204		16.47		16.638	

Mg* = 100 Mg/(Mg + Fe) atomic

Table 2. Major and trace element contents and isotope ratios for low-silica andesite samples.

Trachyandesites

These lavas are present in a small outcrop west of the West Gros Ventre Butte near the Hwy. 22 bridge over the Snake River (Sample JH17) and in a much larger hypabyssal intrusive complex at Indian Peak approximately 25 km to the south-southeast in the Snake River Range (Samples IPK2 and IPK6). Although there is a fairly wide range in silica content between the samples, their petrographic similarity and presence of abundant hornblende and lower-crustal xenoliths suggests that they are of similar origin. Xenoliths, however, preclude both dependable dating and isotope analysis. Based on their greater petrographic and geochemical similarity to the Absaroka volcanic rocks, these rocks are probably Eocene rather than Miocene in age.

High-silica Andesites

This silica range is represented by two flows that are chemically almost identical. One (Sample JH10) is located ~6 km southeast of Teton Pass capping the ridge directly north of Mosquito Creek. The other (Sample 640) lies ~25 km to the southwest, slightly to the southeast of the east abutment of the Palisades Dam. This latter flow, dated by Armstrong et al. (1980) at 6.3 ± 0.2 Ma, is ~ 60 m thick and tends to be slightly more massive than the thinner (~ 20 m ?) Mosquito Creek flow which shows well-developed platy weathering due to flow foliation. Although separated by considerable distance and

Sample	IPK6 J	IPK2 K	JH17 L
SiO[2]	53.4	54.5	60.18
Al[2]O[3]	19.47	19.14	17.23
TiO[2]	0.495	0.506	0.559
FeO*	5.84	6.18	5.9
MnO	0.089	0.129	0.08
CaO	8.19	8.82	5.1
MgO	1.82	2.42	2.52
K[2]O	3.88	3.62	2.78
Na[2]O	4.22	3.98	4.57
P[2]O[5]	0.336	0.302	0.362
Mg*	35.7	41.1	43.2
Ni	7	13	26
Cr	15	43	62
Sc	17	16	15
V	89	98	121
Ba	452	414	924
Rb	92	92	58
Sr	1114	1003	876
Zr	195	183	171
Y	28	28	26
Nb	10	8.2	11.9
Ga	20	20	18
Cu	23	35	38
Zn	52	75	83
Pb	3	22	14
La	40	32	33
Ce	93	92	40
Th	12	9	3

Mg* = 100 Mg/(Mg + Fe) atomic

Table 3. Major and trace element contents and isotope ratios for trachyandesite samples.

Sample	JH10 M	JH640 N
SiO[2]	62.37	63.27
Al[2]O[3]	16.89	16.85
TiO[2]	0.669	0.649
FeO*	5.15	5.39
MnO	0.086	0.083
CaO	5.95	5.75
MgO	2.61	2.7
K[2]O	1.66	1.48
Na[2]O	3.64	3.73
P[2]O[5]	0.194	0.181
Mg*	47.5	47.1
Ni	32	21
Cr	73	56
Sc	18	16
V	94	98
Ba	737	768
Rb	32	24
Sr	284	289
Zr	170	176
Y	28	28
Nb	10.8	10.7
Ga	18	23
Cu	18	15
Zn	71	68
Pb	11	9
La	38	101
Ce	65	61
Th	7	4
87Sr/86Sr	.707731(8)	
143Nd/144	.511591(9)	
208Pb/204	38.41	
207Pb/204	15.463	
206Pb/204	16.653	

Mg* = 100 Mg/(Mg + Fe) atomic

Table 4. Major and trace element contents and isotope ratios for high-silica andesite samples.

different petrographically (unlike 640, JH10 is aphyric), the close chemical similarity suggests these flows may be co-magmatic, if not parts of the same flow.

Dacites

These lavas are present as thick flows (> 300 m) which essentially comprise the northern ends of both the East and West Gros Ventre Buttes, and are of two fundamental types. The dominant lithology is a porphyritic dacite with andesine phenocrysts up to 3 mm in length in a dark gray to black (often red) matrix. These flows are massive to moderately foliated with rare columnar joints. They are quarried for dike rip-rap at the extreme north end of the West Gros Ventre Butte (Sample JH7). They form the top of Hansen Peak (the highest point of the West Gros Ventre Butte) and the prominent cliffs on the east side of the East Gros Ventre Butte.

The slightly less silicic and less voluminous non-porphyritic dacites (Sample JH12) crop out to the south of Hansen Peak and appear to underlie the porphyritic dacites with an non-planar northward-dipping contact. They are distinctly more foliated than the porphyritic dacites and become slightly more porphyritic towards the east, where an apparent vent structure forms a large plug-like outcrop comprised of non-porphyritic dacite blocks up to several meters across (vent breccia ?) suspended in densely porphyritic dacitic matrix (Sample JH6). Just north of this plug are scattered perlite clasts, possibly

Sample	SM4 O	JH12 P	JH7 Q	JH6 R
SiO[2]	66.28	66.49	68.06	68.21
Al[2]O[3]	15.96	16.36	15.67	15.82
TiO[2]	0.44	0.595	0.504	0.463
FeO*	3.49	3.67	3.6	3.35
MnO	0.019	0.048	0.066	0.064
CaO	4.11	4.3	3.7	3.85
MgO	1.68	0.68	0.86	0.94
K[2]O	2.83	2.42	2.42	2.61
Na[2]O	4.11	4.15	4.15	4.05
P[2]O[5]	0.179	0.191	0.152	0.139
Mg*	46.2	24.9	29.8	33.3
Ni	54	7	6	7
Cr	126	1	7	5
Sc	13	7	9	6
V	66	56	50	63
Ba	1649	844	864	866
Rb	60	62	57	64
Sr	636	270	239	244
Zr	148	160	172	151
Y	11	30	27	27
Nb	5.3	11.1	12.2	14.2
Ga	20	21	19	18
Cu	15	10	5	9
Zn	54	60	59	53
Pb	21	20	15	21
La	14	44	39	46
Ce	71	79	83	74
Th	4	10	13	10
87Sr/86Sr		.710403(8)	.709265(8)	
143Nd/144		.511508(5)	.511547(4)	
208Pb/204		40.019	39.093	
207Pb/204		15.527	15.583	
206Pb/204		16.908	17.352	

Mg* = 100 Mg/(Mg + Fe) atomic

Table 5. Major and trace element contents and isotope ratios for dacite samples.

remnants of the glassy chilled intrusive margin. Non-porphyritic dacite has not been found on the East Gros Ventre Butte.

Scopel (1949, 1956) reported lavas as having flowed down the steep eastern sides of the buttes, thus making magmatism post-kinematic. It is clear, however, that these dacitic flows were extremely thick (i.e. dome-like) which is common for phenocryst-rich silicic lavas. Flow foliations are predominantly west-dipping, clearly contrary to flow down these east-dipping fault surfaces. The dacite exposed in these surfaces is therefore most likely pre-kinematic in origin, and the dacites of the two buttes probably formed one large composite dome.

Approximately 25 km to the northeast of the Gros Ventre Buttes, on Ditch Creek east of Shadow Mountain, a monolithologic, block and ash flow deposit (Sample SM4) is very similar in chemistry and phenocryst content to the dacites to the south. However, certain key major and trace elements are sufficiently different as to preclude any direct connection between this flow and those of the buttes. This flow is, nonetheless, much more closely related to the JHV than to the Absaroka volcanic rocks, let alone those of Yellowstone.

Rhyolites

Rhyolitic flows are present south of Teton Pass, on West Gros Ventre Butte, and, to a very limited extent, on East Gros Ventre Butte. Obsidian is found in areally limited

Sample	JH15 S	JH14 T	JH13 U
SiO[2]	73.26	73.83	74.53
Al[2]O[3]	15.28	14.07	14.46
TiO[2]	0.241	0.07	0.068
FeO*	1.75	1.02	0.94
MnO	0.04	0.049	0.016
CaO	2.13	1.38	1.24
MgO	0.1	0	0
K[2]O	3.46	3.95	4.11
Na[2]O	4.22	4.1	3.74
P[2]O[5]	0.082	0.038	0.038
Mg*	9.3		
Ni	7	12	11
Cr	0	5	1
Sc	2	3	1
V	5	0	0
Ba	1156	1177	1214
Rb	88	121	124
Sr	185	125	114
Zr	188	73	70
Y	28	26	22
Nb	15.1	14.2	16.4
Ga	18	15	17
Cu	32	6	4
Zn	65	37	38
Pb	25	27	30
La	40	11	32
Ce	74	57	56
Th	13	14	14
87Sr/86Sr	.711725(8)	.723476(8)	
143Nd/144	.511528(4)	.511414(5)	
208Pb/204	40.116	41.548	
207Pb/204	15.542	15.622	
206Pb/204	16.948	17.364	

Mg* = 100 Mg/(Mg + Fe) atomic

Table 6. Major and trace element contents and isotope ratios for rhyolite samples.

"pipes" on ridges 1 km and 2 km (Sample JH14) southeast of Teton Pass, which have been the sites of prehistoric quarrying. It is also found in excavations and as a consistent subsurface layer in building site assessment drill cores and water wells up to 6 km. southeast of the Pass. Tan-colored flow-banded rhyolite (Sample JH13) also crops out ~5 km southeast of the Pass at the base of Indian Paintbrush Subdivision. Samples from the same sites as JH13 and JH14 were dated at 8.06 ± .08 Ma and 8.48 ± .08 Ma, respectively (Naeser et al., 1980), and the nearly identical chemical composition of these two samples suggests that the rhyolite and obsidian may only be different textural variations of the same flow.

A dark gray and red flow-banded rhyolite (Sample JH15) is well exposed in a quarry on the west side of West Gros Ventre Butte. It is associated with a red and black breccia that is largely altered (hydrothermally ?) to a deep-reddish soil with occasional dark gray dacite (?) clasts and rare obsidian fragments. Foliation in the overlying non-porphyritic dacite is roughly sub-parallel to the contact with the underlying rhyolite body, suggesting that the rhyolite is either an intrusive plug deforming the intruded dacite or a pre-existing dome over which the dacite flowed. No sign is present of a chilled contact, which would confirm the former, but such a margin would be highly susceptible to alteration, of which there is ample evidence. JH15 is chemically similar to, yet distinct from, the flow(s) near Teton Pass and most likely represents a co-genetic but separate eruptive event.

On the east side of East Gros Ventre Butte, porphyritic dacite in places overlies thin beds of orange pumice and pumiceous sandstone. Petrographically, these units show signs of both epiclastic reworking (e.g. rounding) and welding (flattened pumice). As such, this pumice need not be related to the JHV. On Teton Pass, a reddish tuff (Sample JH18) appears to underlie the JH2 basaltic andesite and shows strong chemical affinity to the Yellowstone-Snake River Plain lavas. If it actually overlies the Miocene basaltic andesite, it could be Huckleberry Ridge Tuff, which it roughly resembles. In any case, it appears distinctly unrelated to the JVH.

Petrography

Basaltic Andesites

The basaltic andesites are phenocryst-rich (20 -30%). The dominant mineral phase is euhedral to subhedral olivine phenocrysts (Fo_{80-88}, molar %) up to 2.5 mm in length. They are commonly iddingsitized on their rims and along fractures (Figure 4), suggesting that this is a late-stage, low-temperature reaction (McMillan, pers. comm. 1996) but probably deuteric rather than a weathering product. Other samples (e.g. Sample 81) show signs of extensive replacement of olivine with fine-grained opaques, also along fractures (Figure 5).

Euhedral to subhedral augite phenocrysts up to 1.5 mm in length are slightly less abundant than the olivine. They range from Wo_{38} En_{52} Fs_{10} (Sample JH2) to Wo_{44} En_{43} Fs_{13} (Sample 81) and are often in glomerocrysts associated with plagioclase. Sample JH5

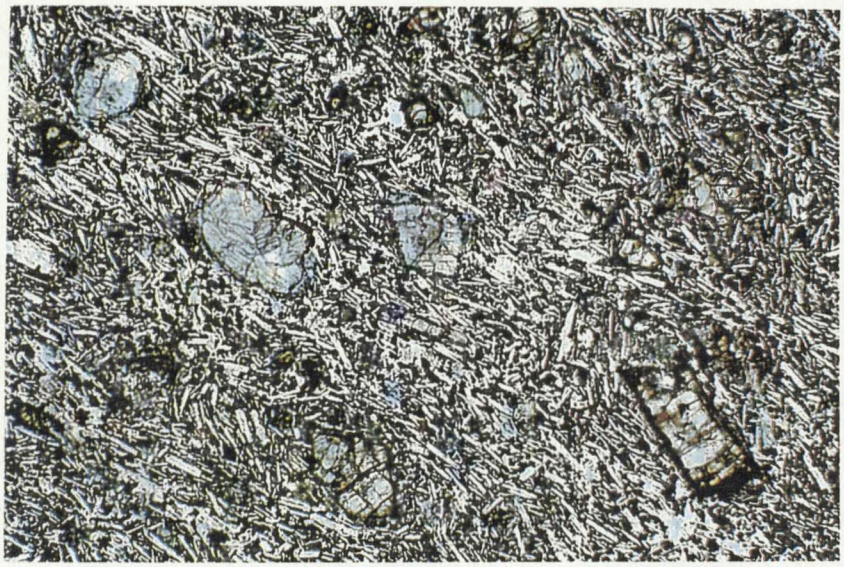

Figure 4. Photomicrograph of Sample JH1 (plane polarized light (PPL), 17x). Olivines show alteration to reddish brown iddingsite; whereas the pale green augite phenocrysts do not.

Figure 5. Photomicrograph of Sample 81 (PPL, 85x). Olivine phenocryst altered to fine-grained opaques.

contains rare bronzite phenocrysts (Wo_2 En_{81} Fs_{17}). These are up to 1.0 mm in length and show irregular exsolution lamellae of augite(?).

Bytownite laths (An74) up to 1.5 mm in length are common, although most plagioclase crystals are present as groundmass laths and microlites with a pilotaxitic to trachytic texture. The plagioclase also appears reasonably fresh and is normally zoned. Aside from the microlites, the matrix contains fine-grained pyroxene, scattered opaques, and some glass. As previously mentioned, Sample 81 from Flat Creek shows signs of extensive vesicle infilling with secondary calcite and silica.

Low-silica Andesites

These rocks are generally less phenocryst-rich than the basaltic andesites, usually with <20 vol.% and as little as 4 vol.% in Sample JH11. Olivine in these samples is corroded and rimmed with, or entirely replaced by, orthopyroxene (Figure 6). Bronzite phenocrysts (Wo_3 En_{74} Fs_{23}) up to 2.0 mm in length are common. Augite phenocrysts (Wo_{42} En_{43} Fs_{15}) are slightly smaller and less abundant. Both pyroxenes are abundant in the groundmass.

Plagioclase (An74) is uncommon as large phenocrysts; it is mainly present as small laths and microlites that comprise the bulk of the moderately to strongly trachytic groundmass. Occasional larger plagioclase phenocrysts up to 2 mm are often corroded with sieve-textured cores. Glass in the matrix ranges from none (Samples JH3 and JH11) to moderate (Samples 617 and 519).

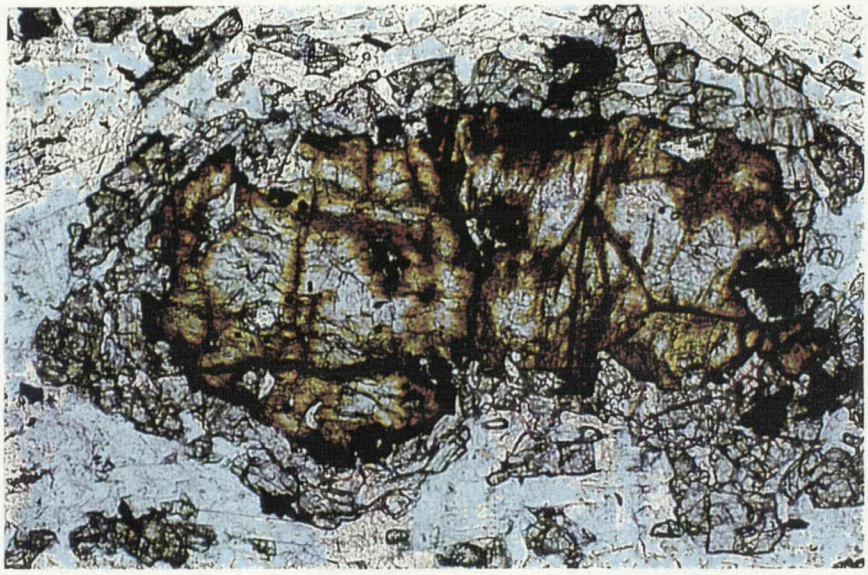

Figure 6. Photomicrograph of Sample 625 (PPL, 85x). Corroded and iddingsitized olivine rimmed with orthopyroxene.

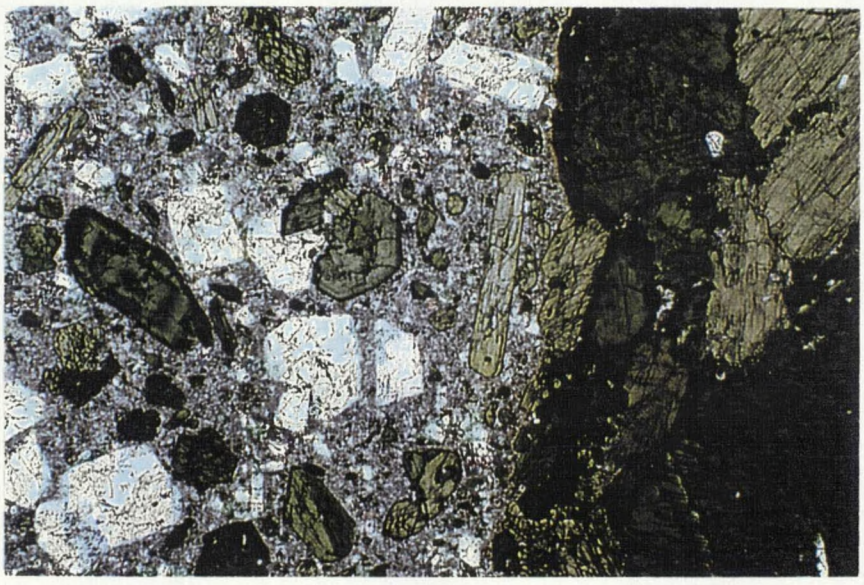

Figure 7. Photomicrograph of Sample 606 (PPL, 17x). Hornblende with oscillatory zoning and rounded plagioclase at left. Hornblendite xenolith at right.

Trachyandesites

These rocks are generally richer in phenocrysts (up to 55%) than the other groups, but their most distinctive petrographic feature is the presence of hornblende, which is absent from other JHV rocks but common in Absaroka volcanic rocks. It is pargasitic in nature and indistinguishable from amphibole crystals in the numerous hornblendite xenoliths present in all the samples (Figure 7). These xenoliths also contain limited amounts of pyroxene and rare garnet, suggesting a lower crustal origin (Green, 1982). Although some of the hornblende crystals may be xenocrysts derived from disaggregated xenoliths, many show overall normal (i.e. Fe/Mg increases from core to rim) oscillatory zoning, which suggests a magmatic rather than metamorphic origin. Further evidence of the complex history of this extensively contaminated magma is seen, on the one hand, in hornblende(?)-rimmed clinopyroxenes (especially within the xenoliths) versus the disequilibrium association of corroded hornblende with fresh, euhedral clinopyroxene (away from the xenoliths) on the other hand.

Plagioclase also shows numerous disequilibrium features (i.e. resorbtion, fritting, calcic overgrowths, etc.). As in the hornblende crystals, many of these may be due to magma mixing (Stimac and Pearce, 1992) or, more likely, to rapid decompression. Rapid ascent from the lower crust, as postulated by Green (1982), could produce both pressure instability of hornblende and sieve-cored and fritted textures in plagioclase (Nelson and Montana, 1992).

High-silica Andesites

These samples, although chemically quite similar, show marked petrographic differences. The Mosquito Creek flow (Sample JH10) is aphyric with only small plagioclase microlites in a mottled matrix probably due to partial devitrification of the original glass. The Palisades Dam andesite has a similar groundmass but also contains numerous glomerocrysts consisting of plagioclase and clinopyroxene.

Dacites

The large (up to 5 mm in length) andesine phenocrysts, which distinguish the porphyritic from the non-porphyritic dacites on the Gros Ventre Buttes, show many of the same disequilibrium textures present in the trachyandesites. Overall, they are normally zoned (An48 core to An12 rim) but also show strong oscillatory zoning. They are noticeably rounded due to resorbtion, have sieve-textured cores (Figure 8), and show strong fritting with and without calcic(?) overgrowths (Figure 9). Plagioclase forms the bulk of the phenocryst content which ranges from 12-18 vol.% in the non-porphyritic and from 28-42 vol.% in the porphyritic dacites.

Subordinate to plagioclase are hypersthene (Wo_2 En_{58} Fs_{40}) phenocrysts up to 1.8 mm. in length. In addition, rare augite (Wo_{45} En_{37} Fs_{18}) is present but may be xenocrystic. The groundmass ranges from nearly holocrystalline comprised of mainly small plagioclase laths (Sample JH6) to nearly holohyaline comprised of dark brown glass (Samples JH7 and 32). The latter also shows acicular Fe-oxide pseudomorphs (after biotite?) and occasional rhomb-shaped pseudomorphs (after hornblende?)(Figure 10).

Figure 8. Photomicrograph of Sample JH6 (Crossed polars (XP), 17x). Rounded andesine phenocrysts with sieve-textured cores.

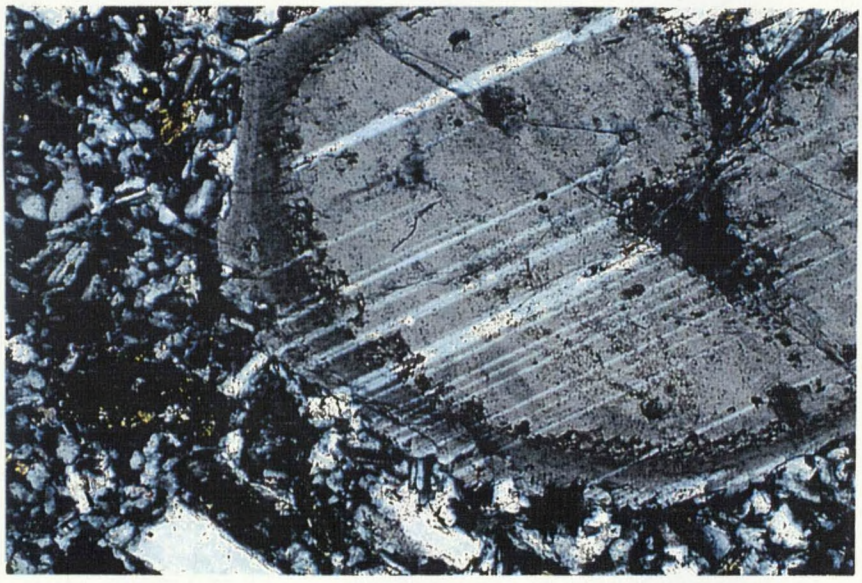

Figure 9. Photomicrograph of Sample JH6 (XP, 85x). Resorbed and fritted plagioclase with zoned overgrowth.

Nixon (1988) has interpreted similar biotite features as the result of dehydration due to magma mixing. Similar biotite dehydration features have been studied by Feeley and Sharp (1996). Dacites from Shadow Mountain (Sample SM2) contain examples of less complete biotite replacement (Figure 11).

That the bulk of these disequilibrium characteristics may be the result of magma mixing is supported by the presence of trachytic-textured inclusions (Figure 12). Possible magma mixing scenarios and their relative importance in the evolution of the Jackson Hole Volcanics will be discussed in a later section.

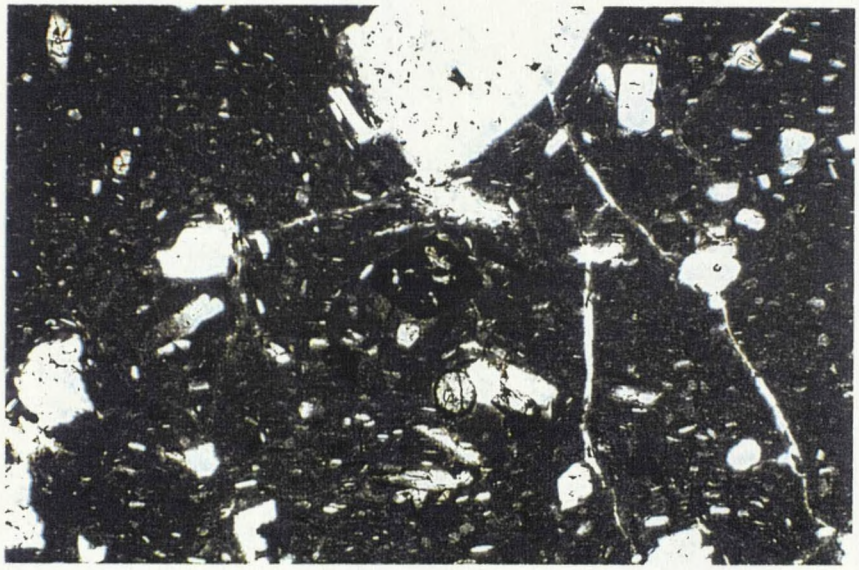

Figure 10. Photomicrograph of Sample 32 (PPL, 17x). Scattered acicular and lath-shaped oxide pseudomorphs after biotite (?). Pseudomorph after hornblende (?) in center.

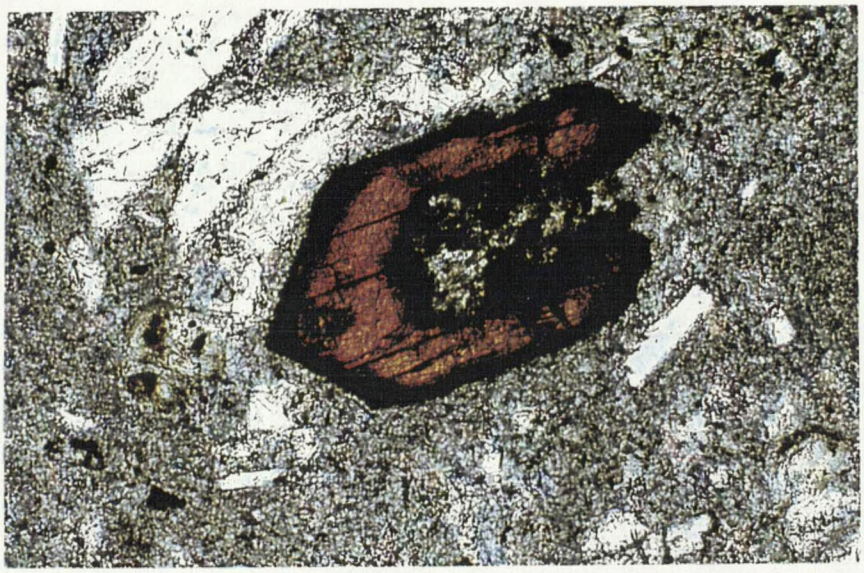

Figure 11. Photomicrograph of Sample SM2 (PPL, 85x). Biotite with oxide reaction rim due to dehydration.

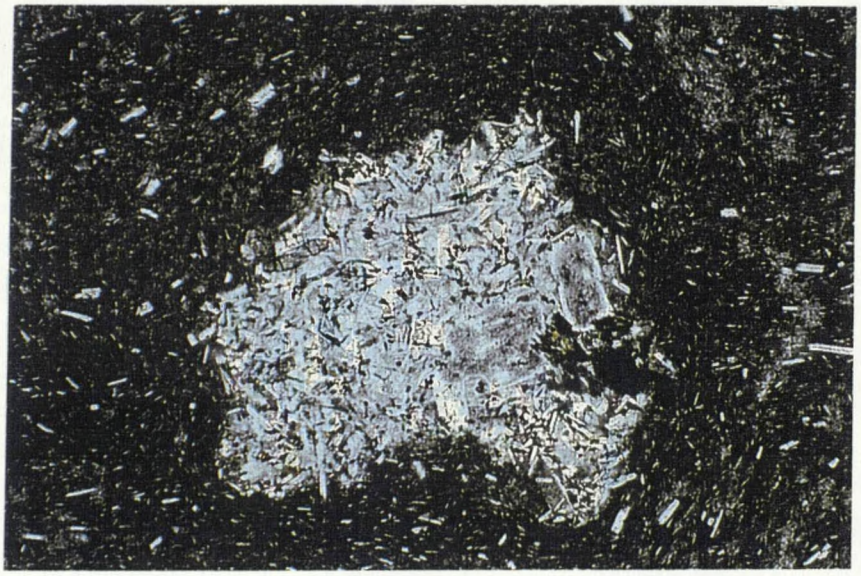

Figure 12. Photomicrograph of Sample JH12 (PPL, 17x). Inclusion of trachytic holocrystalline hypersthene- and plagioclase-bearing andesite(?) within glassy non-porphyritic dacite.

Rhyolites

The rhyolitic samples include obsidian (Sample JH14), flow-banded, aphyric rhyolite (Sample JH13), and red and gray, flow-banded rhyolite with occasional biotite and plagioclase phenocrysts (Sample JH15). In the last, the plagioclase is of both the fresh and disequilibrium (resorbed, etc.) varieties.

It is of note that none of the rhyolites nor any of the other JHV samples contain sanidine. The reddish ash (Sample JH18) on Teton Pass, whose geochemistry is distinct from JHV rocks, does contain abundant sanidine; as do welded tuffs (Sample 701) from the Heise Group Kirkham Hollow volcanic rocks at the mouth of Moose Creek on the west side of Teton Pass. The JHV rocks, however, appear to be too low in potassium to have precipitated sanidine.

Geochemistry

Overview

It is the geochemistry of the JHV rocks that most clearly distinguishes the suite from the other volcanic suites in the region. Silica variation diagrams are consistently coherent and often clearly distinct from similarly coherent trends of other groups of volcanic rocks. For purposes of comparison, three other datasets have been plotted with that of the JHV (see Figure 3). These datasets were chosen not only for their proximity to the JHV but also, and primarily, because they are some of the few available for which major and trace elements and isotope values (for individual samples as opposed to

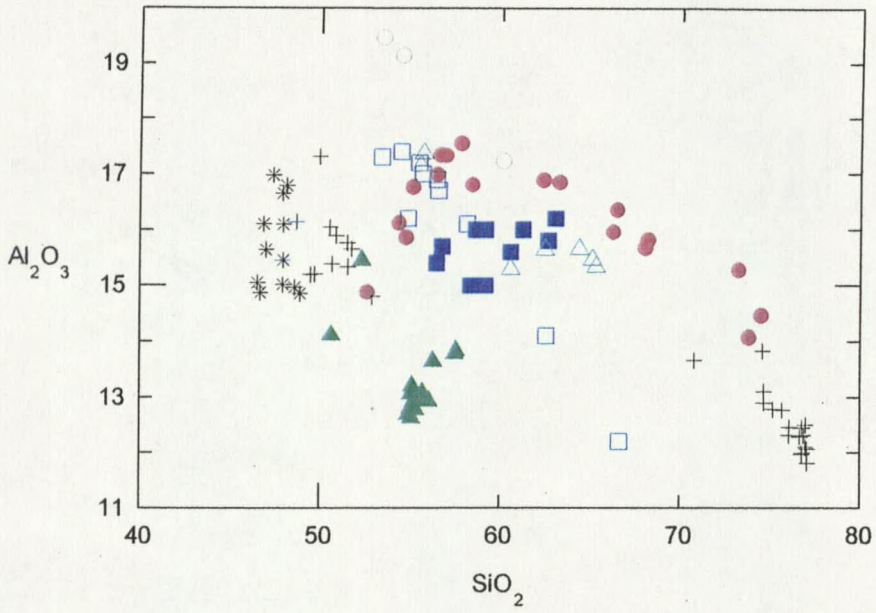

Figure 13. Plot of Al_2O_3 vs. SiO_2 (wt. %). Symbols as in Figure 3.

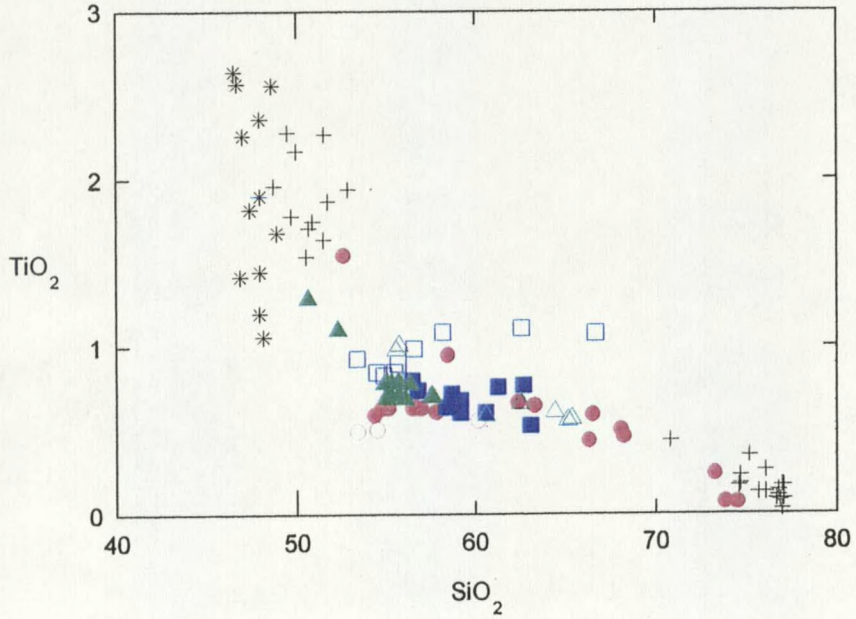

Figure 14. Plot of TiO_2 vs. SiO_2 (wt. %). Symbols as in Figure 3.

averages) have been published. The silica range for the strongly bimodal YSP data shows only minimal overlap with the intermediate values of the other three sets; nevertheless, these plots allow assessment of the potential role of the Yellowstone magmas in the petrogenesis of the JHV, either as end members in a magma mixing or assimilation process or with the YSP basalts as parental in a process dominated by crystal fractionation.

Major Element Variations

Al_2O_3 values in the JHV show a distinct transition from fractionation of non-aluminous (olivine) to aluminous (plagioclase) phases. This has also been interpreted as high-pressure versus low-pressure fractionation (Leeman et al., 1990). The JHV Al_2O_3 values, especially in the more siliceous samples, are distinctly higher than those of the other suites, with some of the trachyandesites (Samples IPK2 and IPK4) showing very high values.

TiO_2 values are flat over the range of 53-62% SiO_2 decrease slightly in rocks with >62% SiO_2 in the JHV. They are similar to the Challis, SCV, and the HABS values but less than those of the HATS. FeO* (total Fe as Fe^{2+}) and MnO contents decrease with increasing SiO_2 for all groups. CaO in the JHV also displays a tightly linear negative correlation with SiO_2, but is noticeably higher at a given silica value than the other groups.

MgO in the JHV rocks shows a steeply negative trend colinear with that of the Challis and HABS suites but shifted from that of the SCV, HATS, and especially YSP groups. The JHV basaltic andesites show very high values while the less siliceous samples

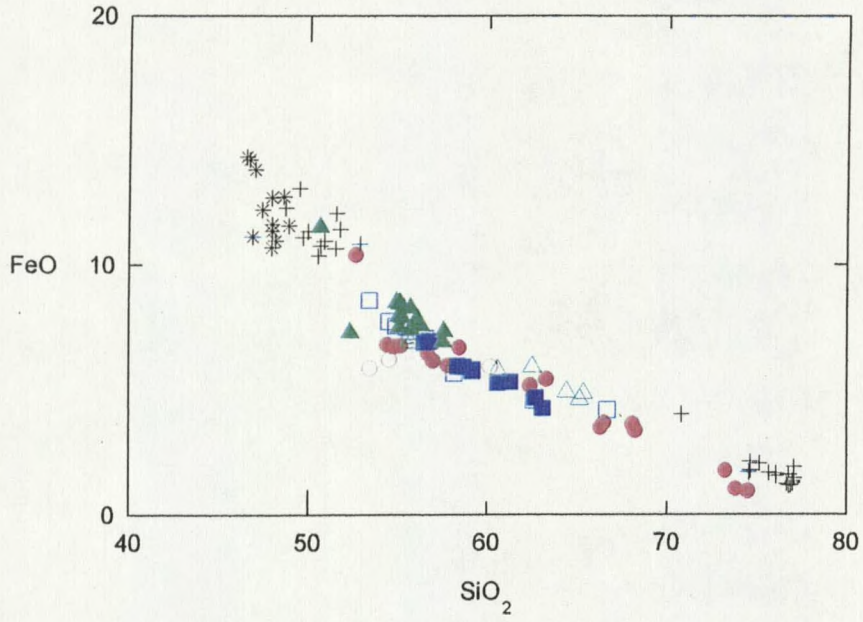

Figure 15. Plot of FeO* vs. SiO_2 (wt. %). Symbols as in Figure 3.

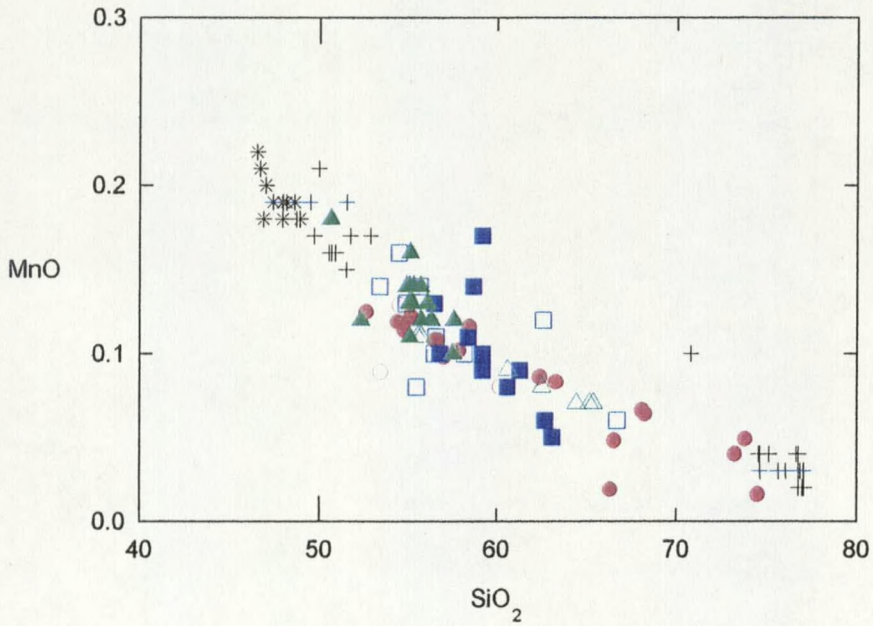

Figure 16. Plot of MnO vs. SiO_2 (wt. %). Symbols as in Figure 3.

of JHV trachyandesites are distinctly lower. K_2O contents in the JHV are markedly lower than the other groups and slightly less positively correlated. The trachyandesites plot with the Eocene volcanics rather than with the rest of the JHV.

Na_2O contents in JHV rocks are higher than the Challis, SCV, and Yellowstone groups yet lower than the Absaroka samples. The shift to a negative trend in the JHV rhyolites may reflect vapor-phase Na-K exchange. The trachyandesites again plot at higher levels than the rest of the JHV. P_2O_5 contents in all suites show a substantial amount of scatter at lower silica values but become more coherent and negatively correlated towards higher values.

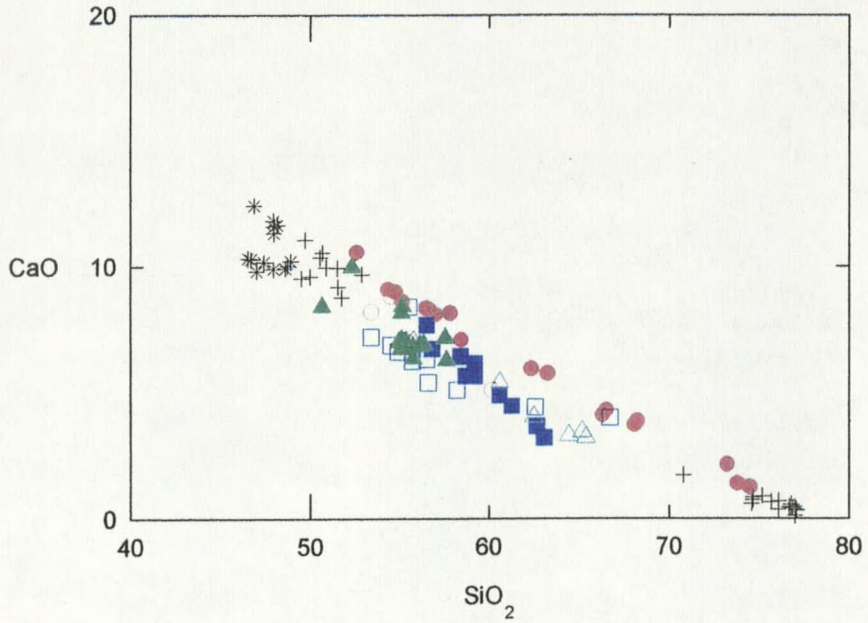

Figure 17. Plot of CaO vs. SiO_2 (wt. %). Symbols as in Figure 3.

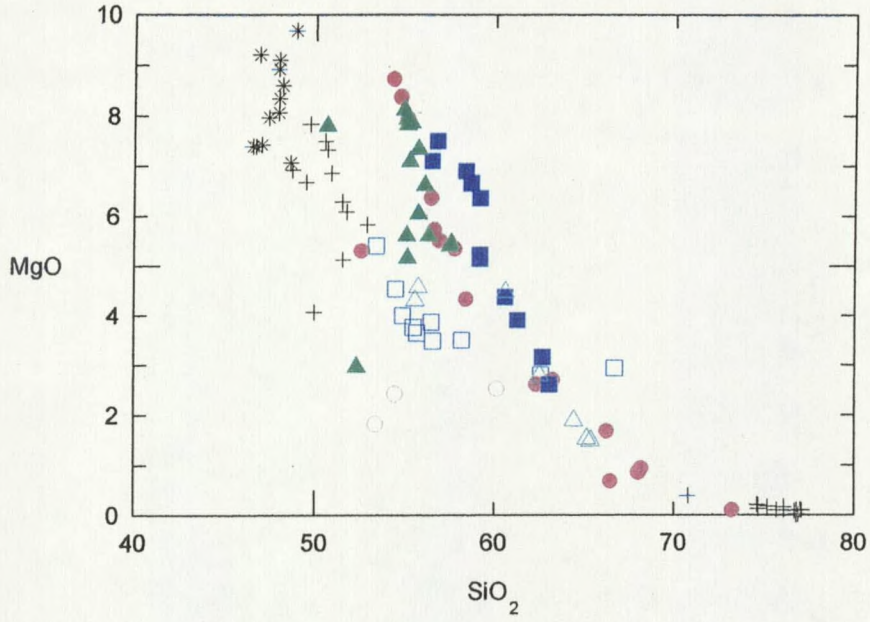

Figure 18. Plot of MgO vs. SiO_2 (wt. %). Symbols as in Figure 3.

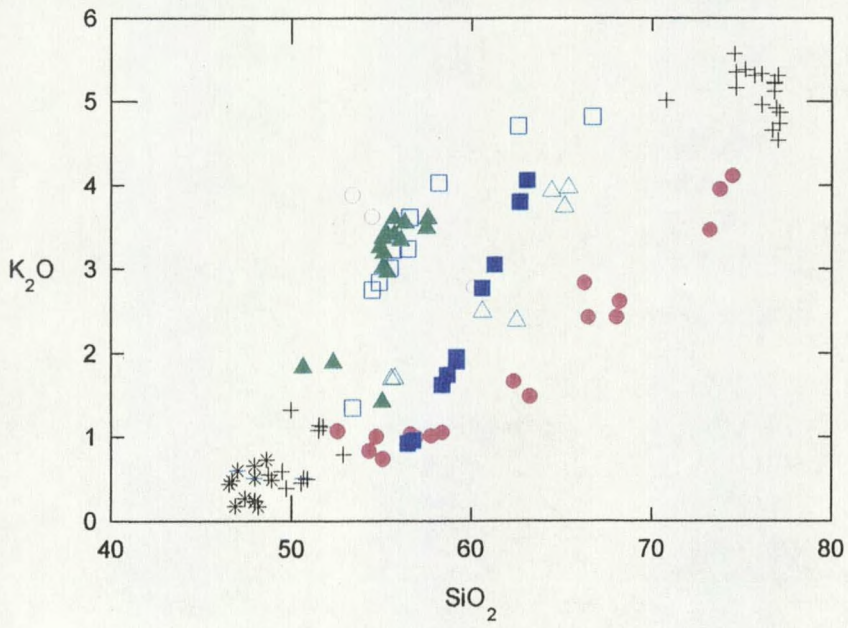

Figure 19. Plot of K_2O vs. SiO_2 (wt. %). Symbols as in Figure 3.

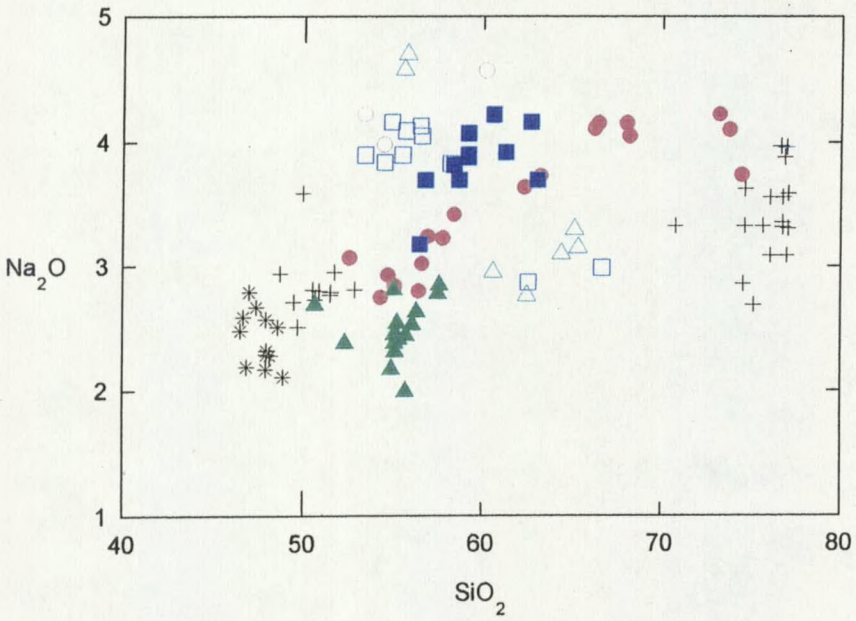

Figure 20. Plot of Na_2O vs. SiO_2 (wt. %). Symbols as in Figure 3.

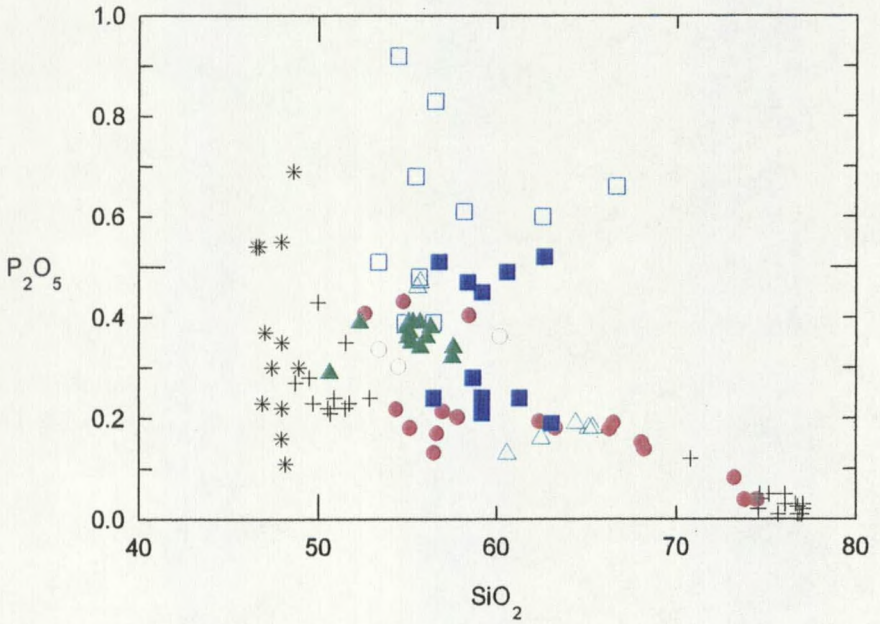

Figure 21. Plot of P_2O_5 vs. SiO_2 (wt. %). Symbols as in Figure 3.

Trace Element Variations

The compatible elements Ni and Cr show steeply negative correlations with SiO_2, with values markedly higher at a given silica content than HATS and YSP, the same or slightly higher than Challis-SCV, and slightly lower than HABS. The trachyandesites also plot lower than the main JHV suite. The highest JHV values, in the basaltic andesites, are in fact higher than all but one of the YSP basalts. These trends mirror those of MgO, but even when plotted against MgO, the Ni and Cr trends for the JHV and Eocene groups are distinctly shifted from that of the Yellowstone group. This is consistent with the olivine-rich nature of the more mafic JHV samples. It is of note, however, that olivine was not detected in the Absaroka samples (Meen and Eggler, 1987).

Sc also shows a negative correlation, although the trend is less steep than those for Ni and Cr , possibly due to the preference for the Sc by pyroxenes only as opposed to the preference for nickel and chromium by olivine only and olivine and pyroxene, respectively. The change in slope for the Ni and Cr trends probably reflects either the gradual cessation of olivine fractionation or the increasing effects of contamination with a crustal component with very low Ni and Cr contents. V in the JHV shows a trend similar to Sc.

Variation of incompatible elements such as the large-ion lithophile elements (LILE), Ba and Rb, are similar to K_2O in that the JHV suite is significantly lower than the Eocene volcanic rocks but close to "colinear" with YSP samples. For Ba, the JHV shows more scatter than for Rb. The trachyandesites plot with the main trend for Ba but higher for Rb. The JHV rhyolites plot higher than theYSP for Ba but lower for Rb.

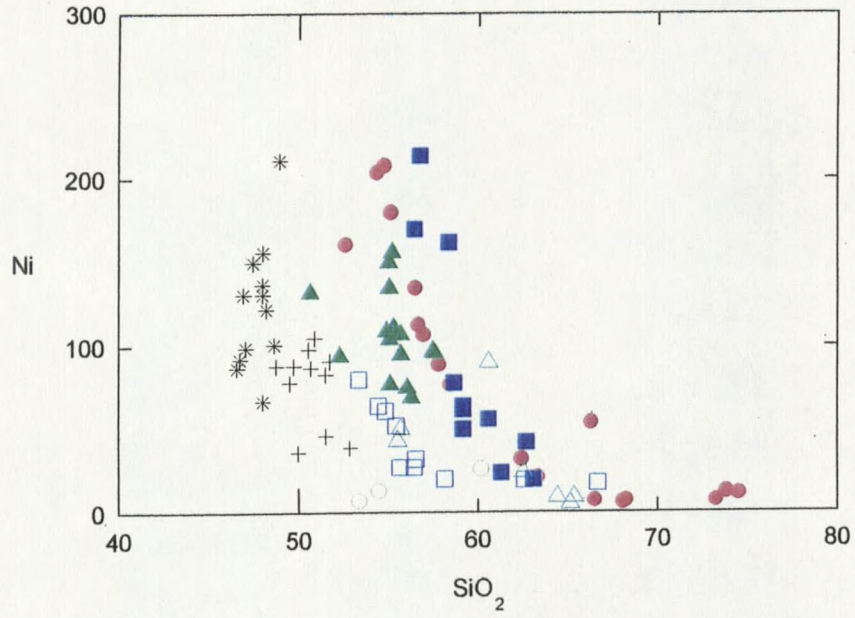

Figure 22. Plot of Ni (ppm.) vs. SiO_2 (wt. %). Symbols as in Figure 3.

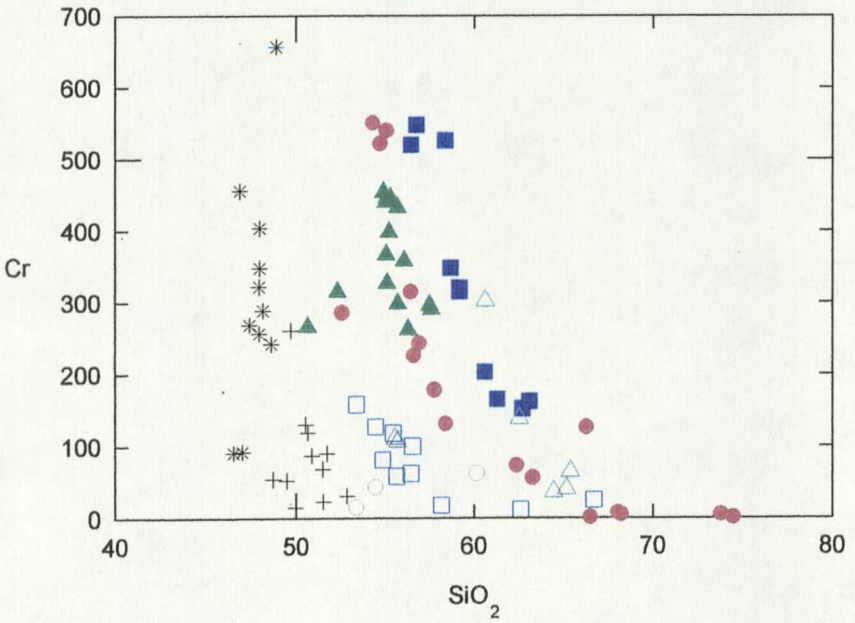

Figure 23. Plot of Cr (ppm.) vs. SiO_2 (wt. %). Symbols as in Figure 3.

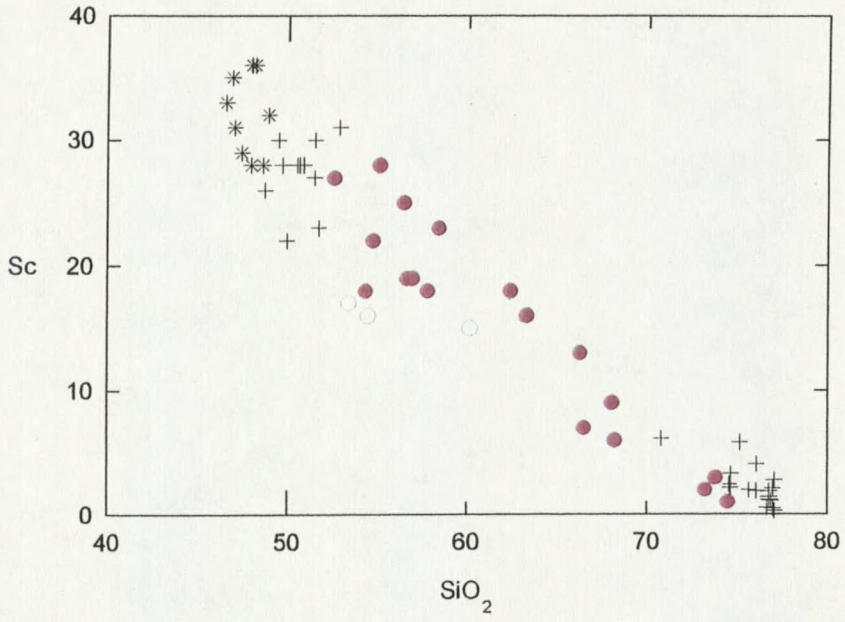

Figure 24. Plot of Sc (ppm.) vs. SiO_2 (wt. %). Symbols as in Figure 3.

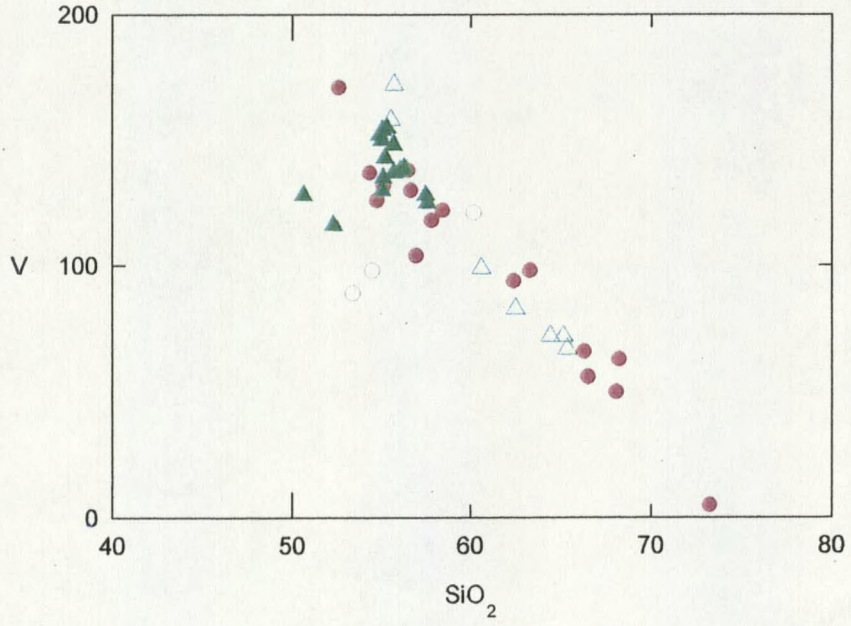

Figure 25. Plot of V (ppm.) vs. SiO_2 (wt. %). Symbols as in Figure 3.

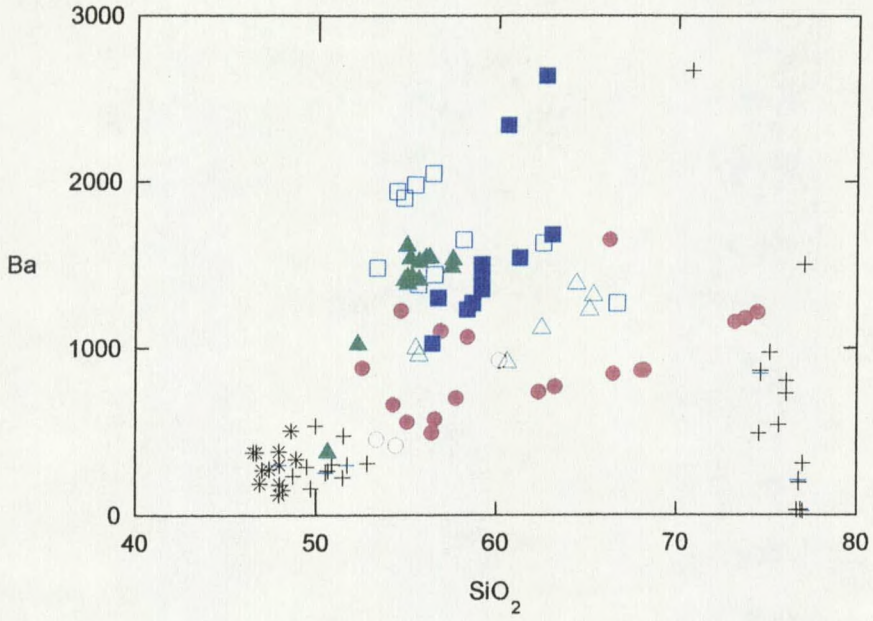

Figure 26. Plot of Ba (ppm.) vs. SiO_2 (wt. %). Symbols as in Figure 3.

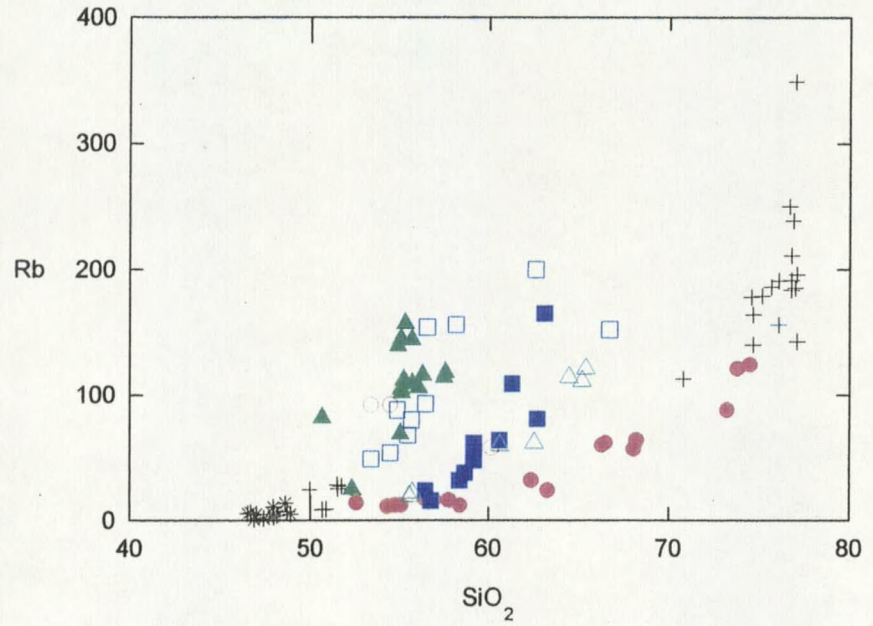

Figure 27. Plot of Rb (ppm.) vs. SiO_2 (wt. %). Symbols as in Figure 3.

Sr in the JHV shows appreciable scatter in the more mafic samples with a shallow negative trend in the dacites and rhyolites. This perhaps reflects the delayed inception of significant plagioclase fractionation (as displayed by Al_2O_3 vs.SiO_2). Compared to the other suites, the JHV plots lower than the Eocene samples and the trachyandesites but slightly higher than the YSP. Zr shows, for the most part, no correlation with silica in the JHV, with perhaps some indication of zircon fractionation in the rhyolites, although none was detected in the mode. The JHV main group plots with HATS and SCV, slightly lower than the intrusive andesites, Challis, and YSP samples, and distinctly higher than the HABS group.

Y in the JHV also shows minimal correlation with SiO_2, although a slight negative trend may exist for the rhyolites. JHV samples have similar to generally higher concentrations than the Eocene samples, suggesting, by proxy, slightly higher HREE levels than the latter which are characterized as flat by Norman and Mertzman (1991).

LREE values as represented by La and Ce show considerable scatter in the JHV but share a similar range with the other groups, with the JHV rhyolites plotting slightly lower than those of the YSP. A plot of La versus Ce, although tightly coherent for the other suites, also shows considerable scatter for the JHV rocks.

Pb values in the more mafic JHV are markedly lower than the Eocene suites and, as a whole, are positively correlated with SiO_2, especially in the more siliceous samples. The Eocene samples, on the other hand, show a slight negative correlation. Th in the JHV

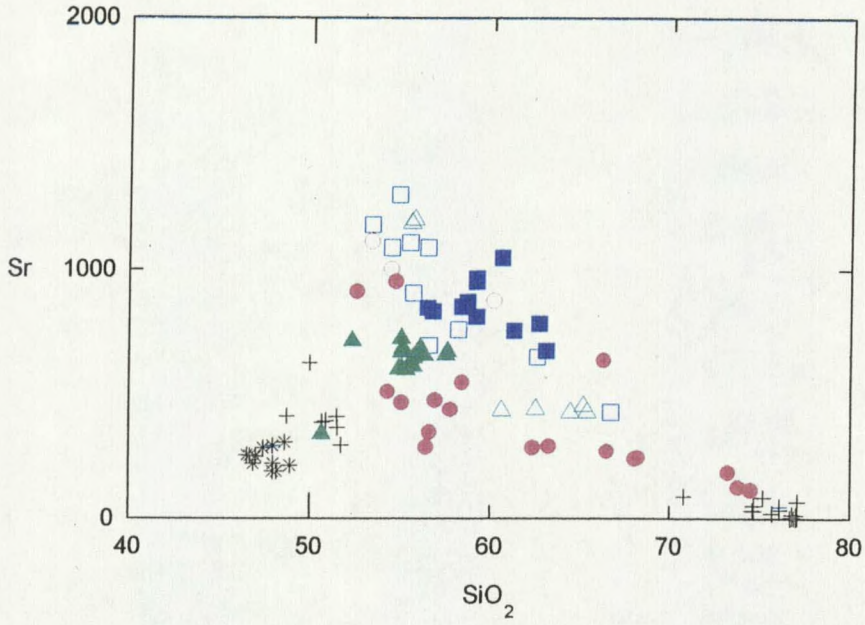

Figure 28. Plot of Sr (ppm.) vs. SiO_2 (wt. %). Symbols as in Figure 3.

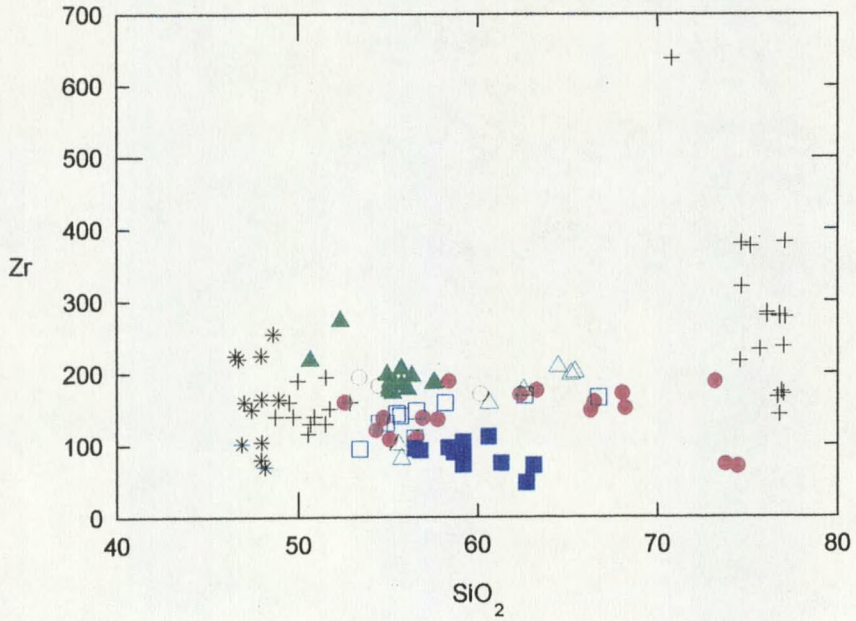

Figure 29. Plot of Zr (ppm.) vs. SiO_2 (wt. %). Symbols as in Figure 3.

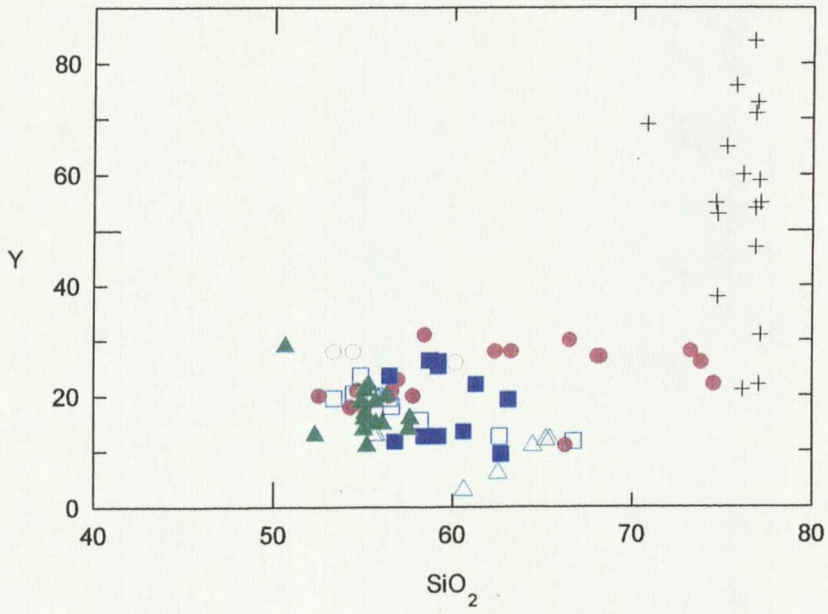

Figure 30. Plot of Y (ppm.) vs. SiO_2 (wt. %). Symbols as in Figure 3.

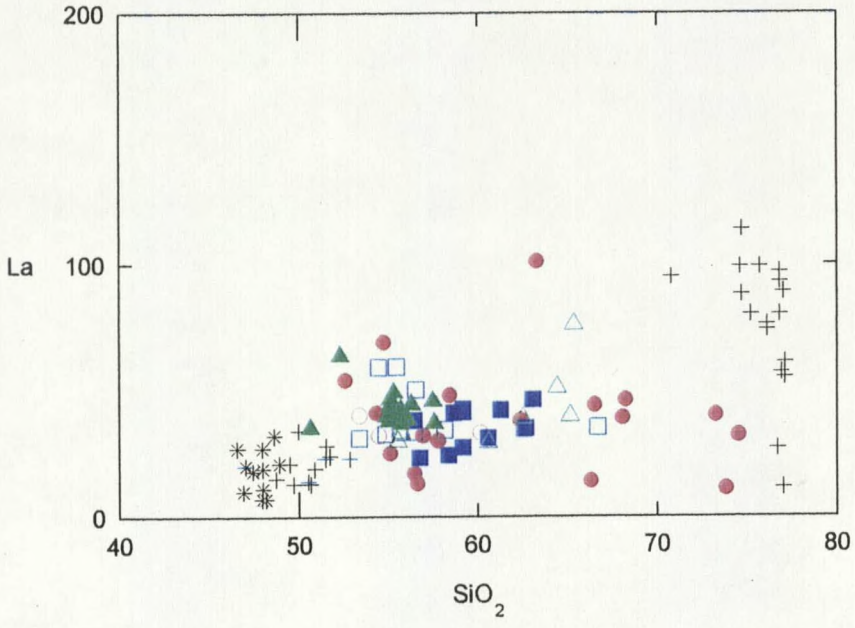

Figure 31. Plot of La (ppm.) vs. SiO_2 (wt. %). Symbols as in Figure 3.

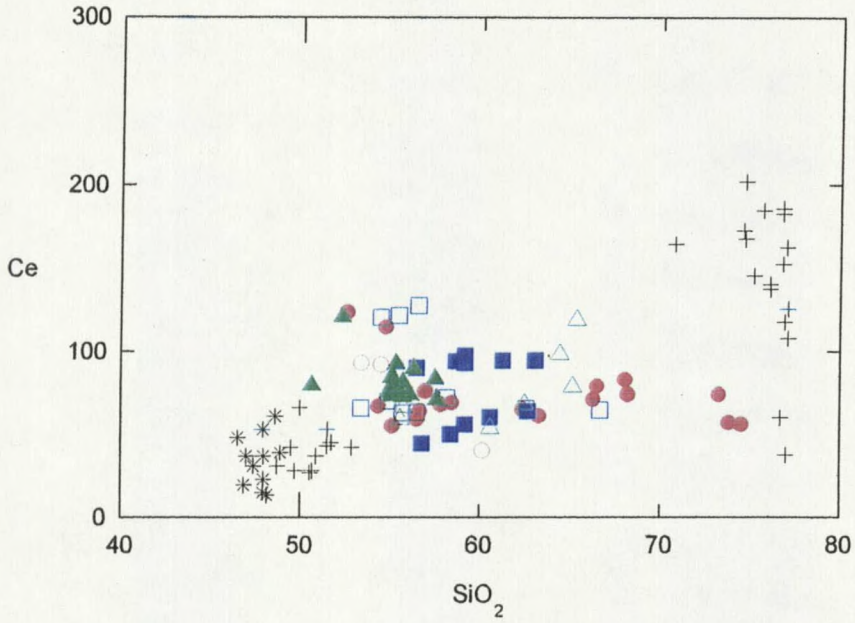

Figure 32. Plot of Ce (ppm.) vs. SiO_2 (wt. %). Symbols as in Figure 3.

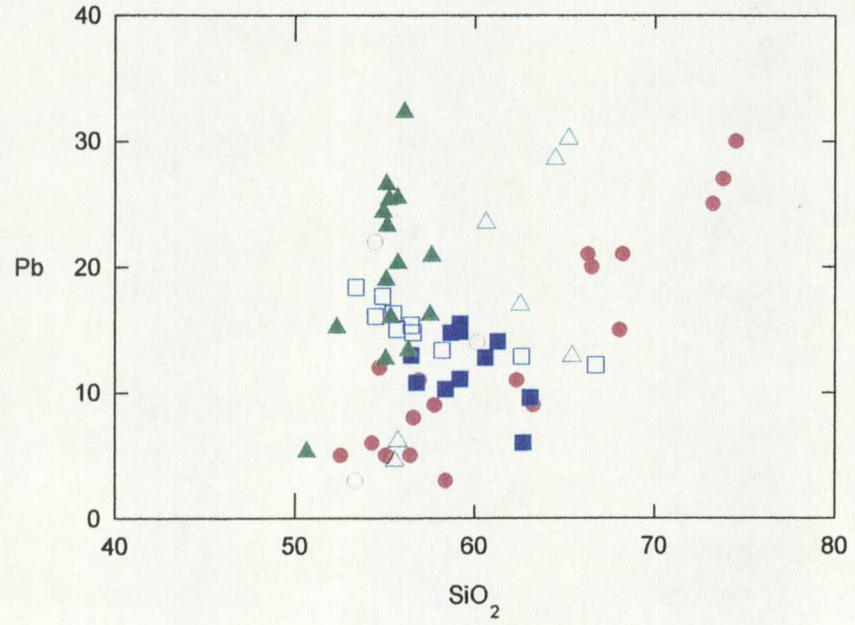

Figure 33. Plot of Pb (ppm.) vs. SiO_2 (wt. %). Symbols as in Figure 3.

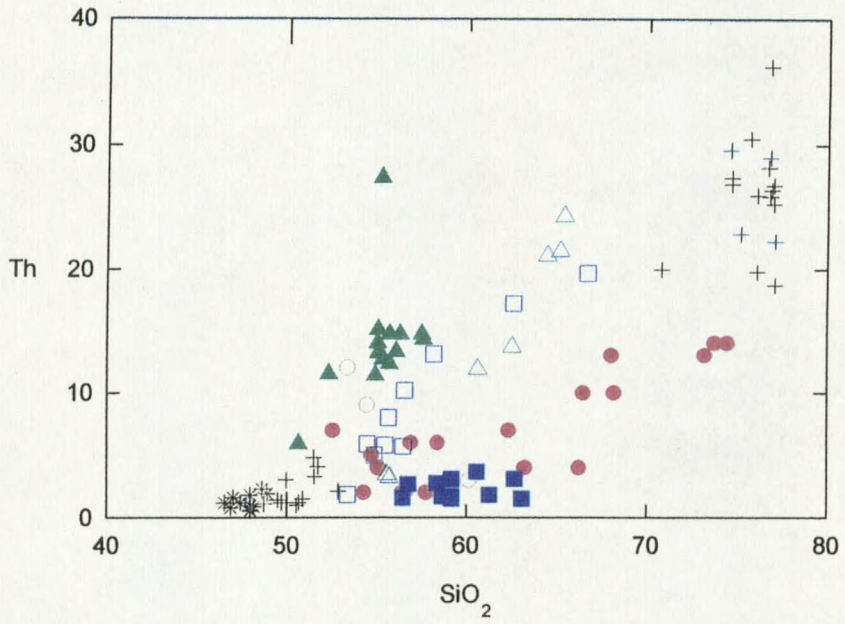

Figure 34. Plot of Th (ppm.) vs. SiO_2 (wt. %). Symbols as in Figure 3.

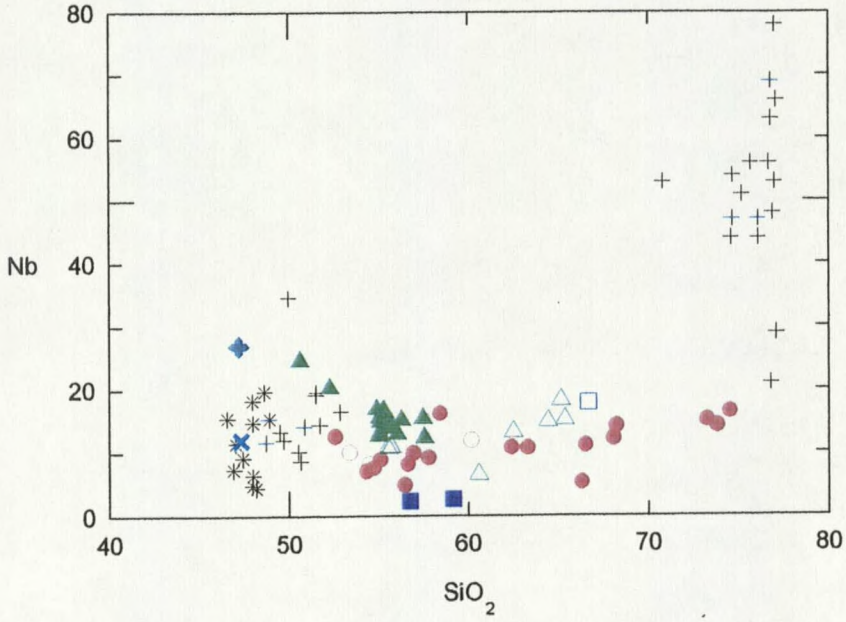

Figure 35. Plot of Nb (ppm.) vs. SiO_2 (wt. %). Symbols as in Figure 3 and, in addition, Snake River Plain basalt averages (Fitton et al., 1991), a blue X for flows > 5 Ma and an olive cross for those < 5 Ma.

is also lower and slightly less positively correlated than the Challis, SCV, HATS, and YSP samples but higher than HABS which appears independent of SiO_2. In neither Th nor Pb do the trachyandesites plot closely with the main JHV group.

Nb values for HATS, HABS, and some YSP samples have been derived from Ta values using a conversion factor of Nb = 13.3 x Ta (as opposed to Gill's (1981) 16 x). This was the average ratio for YSP samples on which both Nb and Ta had been measured. The niobium values for the JHV can be seen to be generally lower than the Challis, SCV, and the bulk of the YSP basalt samples and the Snake River Plain averages, and they are distinctly lower than the YSP rhyolites. JHV samples appear to be higher than the HABS group, but the data for the latter is limited. Of major importance is the lack of correlation with silica in the JHV, suggesting that this is a source characteristic.

Isotopes

A plot of $^{143}Nd/^{144}Nd$ versus $^{87}Sr/^{86}Sr$ shows a lack of relationship between the JHV and the YSP. The latter plots close to the mantle array; while the former plots well below and to the left. The JHV samples plot very close to those of the HABS with a likely contamination trend to higher $^{87}Sr/^{86}Sr$ values. In plots of $^{143}Nd/^{144}Nd$ versus SiO_2 the YSP group shows a very slight negative trend; while the JHV, HATS, and HABS show little or no significant correlation. In a plot of $^{87}Sr/^{86}Sr$ versus SiO_2, HATS and HABS again show no correlation; while the YSP and JHV show a distinct positive trend.

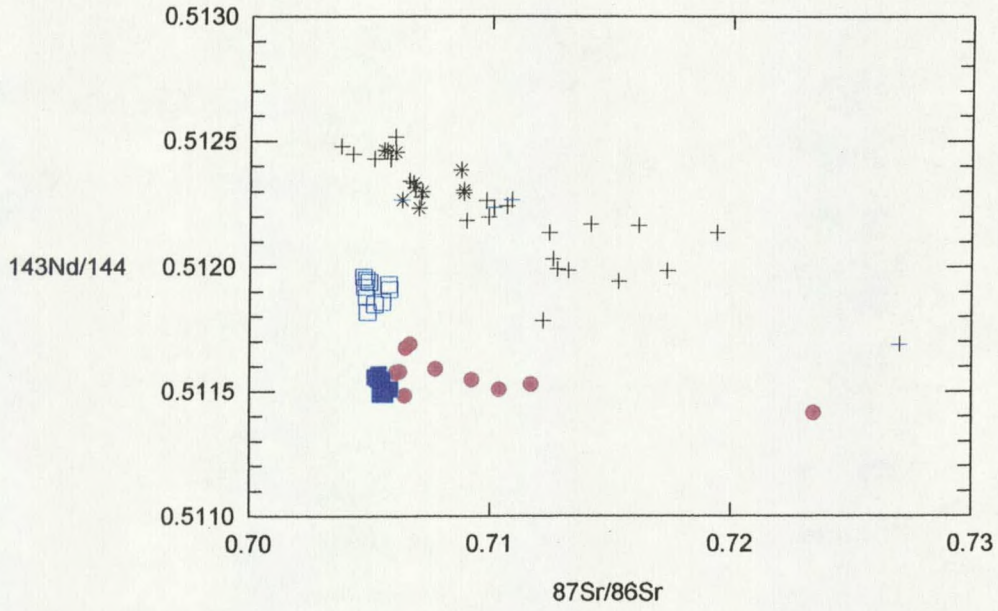

Figure 36. Plot of $^{143}Nd/^{144}Nd$ vs. $^{87}Sr/^{86}Sr$. Symbols as in Figure 3.

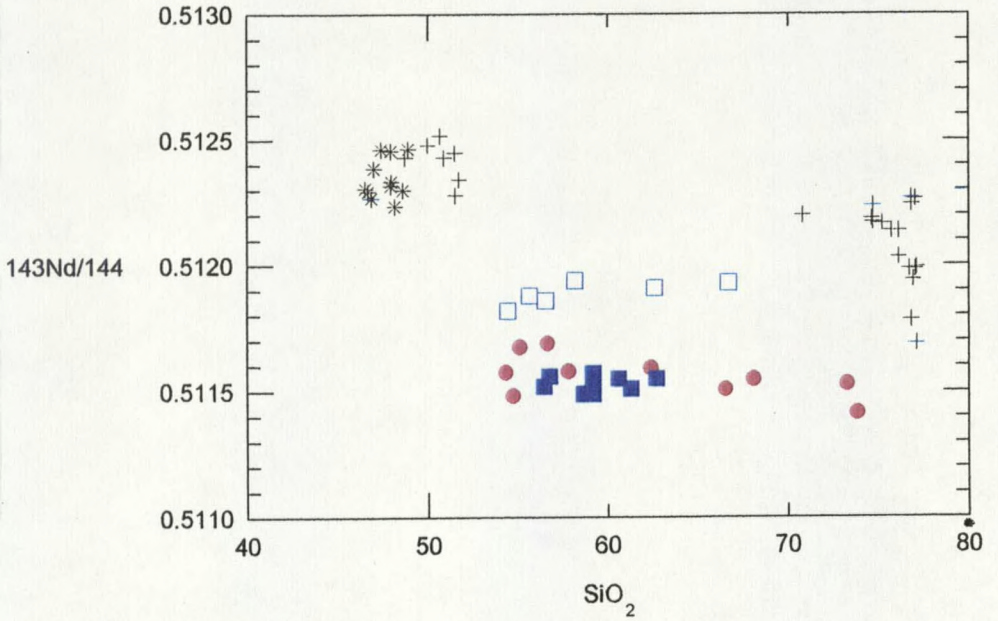

Figure 37. Plot of $^{143}Nd/^{144}Nd$ vs. SiO_2. Symbols as in Figure 3.

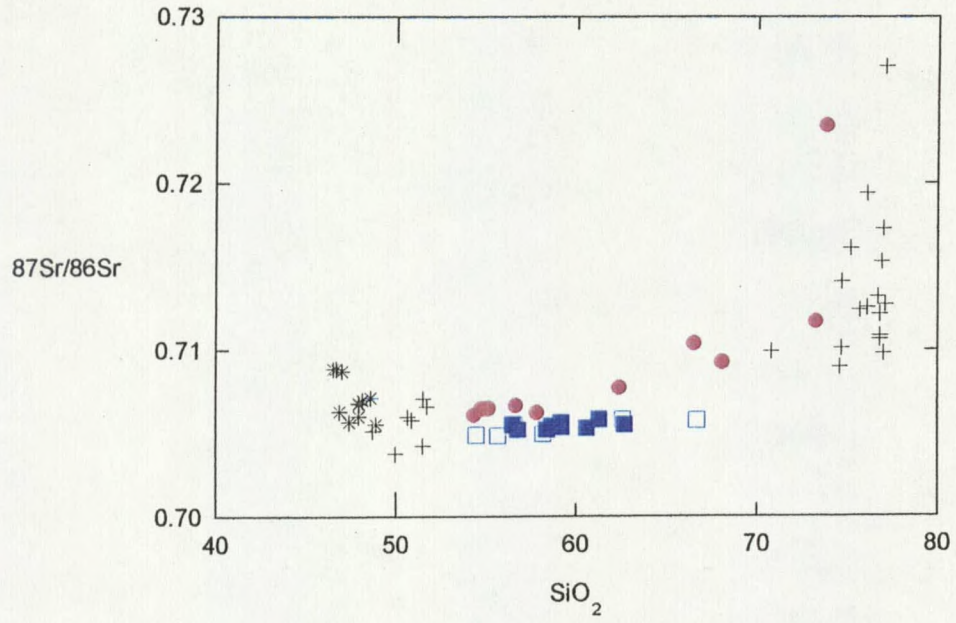

Figure 38. Plot of $^{87}Sr/^{86}Sr$ vs. SiO_2. Symbols as in Figure 3.

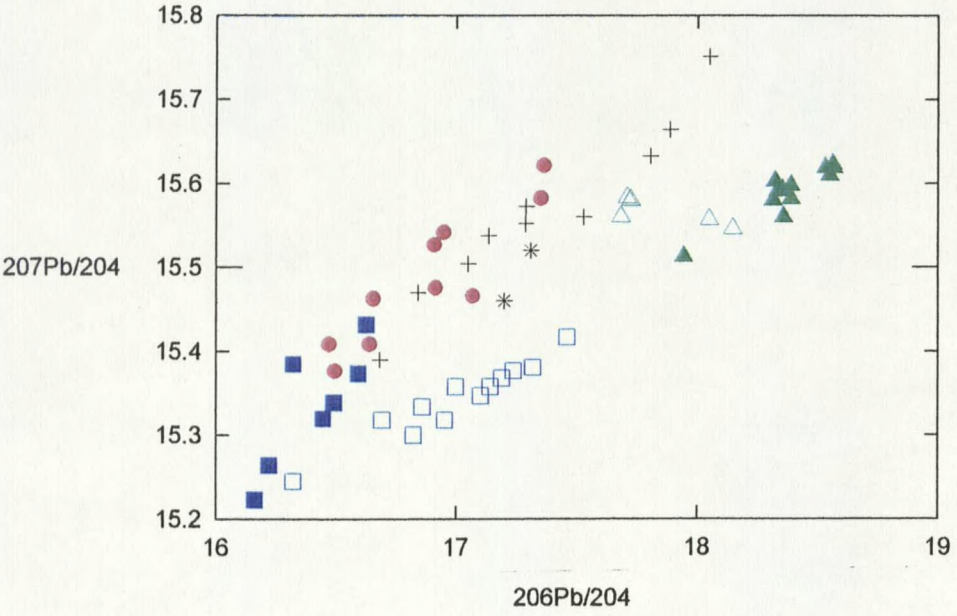

Figure 39. Plot of $^{207}Pb/^{204}Pb$ vs. $^{206}Pb/^{204}Pb$. Symbols as in Figure 3.

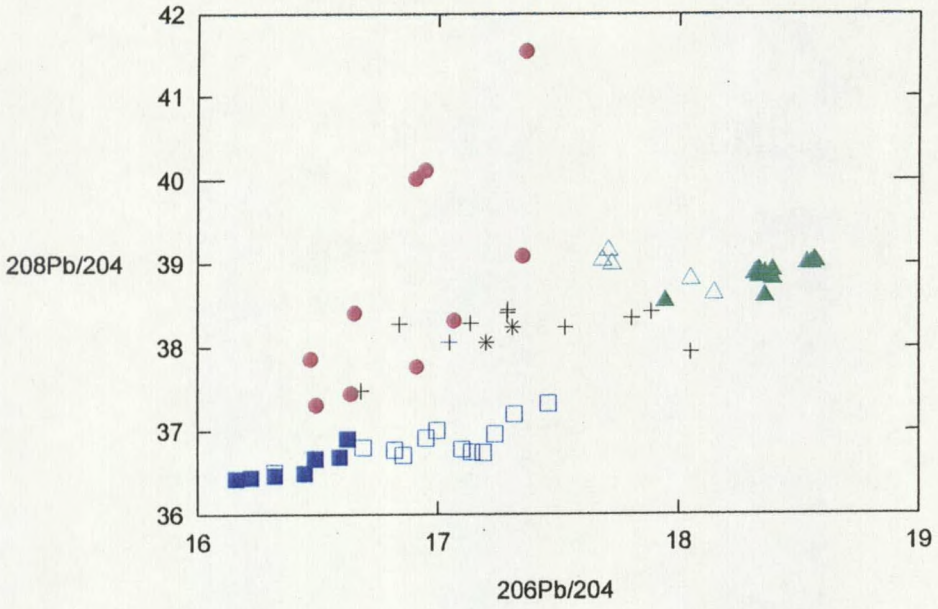

Figure 40. Plot of $^{208}Pb/^{204}Pb$ vs. $^{206}Pb/^{204}Pb$. Symbols as in Figure 3.

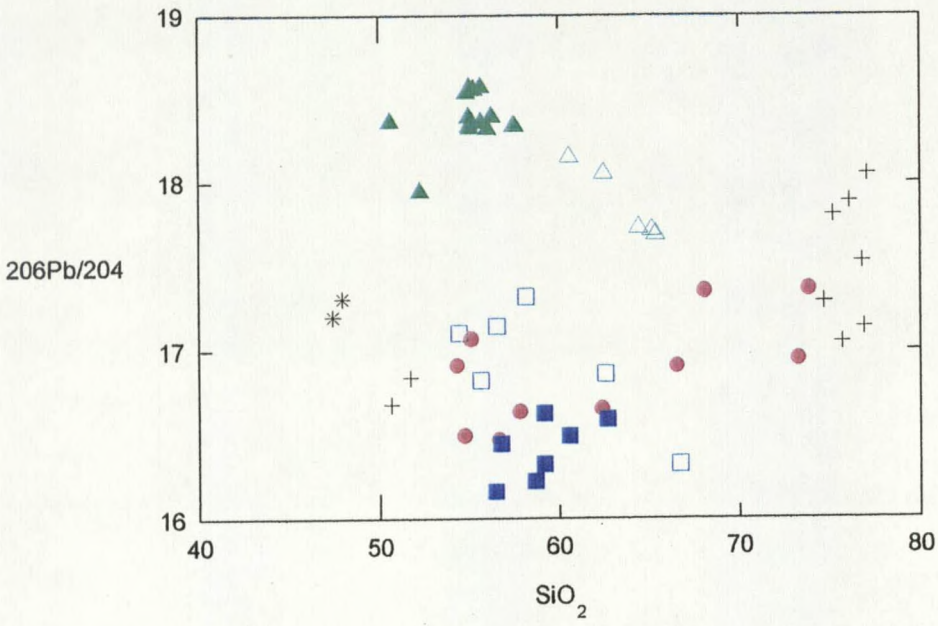

Figure 41. Plot of $^{206}Pb/^{204}Pb$ vs. SiO_2. Symbols as in Figure 3.

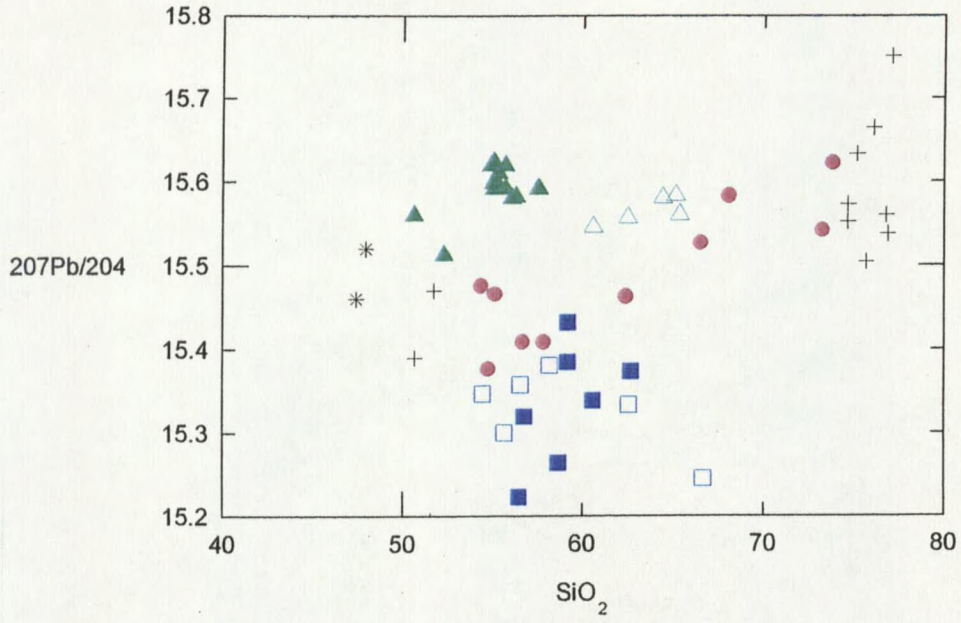

Figure 42. Plot of $^{207}Pb/^{204}Pb$ vs. SiO_2. Symbols as in Figure 3.

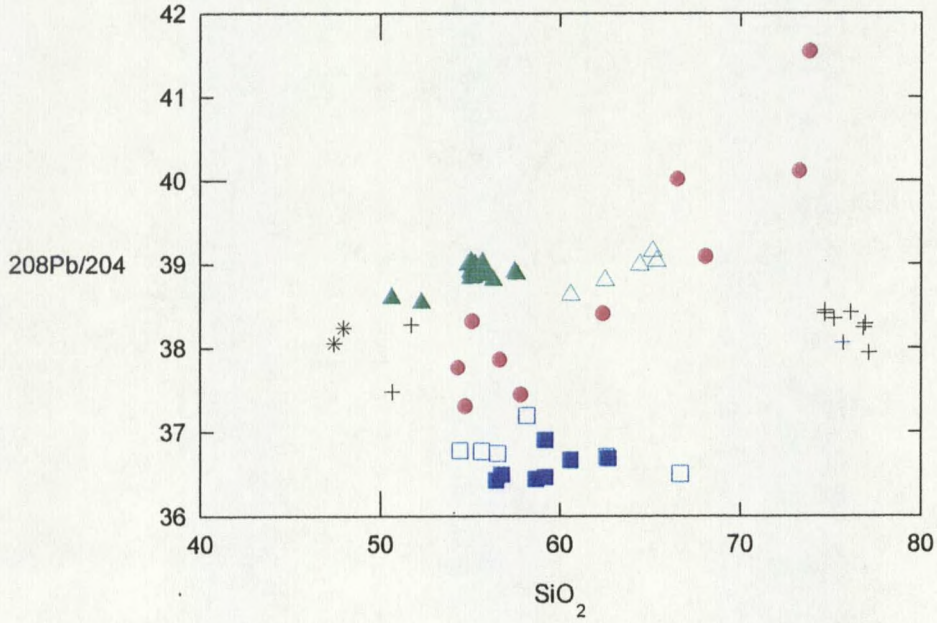

Figure 43. Plot of $^{208}Pb/^{204}Pb$ vs. SiO_2. Symbols as in Figure 3.

Lead isotope ratios, as shown in a plot of $^{207}Pb/^{204}Pb$ versus $^{206}Pb/^{204}Pb$, reveal the similarity of the HABS, JHV, and YSP samples, which share an Archaean-age (pseudo- ?) isochron, as opposed to the HATS and Challis values, which yield a Proterozoic (pseudo-) isochron. The more mafic JHV samples share the low $^{206}Pb/^{204}Pb$ values of the HABS, which are among the lowest values yet detected in North America. $^{208}Pb/^{204}Pb$ values for the JHV, however, are markedly higher than all the other groups and extend to extremely high values in the rhyolitic samples.

Covariation with SiO_2 in the JHV is slightly positive for $^{206}Pb/^{204}Pb$, moderately positive for $^{207}Pb/^{204}Pb$, and strongly positive for $^{208}Pb/^{204}Pb$. The other groups show little correlation with SiO_2 content. The YSP suite is very slightly positive for $^{206}Pb/^{204}Pb$ and $^{207}Pb/^{204}Pb$. SCV is negative for $^{206}Pb/^{204}Pb$ and weakly positive for $^{207}Pb/^{204}Pb$. The Pb isotope ratios for the HATS, HABS, and Challis groups appear to be more or less independent of SiO_2.

CHAPTER 5

DISCUSSION

Overview

As set forth in the introduction, the challenge of identifying the paleotectonic setting associated with a given suite of volcanic deposits is essentially threefold:

1) identify the processes involved in the initial melt production (i.e. heating, hydrous flux, decompression melting, etc.);

2) identify the composition of the source rocks from which the initial melts were produced; and

3) identify the petrologic processes which subsequently modified these primary melts (i.e. crystal fractionation, crustal assimilation, magma mixing, etc.)

In order to determine the tectonic environment associated with volcanism, one must proceed in the reverse order, gradually stripping away effects due to later processes in order to discern the original source rocks, leading *finally* to the physical agents of melt production and thereby the likely tectonic setting. In accordance with this strategy, I will proceed to examine the origin of the JHV rocks and surrounding volcanic suites in the

context of the following aspects in order: 1) magma mixing; 2) assimilation of crustal rocks plus crystal fractionation (AFC); 3) source rocks and their history; 4) agents responsible for initial melting; and 5) tectonic setting.

Magma Mixing

Evidence for the mixing of two distinct magmas is primarily petrographic and can include gross features, such as undercooled inclusions of more mafic magma within the more silicic and magma textures indicative of chemical disequilibrium in phenocrysts. More subtle disequilibrium features are revealed by microprobe analysis of mineral phases. The involvement of magma mixing can also be suggested by chemical trends. Of course, some evidence for the comagmatic origin of a suite is required for magma mixing to be considered. The JHV as a whole is too distributed in time and space to provide such evidence; nevertheless, samples from the East and West Gros Ventre Buttes display several features suggestive of magma mixing.

The inclusion shown in Figure 12 has a rounded, irregular outline suggestive of a magmatic inclusion, although it lacks obvious features of quenching such as a glassy rind or vesicular interior (Bacon, 1986). It could also be interpreted as a partially resorbed xenolith, although plagioclase crystals at its margin appear uncorroded. The orthopyroxene-rimmed olivine phenocrysts in the low-silica andesites (Figure 6) can be interpreted either as a simple peritectic reaction or as a disequilibrium texture due to

magmatic hybridization (Stimac and Pearce, 1992). As mentioned earlier, the contact of these andesites with overlying basaltic andesites as exposed on East Gros Ventre Butte suggests little or no temporal separation of the flows. This implies the two magmas were present simultaneously in the same zoned chamber.

The porphyritic dacites show abundant signs of plagioclase disequilibrium including sieve-textured cores, resorbtion, and fritting with clear (calcic?) overgrowths (Figures 8 &9). They also contain many fine-grained iron-oxide pseudomorphs after biotite (and possibly hornblende and/or olivine)(Figure 10), which elsewhere have been attributed to rapid dehydration (Nixon, 1988; Feeley and Sharp, 1996). Biotite with only partial iron-oxide replacement is seen in the dacites near Shadow Mountain (Figure 11). All these features fit remarkably well with Stimac and Pearce's (1992) model of mixing due to recharge of a chamber containing evolved magma by fresh input of more mafic magma.

There are many examples of volcanic fields, such as the Taos Plateau (McMillan and Dungan, 1986) and Medicine Lake Highlands (Gerlach and Grove,1982) where a magma mixing model successfully accounts for the within suite chemical variation. These cases, however, succeeded in fulfilling three major requirements for invoking magma mixing as a major cause of chemical variation: 1) identification (not postulation) of local end members; 2) demonstrating that these end members more or less bracket the ranges of variation for all elements with samples arranged in generally similar order along the

various mixing lines; and 3) showing that variation for each element falls reasonably close to a mixing line between the end members.

For the JHV, as a whole, the only reasonable candidates for mixing end members are the basalts and rhyolites of the YSP system. Not only are they (i.e. their Miocene counterparts) contemporaneous with the JHV, but they are also of fairly consistent geochemistry (Leeman, 1989) and are far and away the most abundant Neogene volcanic rocks in the region. Silica variation diagrams for many major and trace elements suggest the possibility of deriving the JHV by mixing YSP basalts and rhyolites; however, many elements such as Al_2O_3, MgO, Ni, Cr, and Sr suggest that YSP basalts are unlikely end members. Others such as Na_2O, Ba, and Nb tend to disqualify the YSP rhyolites. And certain isotopic ratios such as $^{143}Nd/^{144}Nd$ serve to preclude any direct relationship whatsoever between the YSP and JHV suites.

Selecting as end members the most mafic and most felsic JHV samples is an obvious option: however, plots of compatible versus incompatible elements (Figures 44, 45, & 46) produce curvilinear trends more readily explained by fractionation (or AFC) than by magma mixing. The plot of Al_2O_3 versus SiO_2 (Figure 13) clearly does not form a mixing line, and to interpret this trend as reflecting plagioclase accumulation would be contrary to petrographic evidence as well as the trend in Sr contents (Figure 28). Instead, this trend is strongly suggestive of a polybaric differentiation history. Trends seen in plots of Sr versus Rb (Figure 47), Rb versus Th (Figure 48), and K/Rb versus SiO_2 (Figure 49) are also best explained by a shift from lower-crustal to upper-crustal processes.

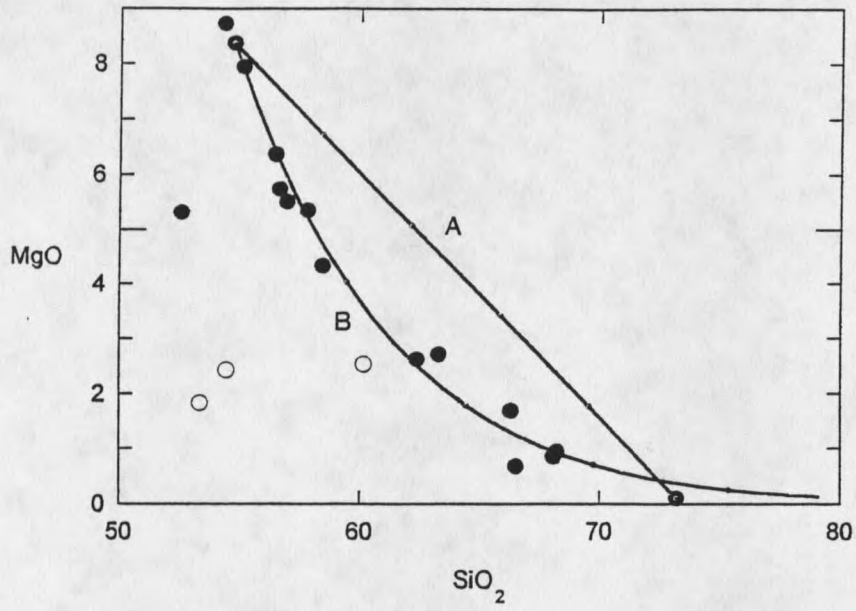

Figure 44. Plot of MgO vs. SiO_2 (wt. %). Line A is a mixing line between end members JH2 and JH13. Line B represents an AFC model between the same samples ($D_{MgO} = 4.0$, $D_{SiO2} = .75$, $r = .5$).

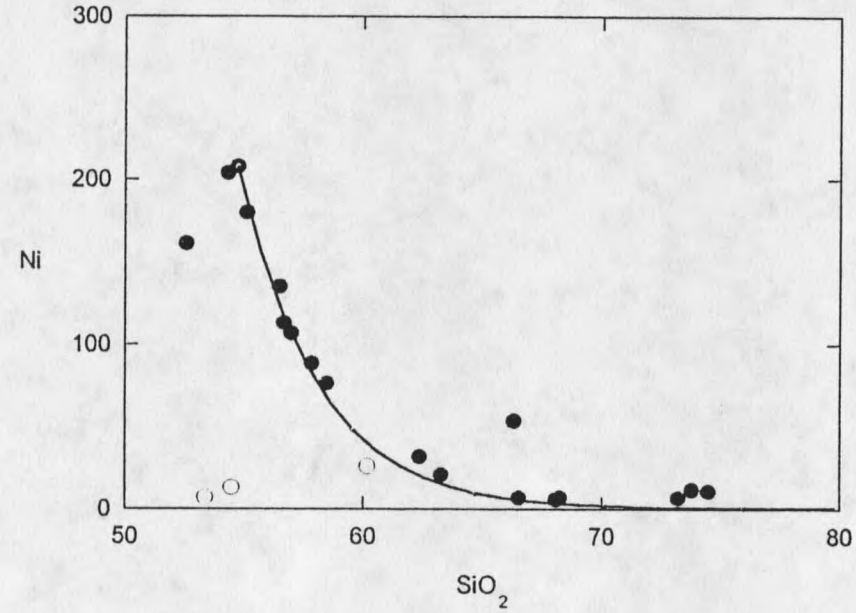

Figure 45. Plot of Ni vs. SiO_2 (ppm, wt. %). Line represents an AFC model between JH2 and JH13 ($D_{Ni} = 7.5$, $D_{SiO2} = .75$, $r = .5$).

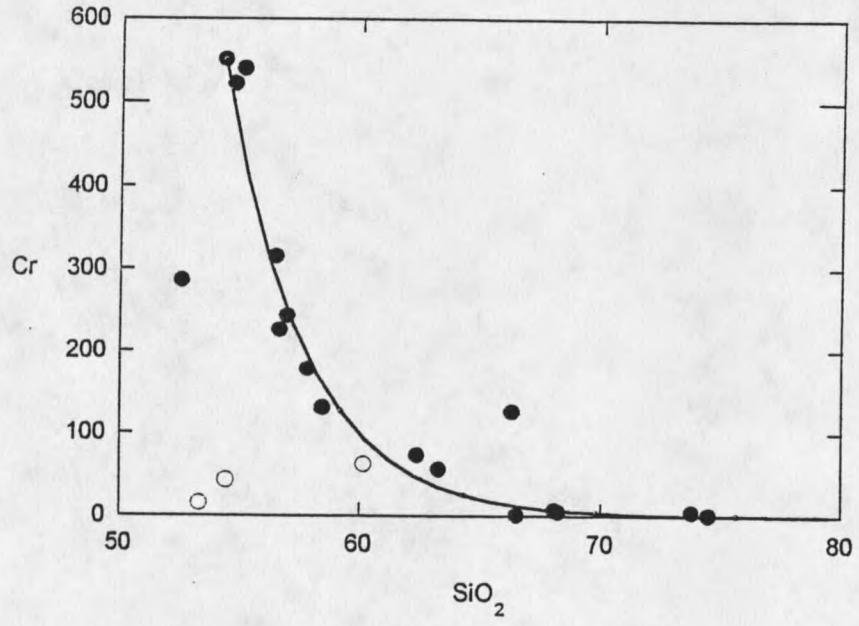

Figure 46. Plot of Cr vs. SiO_2 (ppm, wt. %). Line represents an AFC model between JH5 and JH13 (D_{Cr} = 7.5, D_{SiO2} = .75, r = .5).

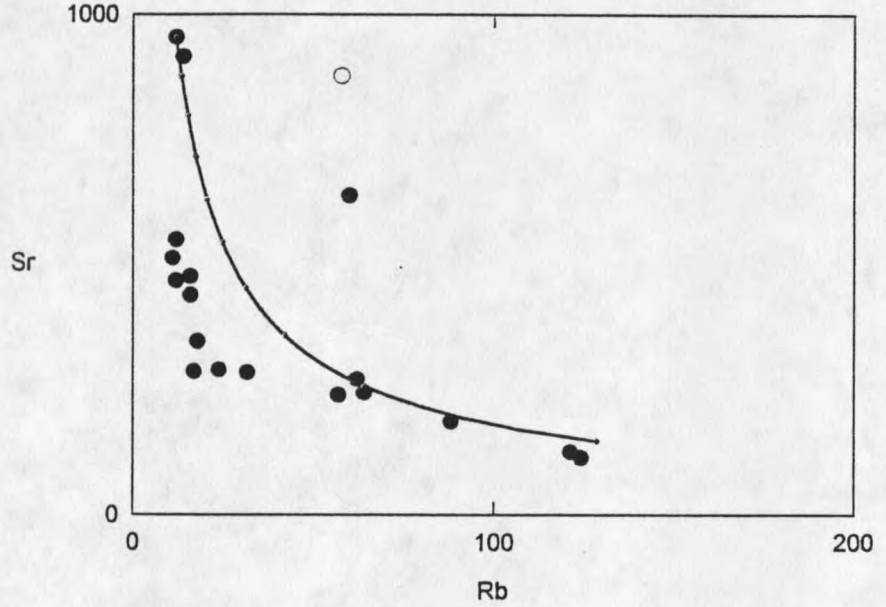

Figure 47. Plot of Sr vs. Rb (ppm). Line represents an AFC model between JH2 and JH13 (D_{Sr} = 1.8, D_{Rb} = .01, r = .01).

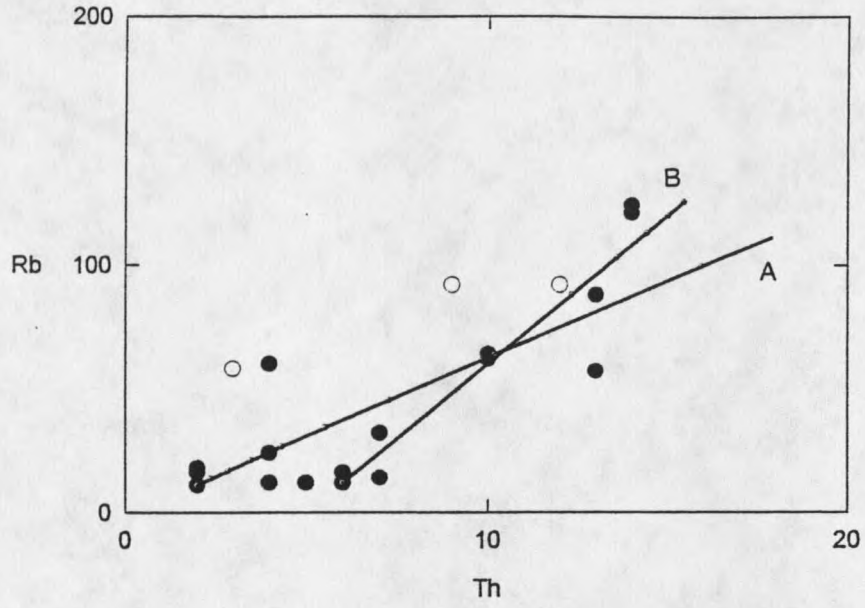

Figure 48. Plot of Rb vs. Th (ppm). Line A represents an AFC model between JH5 and JH13 (D_{Rb} = .07, D_{Th} = .01, r = .1). Line B represents an AFC model between 519 and JH13 (D_{Rb} = .07, D_{Th} = .01, r = 4.0).

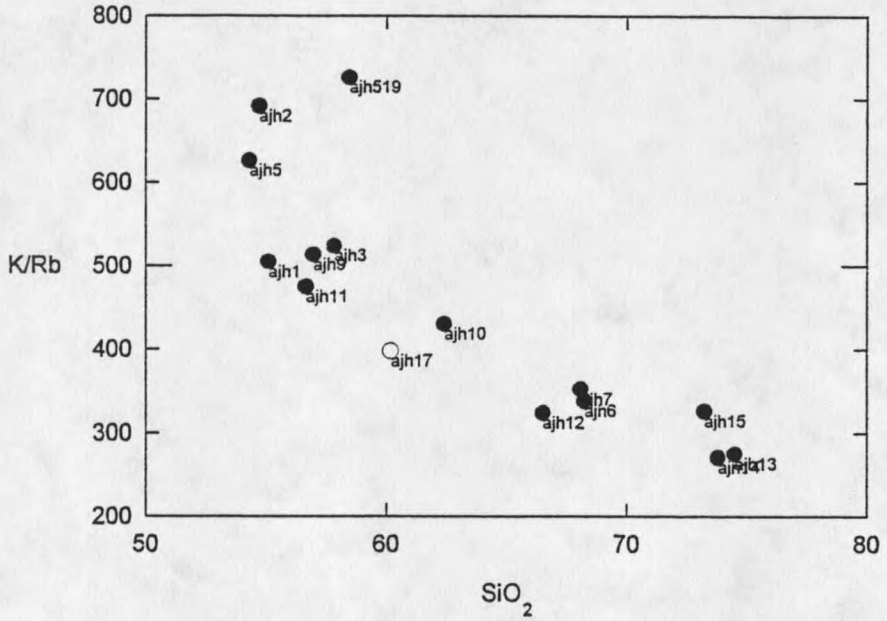

Figure 49. Plot of K/Rb vs. SiO_2 (ppm, wt. %).

Trends in Figures 46-48 suggest that upper-crustal differentiation is dominated by either AFC processes with relatively high r values (DePaolo, 1981) or perhaps magma mixing. Petrologic features characteristic of magma mixing, attributable to a recharge-mixing event, appear to be restricted to flows near the Gros Ventre Buttes. Injection of basaltic andesite at ~ 1200°C (two-pyroxene temperature, Lindsley, 1983) into the base of a chamber filled with 700°C dacite (one-pyroxene temperature, Lindsley, 1983) most likely also served to thermally destabilize the chamber leading to rapid devolatilization and eruption as suggested by Feeley and Sharp (1996).

Fractionation and Assimilation (AFC)

It is necessary for several reasons to consider these two processes together. First, the heat required for fusion of assimilated material is, except in the case of superheated magma, provided by the crystallization of the assimilating magma (DePaolo, 1981). Thus assimilation rarely occurs without some crystallization. Second, it is quite often impossible, when considering the variation in a particular element, to discriminate between the effects of the two processes. As magma ascends, changing conditions of pressure, temperature, oxygen fugacity, and water content lead to changes in the fractionating assemblage and even changes in the partition coefficients for individual fractionating phases. At the same time, different potential assimilants will be encountered by the magma as it ascends through the various levels of the lithosphere.

In order to determine the relative effects of fractionation and assimilation (a.k.a. contamination) responsible for the variation in a particular suite, ratios of similarly incompatible elements such as K and Rb (supposedly unaffected by fractionation) have been used (Davidson et al, 1988). Assuming the near identity of bulk distribution coefficients for K and Rb in a particular assemblage, the amount of change in K/Rb with increasing SiO_2 should be a rough measure of the amount of assimilation. The trend displayed in Figure 48 closely resembles that described by Davidson et al. (1988, Fig. 8c) as a combination of variable parental magma compositions subjected to open-system fractionation (AFC). Petrographically and considering only compatible element variation trends, the lower-crustal differentiation of the JHV appears explainable by olivine and clinopyroxene fractionation alone. This process, however, would not tend to alter K/Rb; nor would the fractionation of any observed phases. Cryptic fractionation of hornblende could produce such a trend (Gill, 1981), but is considered unlikely given the lack of Fe enrichment, lack of Y depletion, and high Na/K. In addition, the JHV sample with the highest K/Rb (Sample 519) is by no means the "least evolved" on the basis of compatible element content. All this suggests that, in addition to olivine fractionation, a significant amount of parental magma variability must exist in order to explain the variation seen in the more mafic JHV samples.

The possibility exists that the basaltic andesites might be cumulates deriving their chemical character from the accumulation of olivine phenocrysts by crystal settling or filter pressing from an originally more silicic magma. However, the high yield strength of

andesitic magmas precludes accumulation by crystal settling unless the chamber were entirely non-convecting (Gill, 1981). Given the small size of the JHV system, such a chamber would be more likely to solidify than to stratify, let alone erupt. Filter pressing, although feasible, does not account for the K/Rb variation which is better explained by parental magma variation.

The one unarguable sign of assimilation of crustal material is variation of isotopic ratios (unaffected by fractionation) with SiO_2 or the bulk elemental values. The JHV show clear signs of covariation for $^{87}Sr/^{86}Sr$, $^{208}Pb/^{204}Pb$, $^{207}Pb/^{204}Pb$, and, to a lesser extent, $^{206}Pb/^{204}Pb$. In this regard, they appear somewhat similar to the YSP but distinct from the Eocene volcanics, which show little or no correlation.

The variation of isotope ratios and SiO_2 seen in the JHV also appear to be restricted to the more silicic samples, suggesting that crustal contamination was important in the evolution of the high-silica andesites, dacites, and rhyolites but not in the low-silica and basaltic andesites. It is possible that the relatively high Sr contents in these samples (300-1000 ppm) could have served to buffer Sr isotope ratios against contaminant alteration; however, other workers in the region (e.g. Norman and Leeman, 1989) have not considered even Sr contents >1000 ppm adequate to prevent such alteration in basalts.

It should be noted that the degree to which the isotope ratios of a magma are affected by contamination is dependent on two things: the relative concentrations of that

element in the end members and degree of difference in isotope ratio between the end members. For example, the relatively low Pb and Sr contents of the JHV make their isotope ratios more susceptible to alteration by contamination than the Eocene suites. On the other hand, the lack of correlation in the JHV between $^{143}Nd/^{144}Nd$ and silica may be due to higher neodymium levels in the magma, lower levels in the assimilant, similar $^{143}Nd/^{144}Nd$ values in the two, or some combination of the three. Thus absence of covariation need not mean absence of contamination.

The lack of covariation of isotope ratios and silica in the more mafic JHV samples, given the evidence for crustal assimilation in the rest of the suite, suggests that the evolution of the lower SiO_2 range was affected much less by crustal contamination than by olivine fractionation and variable parental magma composition, as outlined earlier. Augite and titanomagnetite fractionation played a lesser role which continued into the more siliceous samples, as suggested by the relatively smooth trends seen in plots of Fe, Ti, and Sc versus SiO_2. This assemblage has been interpreted as "high-pressure" as opposed to a plagioclase-dominated "low-pressure" assemblage (Leeman et al., 1990). Analysis using Pearce element ratios (Russell and Nicholls, 1988), suggests that variation seen in the more mafic members of the JHV can be explained by the fractionation of olivine, clinopyroxene, and plagioclase which appears to take place in co-genetic groups of comagmatic samples (Figure 50). The variation seen in the more silicic samples (Figure 51) must be the result of significant crustal assimilation.

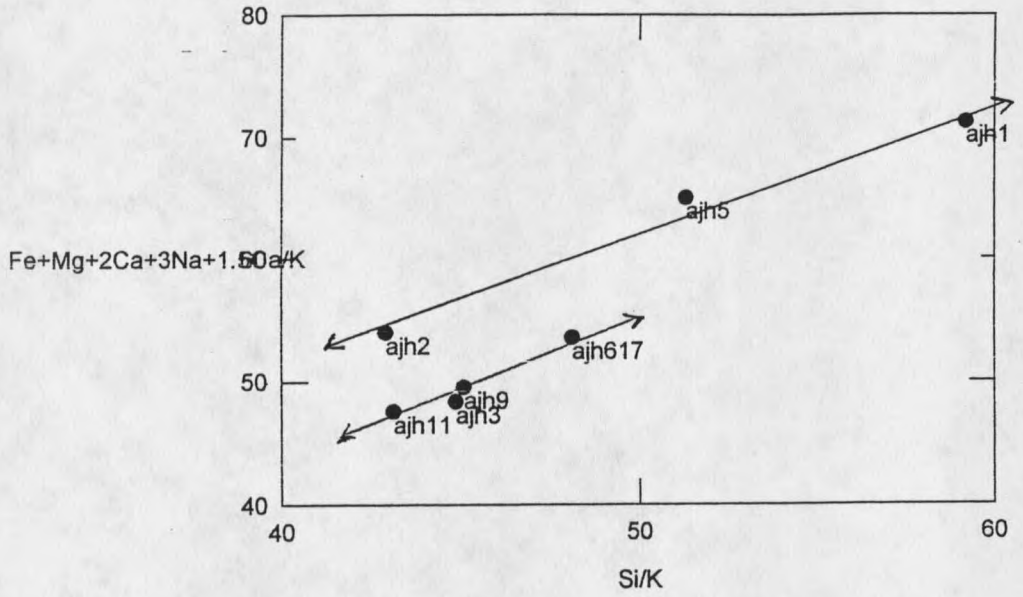

Figure 50. Plot of Pearce element ratios for JHV andesites and basaltic andesites. Lines represent slopes of 1.0, indicative of fractionation of Ol + Cpx + Pl.

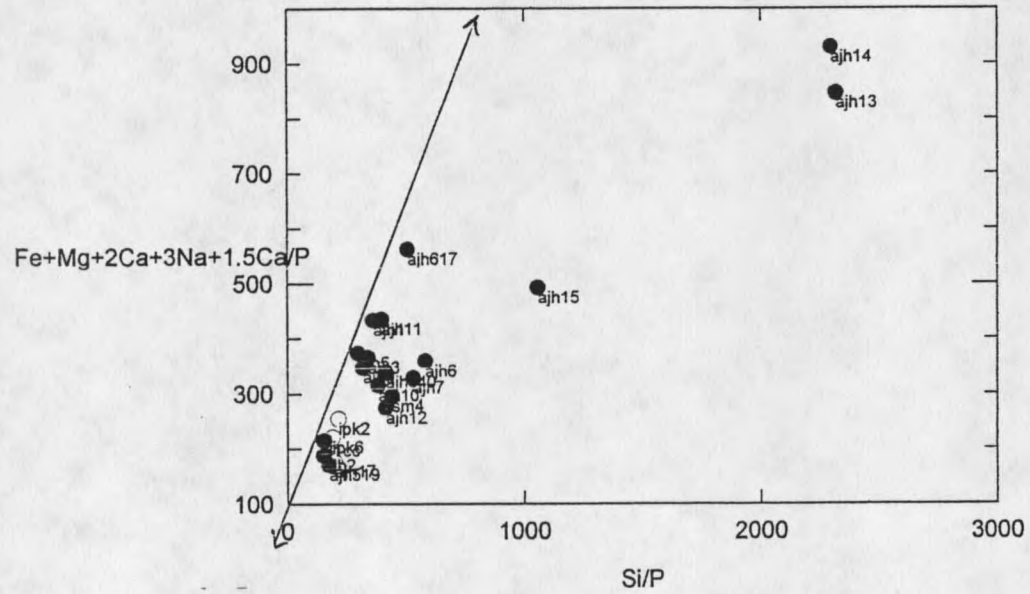

Figure 51. Plot of Pearce element ratios for the JHV. Line represent a slope of 1.0, indicative of fractionation of Ol + Cpx + Pl.

Such evidence for plagioclase involvement in the evolution of the JHV andesites and basaltic andesites appears contrary to the petrographic and trace element evidence mentioned earlier, which suggests that some suppression of plagioclase fractionation did occur. Such suppression can occur due to elevated temperature and pressure but can also be achieved by increased water content, which reduces the stability of plagioclase > pyroxene > olivine (Gill, 1981). That no hydrous phases such as hornblende are present may be due to only moderate water content (2-4 % by weight) or perhaps due to low alkali content (especially K) and thus a higher $aSiO_2$, which would tend to destabilize the relatively low-silica hornblende even at fairly high pH_2O.

Thus the shift to plagioclase-dominated fractionation may have occurred in response to a decrease in pH_2O and/or a decrease in pressure caused by ascent to a mid- to shallow-crustal magma chamber, where the aforementioned contamination processes could also affect the fractionating assemblage by changing bulk chemistry.

Source Rocks and their History

Among the geochemical features most commonly regarded as representative of an unfractionated mantle-derived melt are high MgO, Mg* (100x Mg/ (Mg + Fe)), Ni, and Cr levels. These reflect the high partition coefficient which olivine has for these elements. Any fractionation of a melt originally in equilibrium with mantle peridotite would lower the levels of these elements due to removal of olivine.

Based on a reasonably extensive examination of published analyses of andesites (sensu latu) in the world, the JHV basaltic andesites appear to equal or exceed the Mg, Ni, and Cr values of all other suites yet studied (with the possible exception of some samples from Bonin and the Aleutians). And with Mg* values approaching 70, a mantle origin for the JHV would appear to be reasonable. However, ratios such as K/Zr (~60) and Nb/Th (~2) are much more suggestive of a crustal origin (Norman and Leeman, 1989).

A case could be made for some degree of fractionation from an even more primitive initial melt, but this would require an abnormally high degree of partial melting and/or an unreasonably picritic source rock. It appears more likely that the JHV basaltic andesites represent relatively unfractionated primary melts of a combination of lithospheric mantle and lower crustal rocks.

Clues as to the degree of partial melting which produced the initial melt for the JHV are available by comparison with the geochemistry of the Eocene volcanics. These suites generally share the "primitive" elevated compatible element values of the JHV; however, they vary greatly and generally exceed the JHV in most incompatible element contents (i.e.K, Na, Ba, Rb, Sr, Pb). While the acknowledged heterogeneity of this region's mantle and lower crustal source rocks (to be considered in the next section) may quite well be the dominant reason for this variation, the possible role of a slightly higher degree of partial melting for the JHV initial melt cannot be totally dismissed. In addition, the suppression of plagioclase fractionation, seen in the JHV but not in the Eocene volcanic rocks, suggests that the former may also have had initially higher water content,

which, by lowering solidus temperatures, may have promoted a higher degree of melting than that seen in the Eocene suites.

Numerous authors have noted that the isotope systematics for volcanic rocks in this region indicate that at least some portion of the mantle source rocks has been isolated from the main mantle reservoir for a considerable length of time (Leeman, 1982a; Hildreth et al., 1991; Meen and Eggler, 1987; Dudas, 1991). The more mafic JHV samples appear to share the two-lead isochron of the HABS suite, which according to Meen and Eggler yields an age of 3.8 Ga. As noted by the aforementioned authors, it is often quite difficult to distinguish between the isotopic features of the apparently Archaean lithospheric mantle and those of the equally ancient crust. This 3.8 GA component would appear to represent the lower-crustal and/or lithospheric mantle source rocks for the JHV initial melts. The more silicic JHV samples appear to lie with the YSP suite on a slightly less steep isochron yielding an age of 2.9 Ga. This could be interpreted as the age of the upper-crustal contaminant responsible for the bulk of the chemical variation seen in the JHV dacites and rhyolites. The silicic JHV samples resemble the YSP rhyolites in contents of many major elements and in isotope ratios such as $^{87}Sr/^{86}Sr$, $^{207}Pb/^{204}Pb$, and $^{206}Pb/^{204}Pb$. However, the silicic JHV rocks have distinctly lower values for K, Rb, La, Ce, Th, Y, Zr, and $^{143}Nd/^{144}Nd$ than the YSP rhyolites and distinctly higher values for Na, Ba, Ba/Nb, and $^{208}Pb/^{204}Pb$. These differences may reflect either the heterogeneity of upper-crustal contaminants or differences imposed at the source that were unaffected by the significant assimilation of upper crustal material which apparently took place.

Possible candidates for lower-crustal source rocks for the JHV basaltic andesites are suggested by analyses of xenoliths entrained in Snake River Plain basalts (Leeman et al., 1985). Figures 52-55 compare isotope ratios for the JHV samples and these lower-crustal xenoliths, along with metasediments from the Albion Range, gneisses and metagabbros from the Teton Range (Reed and Zartman, 1973), and Archean rocks from the Beartooth Range (Wooden and Mueller, 1988). The JHV samples consistently plot near xenoliths from the Spencer-Kilgore area, which lies ~130 km to the northwest of the JHV study area. These norite-enderbite-charnockites also share with the JHV basaltic andesites a similar silica range, high MgO, and low K_2O; however, their FeO levels are significantly higher than those of the JHV rocks. It would appear that this lower-crustal component may have been more important than the lithospheric mantle component in the genesis of the JHV. It is, however, highly significant that the YSP rhyolites, ostensibly produced by anatexis of such crustal material as is seen entrained in YSP basalts, would show such vastly different $^{143}Nd/^{144}Nd$ values from both these xenoliths and the JHV.

Isotope ratios suggest that both mantle sources and crustal contaminants are highly heterogeneous in this region. These have been interpreted as the time-integrated products of numerous episodes of enrichment and depletion (Dudas, 1991; Hooper and Hawkesworth, 1993), usually associated with arc magmatism during accretionary assembling of the Wyoming craton during the Pre-Cambrian and the rest of western North America during the Phanerozoic. Such magmatism would, of course, tend to deplete source areas in incompatible elements. At the same time, metasomatic hydrous fluxes

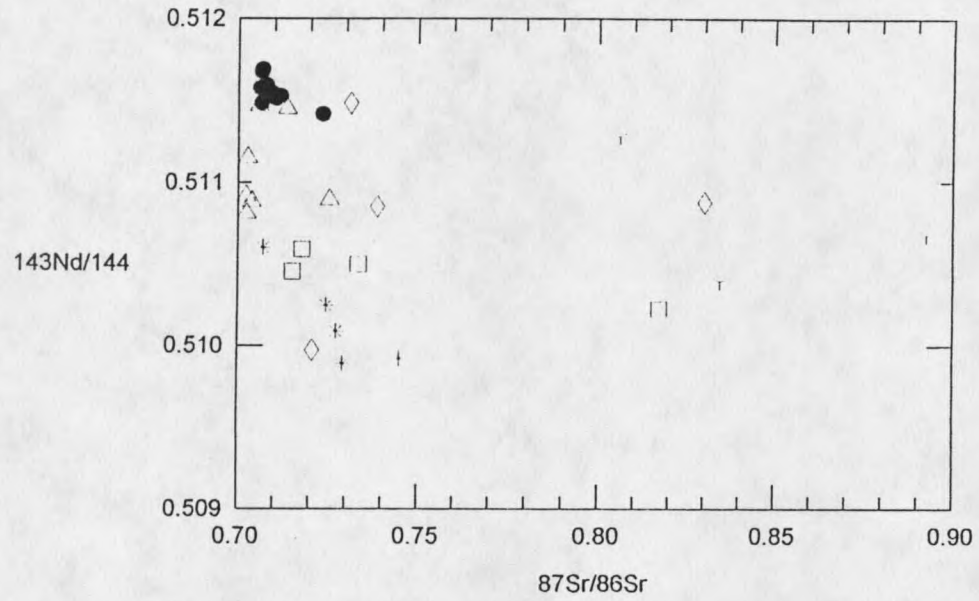

Figure 52. Plot of $^{143}Nd/^{144}Nd$ vs. $^{87}Sr/^{86}Sr$. Solid circles are JHV samples. Spencer-Kilgore xenoliths are hollow triangles, Craters of the Moon xenoliths are hollow squares, Square Mountain xenoliths are hollow diamonds, and Albion Range metasediments are "Y"s (Leeman et al., 1985). Beartooth samples (Wooden and Mueller, 1988) are asterisks. Teton Range samples (Reed and Zartman, 1973) are crosses.

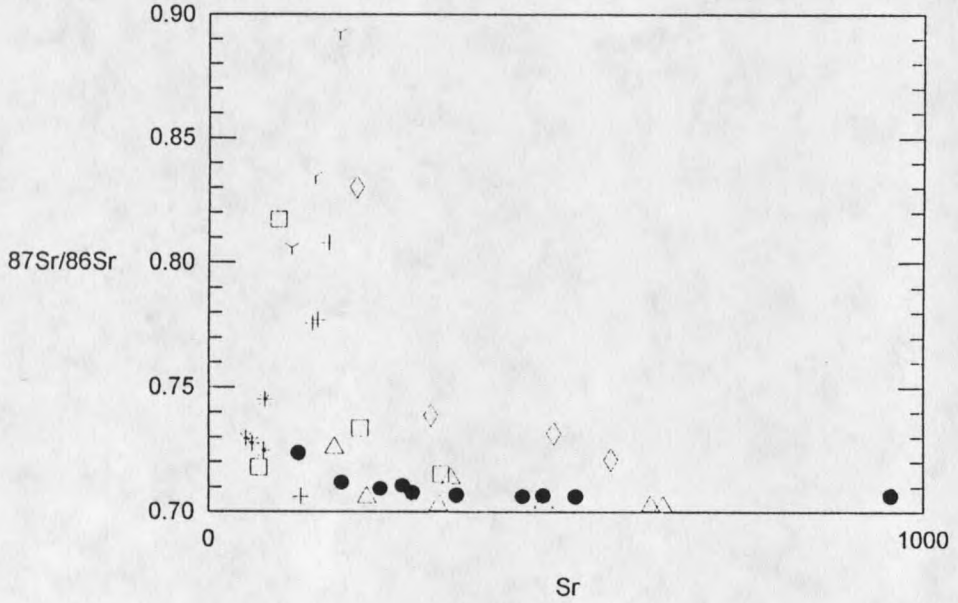

Figure 53. Plot of $^{87}Sr/^{86}Sr$ vs. Sr (ppm). Symbols as in Figure 52.

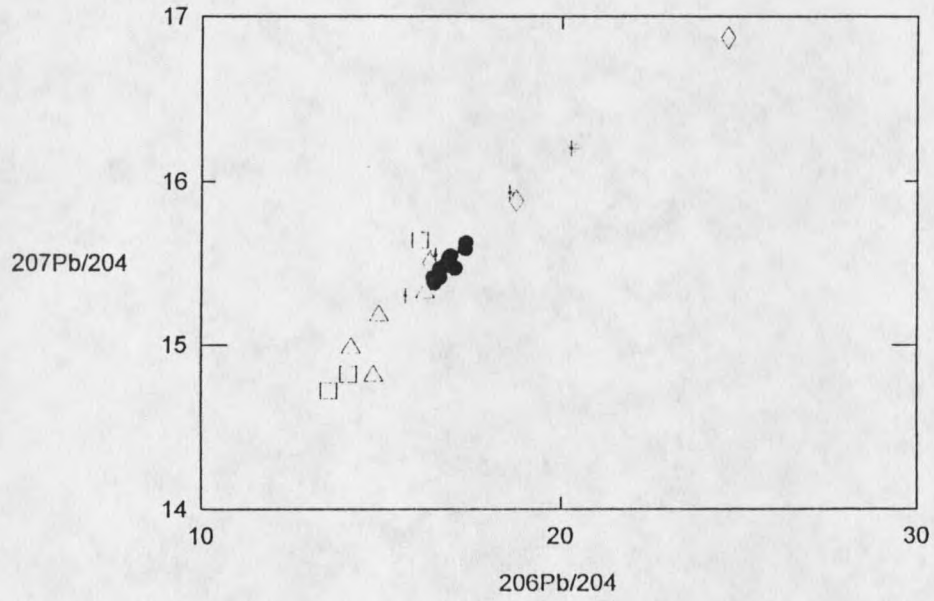

Figure 54. Plot of $^{207}Pb/^{204}Pb$ vs. $^{206}Pb/^{204}Pb$. Symbols as in Figure 52.

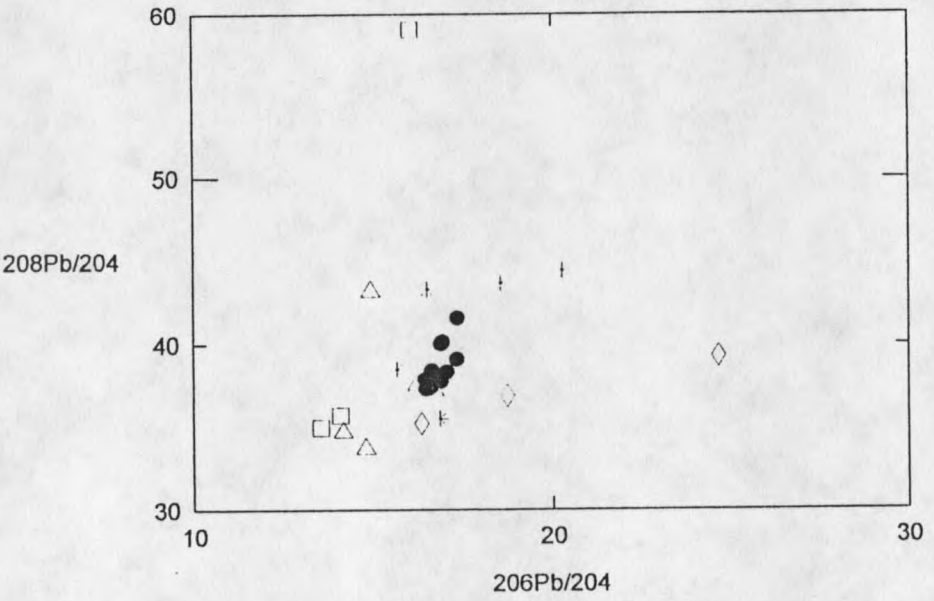

Figure 55. Plot of $^{208}Pb/^{204}Pb$ vs. $^{206}Pb/^{204}Pb$. Symbols as in Figure 52.

from slab-dewatering are postulated to have produced veins in the mantle enriched in some of these same elements. Heterogeneity in mantle-derived melts may therefore be due to the melting of varying amounts of the enriched vein material during later magmatic episodes. Unfortunately, this scenario ignores a major potential source of heterogeneity - that of varying amounts of input from asthenospheric mantle.

As set forth in the introduction, the YSP volcanics show indications of substantial asthenospheric input, and nowhere is the effect of this input more clearly shown than in their high $^{143}Nd/^{144}Nd$ values. The substantially lower Nd isotopic ratios of the JHV and HABS indicate source rocks are, for the most part, restricted to the lithosphere. Other indicators of asthenospheric mantle plume activity such as high niobium (Brandon and Goles, 1988) also tend to support this interpretation. Although bulk neodymium values are not available for the JHV, values for the YSP, HATS, and HABS suites show a distinct lack of correlation between neodymium and $^{143}Nd/^{144}Nd$. This suggests that asthenospheric and lithospheric bulk values are probably similar; while the ratios must differ greatly, making high $^{143}Nd/^{144}Nd$, in this region, a fairly sensitive indicator for even minor amounts of asthenospheric input. (Note that the HATS suite appears to occupy an intermediate position between the YSP and HABS, suggesting some intermediate amount of deeper mantle input.)

Processes Responsible for Initial Melting

It is common for many petrographic explanations either to stop at this point or skip directly to consideration of tectonic setting, as if magmatism could somehow be summoned at will. The degree to which extensional decompression, crustal thickening, hot mantle input, or slab-derived hydrous fluxes are responsible for melting has profound implications for any tectono-magmatic interpretation. Yet, many authors (e.g. Norman and Mertzman, 1991) having established the antiquity of the subduction signature in the volcanic rocks in question, wrongly conclude that a slab-derived hydrous flux melting mechanism (whose geochemical effects would of course be indistinguishable from the effects of the earlier episodes) could thus be disqualified as a potential cause of initial melting. It is instead important to examine thoroughly each of the various melting mechanisms and carefully assess whether each is capable of generating the observed magmas given the particular physical and chemical setting involved.

Extensional Decompression Melting

The eruption of the JHV was approximately coeval with the onset of extensional tectonism in southern Jackson Hole, making melting by decompression an attractive option. However, based on a cross-section of southern Jackson Hole by Lamerson (1983), a stretching factor (β) of at most 1.4 is apparent. Given a mechanical boundary layer of 130 km, such a low stretching factor would be unlikely to generate a melt even

given a potential temperature of 1480° C (McKenzie and Bickle, 1988). Nor could the presence of hydrous minerals from earlier episodes of metasomatism serve to depress the solidus. As such, depression requires water to exist as a separate phase and the dehydration of hydrous minerals such as amphibole requires an increase not a decrease in pressure. Moreover, as set forth in the introduction, it is not clear that non-convecting lithospheric mantle, although ductile, would respond to extension in the same fashion as convecting asthenospheric material. Rather than upwelling, decompressing, and melting, the lithospheric mantle would perhaps be more likely merely to attenuate and allow these processes to occur in the underlying asthenosphere. Lachenbruch and Sass (1978) suggested that lithospheric extension in the western United States is most likely to have occurred by distributed asthenospheric intrusion, making incorporation of this dike material into resulting lithospheric melts highly probable. Lipman (1992) has pointed out several examples in the western United States where crustal magmatism can be shown to be "the unambiguous cause of intense extension." Thus, the coexistence of extension and magmatism may have little petrogenetic significance, let alone automatically indicate decompression melting. Finally, other Miocene normal faulting in the region (i.e. in the Albion, Caribou, and Centennial ranges, among others) produced no such volcanism, suggesting that the JHV melting must have had a much more localized cause.

Crustal Thickening

Melting by this method generally implies volcanism concurrent with or shortly after the compressional episode responsible for the thickening, certainly not 40-50 my. later as

would be the case for the JHV. In addition, this process is more applicable to felsic melts derived from crustal material depressed beneath the isotherm of its relatively lower melting point, and not the high-MgO JHV basaltic andesites, whose source would be much more refractory. Nor is there geophysical evidence for a thickened crust, which maintains a thickness of 40-42 km throughout the region (Leeman, 1989). Finally, the effects of this mechanism would also be expected to be much more regional in extent than the single JHV occurrence.

Injection of Hot Mantle

If high $^{143}Nd/^{144}Nd$ ratios can be taken as a sign of asthenospheric mantle input, it appears that in the case of the JHV little admixture of asthenospheric to lithospheric mantle took place. However, the possibility should be considered that melting of the latter by the former occurred without admixture. Under this scenario, heat flow from the Yellowstone mantle plume caused the localized melting of lithospheric mantle and lower crust particularly rich in less refractory metasomatically enriched veins with slab-dewatering signatures (e.g. high Ba/Nb) derived from much earlier subduction events.

In the case of the JHV, this scenario is unlikely for a number of reasons:

1) With their high levels of compatible and low levels of many incompatible elements, the JHV basaltic andesites more closely resemble depleted (and more refractory) rather than metasomatically enriched lithosphere, yet they consistently show high levels of Ba/Nb.

2) Given a convective heat flow mechanism (i.e. intrusion of the lithosphere by asthenospheric melts), no large viscosity and density contrast would be present to deter the mixing of the asthenospheric melt (most likely basaltic) and the lithospheric basaltic andesite melt, unlike with the YSP basalts and rhyolites. If this melting mechanism is correct, mixing would seem inevitable, yet the $^{143}Nd/^{144}Nd$ ratios indicate that essentially no mixing occurred in the JHV but that significant mixing did occur in the YSP. It is of course quite possible that the differences between the JHV and YSP derive not from different melting mechanisms but from differences in their underlying crust and the partial melts derived therefrom, such that the asthenopheric isotopic signature was swamped by crustal input in the case of the JHV but not in the case of theYSP. Given the fact that many YSP lower crustal xenoliths closely resemble JHV basaltic andesites, support for such major crustal heterogeneity over such relatively short distances would appear minimal. However, without much more rigorous quantitative modelling of these processes than has been attempted here, this alternative hypothesis can in no way be discounted.

3) At 8 Ma., the main focus of YSP mantle plume activity was some 150-200 km to the west of Jackson Hole. Conductive heat flow within the lithosphere is feasible up to 50 km but requires time periods from 10 to 100 my. (Anders et al., 1989). The latent heat of fusion required to melt even preheated lithosphere ($\sim 1260\ MW/m^3$) would require the conductive medium to be very near its own solidus. Heat flowing over such a distance and melting the relatively refractory JHV source rocks therefore seems improbable, especially given the absence of similar melting events more proximal to the plume. The earlier

spreading of an expanded plume head may remove some of this heat transport problem; however, the problem remains of the uniqueness of the JHV given the regional nature of this postulated plume head event. Once again, one could postulate that the lithosphere beneath Jackson Hole was uniquely enriched in hydrous fluids compared to the rest of the region, such that localized melting took place in this area of depressed liquidus temperatures but not in the surrounding anhydrous lithosphere. This enrichment may have occurred during the episode of subduction postulated to have affected the entire region during the Eocene, but why it would have been apparently restricted to only one locality is unclear.

Slab-derived Hydrous Fluxes

The most commonly used geochemical discriminant for subduction-related volcanism (high LILE/HFSE such as Ba/Nb) strongly supports the role of this mechanism in the derivation of the JHV and clearly distinguishes them from the YSP (Figure 56). Although this characteristic is an extremely consistent feature of arc volcanism, it is by no means completely understood or unique to subduction environments (Arculus, 1987). High LILE/HFSE ratios are therefore here considered as only permissive evidence of subducted slab involvement. More definitive evidence lies in the other, more physical attributes of slab-derived hydrous melting which commend it as the cause of JHV magmatism where the other mechanisms have failed.

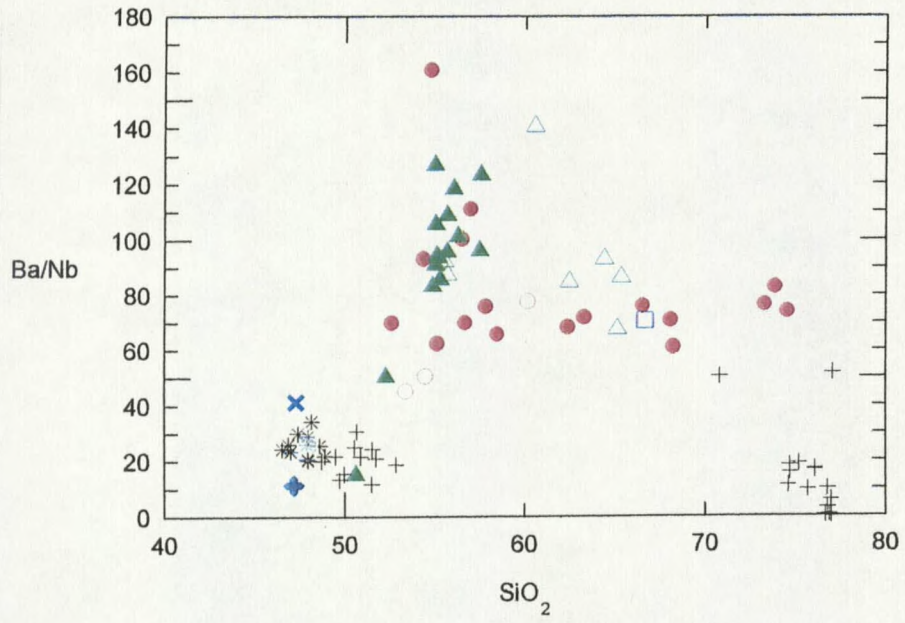

Figure 56. Plot of Ba/Nb (ppm) vs. SiO_2. Symbols as in Figure 35.

1) The uniqueness and highly localized nature of the JHV requires either that their source rocks be unique in this region or that the melting mechanism be locally focused and of unique occurrence. The descent and dewatering of an isolated fragment of subducted oceanic slab could clearly satisfy the latter requirement.

2) Slab-dewatering at the depths where arc magmatic melts are produced (80 to 120 km.) is the result of the breakdown of amphiboles rather than chlorites, which dehydrate at much shallower levels (Gill, 1981). The upper limit of amphibole stability in water-saturated tholeiitic basalt (oceanic crust) is subhorizontal in P-T space (Green, 1982), making this reaction pressure rather than temperature-dependent. This removes

the necessity for special heat flow conditions in the genesis of the JHV magmas. The Yellowstone mantle plume head may have served to raise slightly the temperature of the entire region but would not have produced localized effects. An isolated slab fragment buoyed and carried eastward by the spreading plume head would have been heated , but it would not have dewatered until it encountered the lithospheric root of the Wyoming craton, the western boundary of which is interpreted to coincide with the Idaho-Wyoming border (Blackstone, 1977). Here it would be driven to deeper levels where increased pressure would have led to amphibole breakdown and the release of hydrous fluids. As the temperature at the base of the crust at this time could be expected to be in the range of 1000° to 1200°C (Brott et al., 1981), introduction of water could easily trigger melting. The absence of an overlying convecting mantle wedge need not pose a problem in that no replenishment of the wedge is required for such a short-lived magmatic event and the geochemical and temperature characteristics of both slab and lithosphere, in this case, are not necessarily analogous to a typical arc magmatic system.

3) In the absence of high heat input, only the influx of locally high water concentrations could lead to the higher degrees of partial melting in the JHV basaltic andesites suggested by the high contents of compatible and low contents of many incompatible elements. The "primitive" yet siliceous nature of these rocks reflects the tendency of water to produce magmas enriched in silica (Wyllie, 1982). The stabilization of olivine and suppression of plagioclase fractionation seen in these samples is further evidence of elevated water content. The low volatile contents (as measured by loss on

ignition values) of the JHV samples are post-eruptive and cannot be taken as measures of pre-eruptive, let alone mantle level, water contents.

It appears that a slab-derived hydrous flux melting mechanism can explain the features of the JHV and reconcile them with their spatial and temporal setting. It now remains to examine how a fragment of subducted oceanic slab could have traveled the 1200 km from the Miocene subduction zone off the Pacific Northwest coast to western Wyoming.

Tectonic Setting

The concept of shallow subduction is neither new nor merely speculative. As described in the introduction, shallow subduction of the Farallon Plate in the late Cretaceous and early Tertiary is widely credited with facilitating the shortening associated with the Sevier and Laramide orogenies in the western United States. Seismic tomography has detected slab-like structures in the mantle beneath the North American mid-continent (Grand, 1987). Two points must be made clear regarding the proposed slab involvement in the genesis of the JHV: first, this event is in no way connected with the earlier Laramide episode of shallow subduction; and second, the JHV involves a slab fragment totally detached from its original trench and subduction zone.

There is little doubt that an actively convergent plate margin has been present near the coast of northern California, Oregon, and Washington for most of the Cenozoic. Although reorganization of the Farallon and Kula Plates during this period makes

paleoconvergence vectors somewhat unclear (Engebretson et al., 1985), it appears that arc magmatism was strongly episodic and somewhat synchronized with volcanic cycles elsewhere on the Pacific Rim (McBirney et al., 1974; Armstrong, 1975).

One major hiatus appears associated with the other major Cenozoic magmatic event(s) in the Pacific Northwest, the eruption of the Columbia River Basalts (17-12 Ma.) and inception of Snake River Plain volcanism (i.e. mantle plume activity) in southeast Oregon (17 Ma.). Alt and Hyndman (1981,1995) note the abrupt cessation of volcanism in the Western Cascades at ~20 Ma with a resumption of activity at ~15Ma. Priest (1990) placed this non-volcanic period between early and late Western Cascade volcanic episodes (~18 to ~14 Ma.). Beeson and Tolan (1990) noted the absence of active volcanic centers in the Columbia transarc lowland from ~17 to ~14.5 Ma. Hart and Carlson (1987) identified a regional hiatus in volcanic activity from ~20 to ~17 Ma. And Geist and Richards (1993) pointed out the lack of Cascade tephra in the interbeds of the main phase Columbia River basalts.

With regard to the YSP mantle plume, some question remains as to its actual time and place of inception and therefore whether a broad plume head or only a narrowly-focused plume tail was present beneath the North American Plate. Duncan (1982), citing the ages of accreted seamounts on the Oregon coast, suggested the presence of a plume astride a spreading ridge off the coast, over which the coast would have drifted at ~35 Ma. However, the termination of the YSP "track" with the McDermitt volcanic field with no

signs of plume-related volcanism to the west led Draper (1991) and Pierce and Morgan (1992) to suggest that the plume first arose beneath southeast Oregon.

The geochemistry of the Columbia River Basalts has been interpreted as reflecting varying amounts of shallower mantle entrained with material from deeper sources in the evolving plume head (Campbell and Griffiths, 1990); whereas the Snake River Plain magmas would represent the unmodified deep mantle material of the plume tail. Numerous authors (Hart, 1985; Church, 1985; Hart and Carlson, 1987; Goles et al., 1989; Norman and Leeman, 1989; and Hooper and Hawkesworth, 1993) have also identified a subduction-related component in the geochemistry of the Columbia River Basalts and coeval neighboring volcanic rocks, which most have ascribed to much earlier episodes of subduction-related metasomatic enrichment.

A possible scenario relating the Columbia River Basalts to cessation of arc magmatism without the involvement of a mantle plume was proposed by Alt and Hyndman (1981) and is shown in Figure 57 compared to a model including the Snake River Plain and a mantle plume, proposed by Geist and Richards (1993). The former suggests that a slab window opening behind a self-detaching slab could somehow induce the upwelling of the monumental volumes of the Columbia River Basalts, bolide impacts (Alt et al., 1988) notwithstanding. The latter theory suggests that prior to slab detachment caused by the upwelling mantle plume, the slab served to deflect the plume head northward from Oregon to southern Washington, where it erupted as the Columbia River Basalts. After slab detachment, the undeflected plume tail began its more narrowly focused track towards

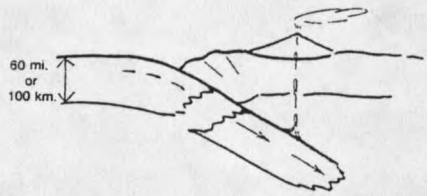

1) The descending slab breaks free and begins to sink more rapidly.

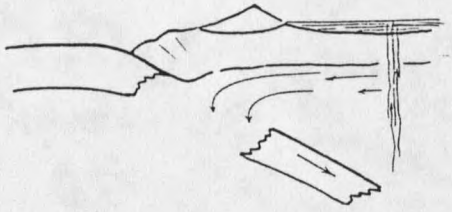

2) Activity ceases in the western Cascades because there is no longer a sinking slab of seafloor beneath them and material flows westward beneath Oregon to fill behind the sinking slab. Flood basalts erupt in central and eastern Oregon.

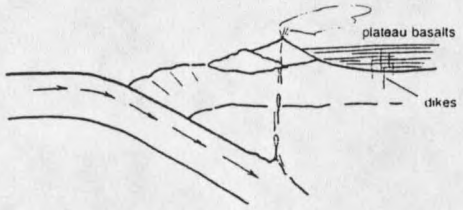

3) A new slab of seafloor descends to the level beneath the western Cascades to put them back in business; slowing westward movement of rock beneath Oregon halts the flood basalt eruptions.

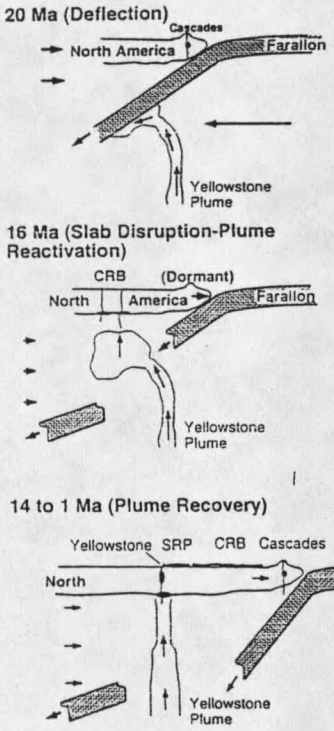

Figure 2. Schematic representation of proposed model as viewed in cross section from northwest. Top: At 20 Ma, Yellowstone plume was shielded from surface and deflected northnortheast by Farallon plate. Middle: At 16 Ma, Farallon plate allowed plume to pass through, and deflected part rose to create Columbia River Basalt. Bottom: Most recently, plume is only slightly deflected by slow (1 cm/yr) motion of North American plate. JdF—Juan de Fuca plate. Other abbreviations as in Figure 1.

Figure 57. Models relating Cascade volcanism, Columbia River Basalt eruption, and the Yellowstone mantle plume. At left, from Alt and Hyndman (1981). At right, from Geist and Richards (1993).

Yellowstone, as the North American Plate drifted to the southwest. The subduction-related geochemical component noted above could reflect the incorporation of portions of the slab into the plume-derived magmas as they pierce the previously intact subducted plate. Seismic tomography of the present-day Juan de Fuca plate beneath southern

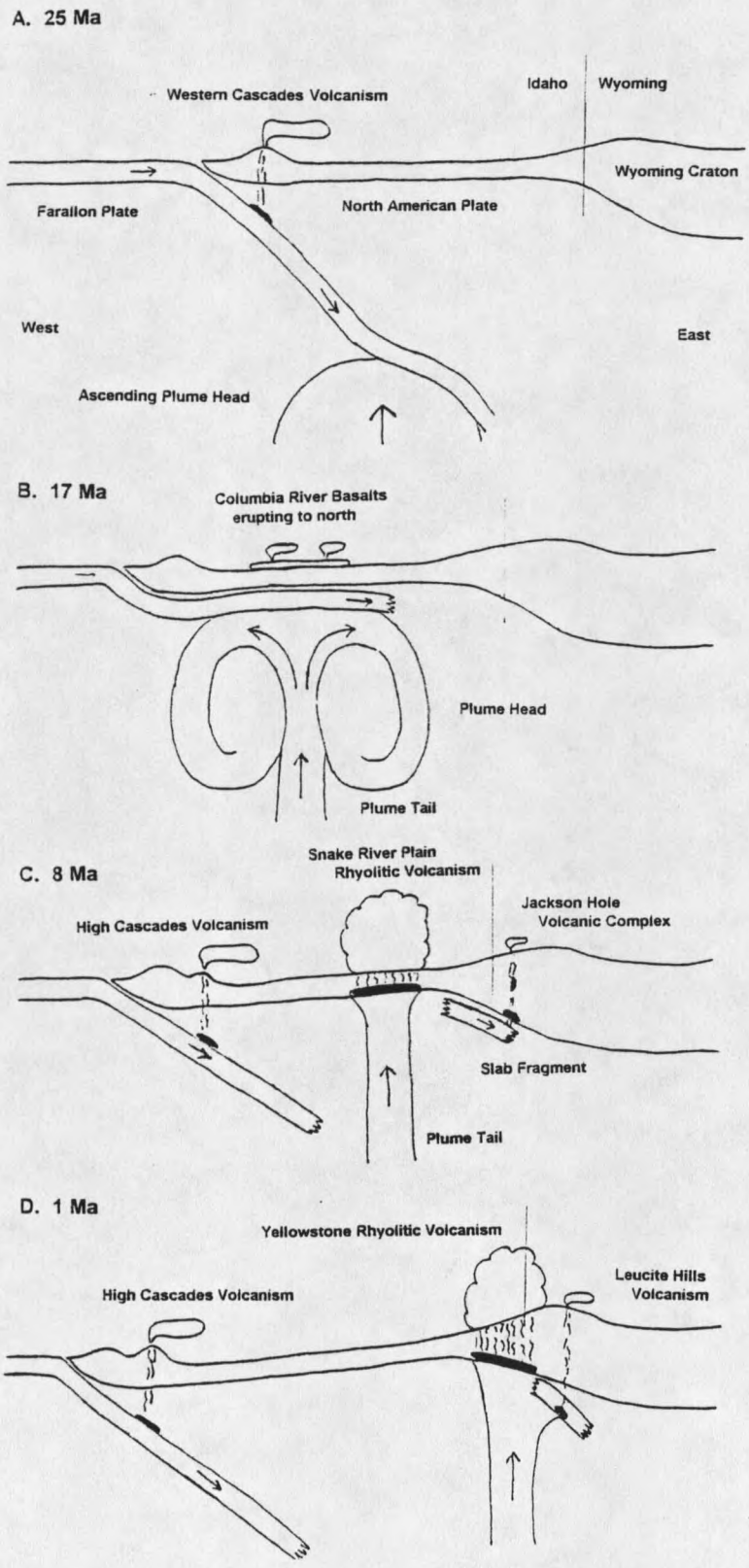
A. 25 Ma
Western Cascades Volcanism
Idaho
Wyoming
Wyoming Craton
Farallon Plate
North American Plate
West
East
Ascending Plume Head
B. 17 Ma
Columbia River Basalts
erupting to north
Plume Head
Plume Tail
C. 8 Ma
Snake River Plain
Rhyolitic Volcanism
Jackson Hole
Volcanic Complex
High Cascades Volcanism
Slab Fragment
Plume Tail
D. 1 Ma
Yellowstone Rhyolitic Volcanism
Leucite Hills
Volcanism
High Cascades Volcanism

Figure 58.

Figure 58. Cartoon depicting the sequence and relationship of magmatic and tectonic events in the northwestern United States during the late Cenozoic. A. At 25 Ma, the ascending mantle plume head begins to deflect the descending slab. B. At 17 Ma, the plume head has buoyed the subducted slab, preventing dewatering and thus Cascade volcanism. The slab serves to deflect plume-derived melts to the north, producing the voluminous Columbia River Basalts. C. At 8 Ma, the plume has pierced the slab, isolating a fragment which then descends against the cratonic lithospheric root and dewaters, producing the JHV magmas. The plume tail causes the more focused Snake River Plain volcanism. Subduction-related volcanism resumes in the Cascades. D. At 1 Ma, The plume tail causes rhyolitic volcanism in Yellowstone and, by direct melting of the phlogopite-rich slab fragment, the ultrapotassic Leucite Hills magmas.

Washington suggests that the descending slab may indeed terminate at a depth of ~300 km. (Rasmussen and Humphreys, 1988).

As pertains to the JHV, the two models in Figure 57 have two things in common: first, in both cases Cascade volcanism was interrupted due to lack of slab descent and dewatering beneath the arc; and second, in each case a slab fragment is seen exiting to the east. In the preferred model (Figure 58), the subducted slab is prevented from descent and dewatering not only due to the actively upwelling mantle but also due to increased thermal buoyancy from plume heat input. A slab fragment is then isolated from slab to the north and south by scissor-like shearing due to differential dip off the flanks of the plume head and from slab to the west by eventual piercing of the slab by the plume. Traction from the horizontally spreading plume head could further deflect slab trajectory eastward. All this

plume activity would have little effect on the slab's cargo of water-laden amphibole, whose breakdown would await descent to higher pressures imposed by encounter with the cratonic root.

In short, there seems to be ample indirect evidence that a portion of subducting slab may have been prevented from dewatering descent under the Cascades in the early Miocene and ample evidence that a slab fragment may have descended and dewatered under western Wyoming in the late Miocene. A slab fragment with an initial velocity relative to the North American plate of 47mm/yr, N51°E, would have a velocity relative to the Yellowstone mantle plume of 36 mm/yr, N52°E (Engebretson et al., 1985). In the 8 my between the time of slab disruption by the plume at 16 Ma and the eruption of the JHV at 8 Ma., the slab fragment would have traveled ~ 288 km NE relative to the plume, assuming no decrease in velocity. When corrected for an average NE-SW extension rate of 15mm/yr (Rodgers et al., 1990), the distance between the surface expression of plume activity at 8 Ma and the site of JHV volcanism would be ~ 408 km. The distance between Jackson Hole and Twin Falls, Idaho, the projected locus of Snake River Plain volcanism at 8 Ma., is ~ 340 km. Given some frictional decrease in the velocity of the detached slab fragment, these distances suggest that such slab transport is at least tectonically reasonable. In addition, the distance from the plume axis to the stagnation line, as determined by modern day topography (Pierce and Morgan, 1992) is ~ 320 km. This line marks the boundary where upper mantle flow outward from the plume axis is counterbalanced by the opposing flow induced by the overriding plate (Sleep, 1990;

Anders and Sleep, 1992). This boundary could thus also serve to localize slab deceleration and descent.

As the slab fragment continued to descend beneath the Wyoming craton, it may have become involved in the petrogenesis of other volcanic suites such as the 1 Ma ultrapotassic Leucite Hills volcanic field in southwest Wyoming. Wyllie (1982) suggested that subduction-related phlogopite peridotite transported to deeper levels could be a source for alkalic magmas. Rowell and Edgar (1983) linked much of the late Cenozoic ultrapotassic mafic volcanism to deep subduction processes. The Leucite Hills rocks have high Ba/Nb and Nd and Sr isotope ratios similar to the JHV (Vollmer et al., 1984). The madupites in particular show slightly higher Nb and $^{143}Nd/^{144}Nd$ values than the JHV, suggesting some input of asthenospheric mantle plume material. An off-axis eruption of Yellowstone mantle plume magma, similar to the South Arch field south of Hawaii (Lipman et al., 1989), may have incorporated phlogopite-rich slab material by direct fusion, a process suggested by the petrology of the Leucite Hills rocks (Kuehner et al., 1981).

CHAPTER 6

CONCLUSIONS

The geochemical and petrologic features of the late-Miocene Jackson Hole Volcanics provide evidence for the involvement of subducted slab-derived fluids not only during some pre-Miocene episode(s) of subduction-related mantle enrichment but also during the late-Miocene melting event itself. Solidus depression due to hydrous flux from amphibole breakdown in a descending fragment of oceanic slab is clearly suitable as a melt-generating mechanism for the JHV. All other mechanisms fail to explain either the petrology or spatial and temporal aspects of this volcanism.

In addition, most syntheses of the Neogene tectonics of the Pacific Northwest imply an interruption of subduction-related Cascade volcanism and thereby the presence of some amount of un-dewatered oceanic slab some distance inland from the Cascade arc. This study of the JHV serves to confirm these theories, in that it provides a likely destination for this previously postulated detached fragment of subducted oceanic crust.

This study has benefited greatly from the close juxtaposition, in both time and/or space, of the voluminous Yellowstone-Snake River Plain and Challis-Absaroka volcanic suites and the excellent and extensive work performed thereon by the authors cited here. These suites provide critical petrogenetic constraints and comparative points of reference for the description and deciphering of the JHV. Petrogenetic studies in other areas are often without the benefit of such information regarding the nature of the underlying mantle

and lower crust, forcing reliance on such nebulous chemical entities as "bulk silicate earth" or xenoliths from far-flung continents.

Even when such constraints are not available, however, a complete petrogenetic explanation, including a consideration of the conditions required for melt generation, is never "beyond the scope of" any study which wishes to treat the tectonic implications of magmatism. Indeed, the increasing number of analyses available for volcanism in the western United States may soon allow a more comprehensive re-examination of the numerous calc-alkaline Cenozoic volcanic suites in the western interior which bear an "anomalous" chemical resemblance to arc magmas. It is not unlikely that in some cases the dewatering of an isolated fragment of oceanic slab may prove the most reasonable candidate for the cause of initial melting.

REFERENCES CITED

Albee, H.F., 1968, Geologic Map of the Munger Mountain Quadrangle, Teton and Lincoln Counties, Wyoming: United States Geological Survey Map GQ-705.

Albee, H.F., 1973, Geologic Map of the Observation Peak Quadrangle, Teton and Lincoln Counties, Wyoming: United States Geological Survey Map GQ-1081.

Alt, D.D., and Hyndman, D.W., 1981, Roadside Geology of Oregon: Mountain Press Publishing, Missoula, Montana, 272p.

Alt, D.D., and Hyndman, D.W., 1995, Northwest Exposures: A Geologic Story of the Pacific Northwest: Mountain Press Publishing, Missoula, Montana, 443p.

Alt, D., Sears, J.M., and Hyndman, D.W., 1988, Terrestrial maria: The origins of large basalt plateaus, hotspot tracks, and spreading ridges: Journal of Geology, v. 96, p. 647-662.

Allmendinger, R.W., 1982, Sequence of Late Cenozoic Deformation in the Blackfoot Mountains, Southeastern Idaho: *in* Cenozoic Geology of Idaho, Bonnichsen, B., and Breckenridge, R.M., eds., Idaho Bureau of Mines and Geology Bulletin 26, p. 505-516.

Anders, M.H., Geissman, J.W., Piety, L.A., and Sullivan, J.T., 1989, Parabolic distribution of circumeastern Snake River Plain seismicity and latest Quaternary faulting: Migratory pattern and association with the Yellowstone hotspot: Journal of Geophysical Research, v. 94, no. B2, p. 1589-1621.

Anders, M.H., and Sleep, N.H., 1992, Magmatism and extension: The thermal and mechanical effects of the Yellowstone hotspot: Journal of Geophysical Research, v. 97, no. B11, p. 15379-15393.

Arculus, R.J., 1987, The significance of source versus process in the tectonic controls of magma genesis: Journal of Volcanology and Geothermal Research, v. 32, p. 1-12.

Arculus, R.J., and Johnson, R.W., 1978, Criticism of generalized models for the magmatic evolution of arc-trench systems: Earth and Planetary Science Letters, v. 39, p. 118-126.

Armstrong, R.L., 1975, Episodic volcanism in the central Oregon Cascade Range: confirmation and correlation with the Snake River Plain: Geology, v. 87, p. 356-357.

Armstrong, R.L., Leeman, W.P., and Malde, H.E., 1975, K-Ar Dating, Quaternary and Neogene volcanic rocks of the Snake River Plain, Idaho: American Journal of Science, v. 275, p. 225-251.

Armstrong, R.L., Harakal, J.E., and Neill, W.M., 1980, K-Ar dating of Snake River Plain (Idaho) volcanic rocks - New results: Geochron/West, no. 27, p. 5-10.

Bacon, C.R., 1986, Magmatic inclusions in silicic and intermediate volcanic rocks: Journal of Geophysical Research, v. 91, no. B6, p. 6091-6112.

Barnosky, A.D., 1984, The Colter Formation: Evidence for Miocene volcanism in Jackson Hole, Teton County, Wyoming: Wyoming Geological Association, Earth Science Bulletin, v. 16, p.49-101.

Barnosky, A.D., 1985, Late Blancan (Pliocene) Microtine rodents from Jackson Hole, Wyoming: Biostratigraphy and biogeography: Journal of Vertebrate Paleontology, v. 5, p. 255-271.

Barnosky, A.D., 1986, Arikareean, Hemingfordian, and Barstovian mammals from the Miocene Colter Formation, Jackson Hole, Teton County, Wyoming: Bulletin of the Carnegie Museum of Natural History, no. 26, 69p.

Barnosky, C.W., 1984, Late Miocene vegetational and climatic variations inferred from a pollen record in northwest Wyoming: Science, v. 223, p. 49-51.

Beeson, M.H., and Tolan, T.L., 1990, The Columbia River Basalt Group in the Cascade Range: A middle Miocene reference datum for structural analysis: Journal of Geophysical Research, v. 95, no. B12, p. 19547-19559.

Behrendt, J.C., Tibbetts, B.L., Bonini, W.E., and Lavin, P.M, 1968, A geophysical study in Grand Teton National Park and vicinity, Teton County, Wyoming: United States Geological Survey Professional Paper 516-E, 23p.

Blackstone, D.L., 1966, Pliocene vulcanism, southern Absaroka Mountains, Wyoming: p. 21-30.

Blackstone, D.L., 1977, The Overthrust Belt salient of the Cordilleran Fold Belt, western Wyoming-southeastern Idaho-northeastern Utah: Wyoming Geological Association Guidebook, 29th Annual Field Conference, p. 367-384.

Blackwelder, E., 1915, Post-Cretaceous history of the mountains of central western Wyoming: Journal of Geology, v. 23, p. 97-117, 193-217, 307-340.

Blackwell, D.D., 1989, Regional implications of heat flow of the Snake River Plain, northwestern United States: Tectonophysics, v. 164, p. 323-343.

Bradley, C.C., 1956, The Pre-Cambrian complex of Grand Teton National Park, Wyoming: Wyoming Geological Association Guidebook, 11th Annual Field Conference, p. 34-42.

Brandon, A.D., and Goles, G.G., 1988, A Miocene subcontinental plume in the Pacific Northwest: geochemical evidence: Earth and Planetary Science Letters, v. 88, p. 273-283.

Brott, C.A., Blackwell, D.D., and Ziagos, J.P., 1981, Thermal and tectonic implications of heat flow in the eastern Snake River Plain, Idaho: Journal of Geophysical Research, v. 86, no. B12, p. 11709-11734.

Burbank, D.W. and Barnosky, A.D., 1990, The magnetostratigraphy of Barstovian mammals in southwestern Montana and implications for the initiation of Neogene crustal extension in the northern Rocky Mountains: Geological Society of America Bulletin, v. 102, p. 1093-1104.

Byrd, J.O., Smith, R.B., and Geissman, J.W., 1994, The Teton Fault, Wyoming: topographic signature, neotectonics, and mechanisms of deformation: Journal Geophysical Research, v. 99, no. B10., p. 20095-20122.

Campbell, I.H., and Griffiths, R.W., 1990, Implications of mantle plume structure for the evolution of flood basalts: Earth and Planetary Science Letters, v. 99, p. 79-93.

Carlson, R.W., and Hart, W.K., 1987, Crustal genesis on the Oregon Plateau, Journal of Geophysical Reseach, v. 92, no. B7, p. 6191-6206.

Cather. S.M., 1990, Stress and volcanism in the northern Mogollon-Datil volcanic field, New Mexico: Effects of the post-Laramide tectonic transition: Geological Society of America Bulletin, v. 102, p. 1447-1458.

Christiansen, R.L., 1995, The Quaternary and Pliocene Yellowstone Plateau Volcanic Field of Wyoming, Idaho, and Montana: United States Geological Survey Professional Paper 729-G, 187 p.

Christiansen, R.L. and Lipman, P.W., 1972, Cenozoic volcanism and plate-tectonic evolution of the western United States. II. Late Cenozoic: Philosophic Transactions of the Royal Society of London, Series A.271, p.249-284.

Christiansen, R.L. and Love, J.D., 1978, The Pliocene Conant Creek Tuff in the northern part of the Teton Range and Jackson Hole, Wyoming: United States Geological Survey Bulletin 1435-C, 9p.

Christiansen, R.L. and McKee, E.H., 1978, Late Cenozoic volcanic and tectonic evolution of the Great Basin and Columbia intermontane regions: *in* Smith, R.B., and Eaton, G.P., eds., Cenozoic tectonics and regional geophysics of the western Cordillera: Geological Society of America Memoir 152, p.283-311.

Church, S.E., 1985, Genetic interpretation of lead-isotope data from the Columbia River Basalt Group, Oregon, Washington, and Idaho: Geological Society of America Bulletin, v. 96, p. 676-690.

Condie, K.C., Leech, A.P., and Baadsgaard, H., 1969, Potassium-argon ages of Precambrian mafic dikes in Wyoming: Geological Society of America Bulletin v. 80, p. 899-906.

Craig, H., Lupton, J.E., Welhan, J.A., and Poreda, R., 1978, Helium isotope ratios in Yellowstone and Lassen Park volcanic gases: Geophysical Research Letters, v. 5, p. 897-900.

Davidson, J.P., Ferguson, K.M., Colucci, M.T., and Dungan, M.A., 1988, The origin and evolution of magmas from the San Pedro-Pellado Volcanic Complex, S. Chile: multicomponent sources and open system evolution: Contributions to Mineralogy and Petrology, v. 100, p. 429-445.

Davis, R.L. and Wilkinson, B.H., 1983, Sedimentology and petrology of freshwater lacustrine carbonate: Mid-Tertiary Camp Davis Formation, northwestern Wyoming: Contributions to Geology, University of Wyoming, v. 22, p. 45-55.

DePaolo, D.J., 1981, Trace element and isotopic effects of combined wallrock assimilation and fractional crystallization: Earth and Planetary Science Letters, v. 53, p. 189-202.

Doe, B.R., Leeman, W.P., Christiansen, R.L., and Hedge, C.E., 1982, Lead and strontium isotopes and related elements as genetic tracers in the upper Cenozoic rhyolite-basalt association of the Yellowstone Plateau volcanic field: Journal of Geophysical Research, v. 87, no. B6, p. 4785-4806.

Doser, D.I. and Smith, R.B., 1983, Seismicity of the Teton-southern Yellowstone region, Wyoming: Bulletin of the Seismological Society of America, v. 73, p. 1369-1394.

Draper, D.S., 1991, Late Cenozoic bimodal magmatism in the northern Basin and Range province of southeastern Oregon: Journal of Volcanology and Geothermal Research, v. 47, p. 299-328.

Dudas, F.O., 1991, Geochemistry of igneous rocks from the Crazy Mountains, Montana, and tectonic models for the Montana Alkalic Province: Journal of Geophysical Research, v. 96, no. B8, p. 13261-13277.

Duncan, R.A., 1982, A captured island chain in the Coast Range of Oregon and Washington: Journal of Geophysical Research, v. 87, no. B13, p. 10827-10837.

Dunn, S.L.D., 1983, Timing of foreland and thrust-belt deformation in an overlap area, Teton Pass, Idaho and Wyoming: *in* Lowell, J.D., ed., Rocky Mountain foreland basins and uplifts: Denver, Rocky Mountain Association of Geologists, p. 263-269.

Eaton, G.P., Christiansen, R.L., Iyer, H.M., Pitt, A.M., Mabey, D.R., Blank, H.R., Zietz, I., and Gettings, M.E., 1975, Magma beneath Yellowstone National Park: Science, v. 188, p.787-796.

Edmund, R.W., 1956, Resume of Structures and Physiography in the Northern Teton Mountains, Wyoming: Wyoming Geological Association Guidebook, 11th Annual Field Conference, p.151-157.

Eggler, D.H., 1972, Water-saturated and undersaturated melting relations in a Paricutin andesite and an estimate of water content in the natural magma: Contributions to Mineralogy and Petrology, v. 34, p. 261-271.

Eggler, D.H., 1974, Application of a portion of the system $CaAl_2Si_2O_8$-$NaAlSi_3O_8$-MgO-Fe-O_2-H_2-CO_2 to genesis of the calc-alkaline suite: American Journal of Science, vol.274, p. 297-315.

Eggler, D.H., 1987, Solubility of major and trace elements in mantle metasomatic fluids: Experimental constraints: *in* Menzies, M.A., and Hawkesworth, C.J., eds., Mantle Metasomatism, Academic Press, London, p. 21-39.

Eggler, D.H., and Burnham, C.W., 1973, Crystallization and fractionation trends in the system andesite-H_2O-CO_2-O_2 at pressures to 10 Kb: Geological Society of America Bulletin, v. 84, p. 2517-2532.

Engebretson, D.C., Cox, A., and Gordon, R.G., 1985, Relative motions between oceanic and continental plates in the Pacific basin: Geological Society of America Special Paper 206, 59p.

Erslev, E.A., and Rogers, J.L., 1993, Basement-cover geometry of Laramide fault-propagation folds: *in* Schmidt, C.J., Chase, R.B., and Erslev, E.A., eds., Laramide Basement Deformation in the Rocky Mountain Foreland of the Western United States: Boulder, Colorado, Geological Society of America Special Paper 280, p. 125-146.

Evernden, J.F., Savage, D.E., Curtis, G.H., and James, G.T., 1964, Potassium- argon dates and the Cenozoic mammalian chronology of North America: American Journal Science, v. 262, p. 145-198.

Ewart, A., 1982, The mineralogy and petrology of Tertiary-Recent orogenic volcanic rocks: with special reference to the andesitic-basaltic compositional range: *in* Andesites, Thorpe, R.S., ed., John Wiley and Sons, New York, p.25-95.

Feeley, T.C., and Sharp, Z.D., 1996, Chemical and hydrogen isotope evidence for in situ dehydrogenation of biotite in silicic magma chambers: Geology, v. 24, p. 1021-1024.

Fitton, J.G., James, D., and Leeman,W.P., 1991, Basic magmatism associated with Late-Cenozoic extension in the western United States: Compositional variations in space and time: Journal of Geophysical Research, v. 96, no. B8, p. 13693-13711.

Fritz, W.J. and Sears, J.W., 1993, Tectonics of the Yellowstone hotspot wake in southwestern Montana: Geology, v. 21, p. 427-430.

Fryxell, F.M., 1930, Glacial features of Jackson Hole, Wyoming: Augustana Library Publication, Rock Island, Illinois.

Gans, P.B., Mahood, G.A., and Schermer, E., 1989, Synextensional magmatism in the Basin and Range Province; A case study from the eastern Great Basin: Geological Society of America Special Paper 233, 53p.

Geist, D. and Richards, M., 1993, Origin of the Columbia Plateau and Snake River Plain: deflection of the Yellowstone plume: Geology, v. 21, no. 9, p. 789-792.

Gerlach, D.C., and Grove, T.L., 1982, Petrology of Medicine Lake Highland volcanics: Characterization of endmembers of magma mixing: Contributions to Mineralogy and Petrology, v. 80, p. 147-159.

Gilbert, J.D., Ostenaa, D., and Wood, C., 1983, Seismotectonic study: Jackson Lake Dam Minidoka Project, Wyoming: United States Bureau of Reclamation, Engineering and Research Center., Denver, Colorado, 123p.

Gill, J.B., 1981, Orogenic Andesites and Plate Tectonics: Springer-Verlag, New York, 390p.

Glenn, W.R., Nettleton, W.D., Fowkes, C.J., and Daniels, D.M., 1983, Loessial deposits and soils of the Snake and tributary river valleys of Wyoming and eastern Idaho: Soil Science Society of America Journal, v. 47, p. 547-552.

Goles, G.G., 1986, Miocene basalts of the Blue Mountains province in Oregon. I: Compositional types and their geological settings: Journal of Petrology, v. 27, p. 495-520.

Goles, G.G., Brandon, A.D., and Lambert, R.S., 1989, Miocene basalts of the Blue Mountains Province in Oregon; Part 2, Sr isotopic ratios and trace element features of little-known Miocene basalts of central and eastern Oregon: *in* Reidel, S.P., and Hooper, P.R., eds., Volcanism and tectonism in the Columbia River flood-basalt province: Boulder, Colorado, Geological Society of America Special Paper 239, p. 357-36

Grand, S.P., 1987, Tomographic inversion for shear velocity beneath the North American Plate: Journal of Geophysical Research, v. 92, no. B13, p. 14065-14090.

Green, D.H., 1973, Experimental melting studies on a model upper mantle composition at high pressure under water-saturated and water-undersaturated conditions: Earth and Planetary Science Letters, v. 19, p. 37-53.

Green, D.H., 1982, Anatexis of mafic crust and high pressure crystallization of andesite: *in* R.S.Thorpe, ed., Andesites: Orogenic andesites and related rocks, John Wiley and Sons, New York.

Harrington, C.D., 1985, A revision in the glacial history of Jackson Hole, Wyoming: The Mountain Geologist, v. 22, p. 28-32.

Hart, W.K., 1985, Chemical and isotopic evidence for mixing between depleted and enriched mantle,northwestern U.S.A.: Geochimica et Cosmochimica Acta, v. 49, p. 131-144.

Hart, W.K., and Carlson, R.W., 1987, Tectonic controls on magma genesis and evolution in the northwestern United States: Journal of Volcanology and Geothermal Research, v. 32, p. 119-135.

Hawkesworth, C.J., 1982, Isotope characteristics of magmas erupted along destructive plate margins: *in* R.S. Thorpe, ed., Andesites: Orogenic andesites and related rocks, John Wiley and Sons, New York.

Hidebrandt, P.K., 1989, Petrology, thermobarometry, and geochemistry of the Archean layered gneiss, Teton Range, Wyoming [M.S. Thesis]: Fort Collins, Colorado, Colorado State University, 70p.

Hildreth, W., 1981, Gradients in silicic magma chambers: Implications for lithospheric magmatism: Journal of Geophysical Research, v. 86, no. B11, p. 10153-10192.

Hildreth, W., Halliday, A.N., and Christiansen, R.L., 1991, Isotopic and chemical evidence concerning the genesis and contamination of basaltic and rhyolitic magma beneath the Yellowstone volcanic field: Journal of Petrology, v. 32, p. 63-138.

Hooper, P.R., 1990, The Timing of Crustal Extension and the Eruption of Continental Flood Basalts: Nature, vol. 345, p. 246-249.

Hooper, P.R., and Hawkesworth, C.J., 1993, Isotopic and geochemical constraints on the origin and evolution of the Columbia River Basalt Group: Journal of Petrology, v. 34, p. 1203-1246.

Hooper, P.R., Johnson, D.M., and Conrey, R.M., 1993, Major and trace element analyses of rocks and minerals by automated X-ray spectometry: Washington State University, Open File Report, 36p.

Hooper, P.R., Bailey, D.G., and Holder, G.A.M., 1995, Tertiary calc-alkaline magmatism associated with lithospheric extension in the Pacific Northwest: Journal of Geophysical Research, v. 100, no. B7, p. 10303-10319.

Horberg, L. and Fryxell,F., 1942, Pre-Cambrian metasediments in Grand Teton National Park, Wyoming: American Journal of Science, v. 240, no. 6, p. 385-393.

Horberg, L., Nelson, V., and Church, V., 1949, Structural trends in central western Wyoming: Geological Society of America Bulletin, v. 60, p. 183-216.

Houston, R.S., 1956, Preliminary report on the petrography of Tertiary volcanic rocks of the Jackson Hole area, Teton County, Wyoming: Wyoming Geological Association Guidebook, 11th Annual Field Conference, p. 133-139.

Jakes, P. and White, A.J.R., 1972, Major and trace element abundances in volcanic rocks of orogenic areas: Geological Society of America Bulletin, v. 83, p. 29-40.

Kempton, P.D., Fitton, J.G., Hawkesworth, C.J., and Ormerod, D.S., 1991, Isotopic and trace element constraints on the composition and evolution of the lithosphere beneath the southwestern United States: Journal of Geophysical Research, v. 96, no. B8, p. 13713-13735.

Kennedy, B.M., Reynolds, J.H., Smith, S.P., and Truesdale, A.H., 1987, Helium isotopes: Lower Geyser Basin, Yellowstone National Park: Journal of Geophysical Research, v. 92, p. 12477-12489.

Kuehner, S.M., Edgar, A.D., and Arima, M., 1981, Petrogenesis of the ultrapotassic rocks from the Leucite Hills, Wyoming: American Mineralogist, v. 66, p. 663-677.

Kuntz, M.A., 1992, A model-based perspective of basaltic volcanism, eastern Snake River Plain, Idaho: *in* Link, P.K., Kuntz, M.A., and Platt, L.B., eds., Regional Geology of Eastern Idaho and Western Wyoming: Geological Society of America Memoir 179, p. 289-304.

Kuntz, M.A., Covington, H.R., and Schorr, L.J., 1992, An overview of basaltic volcanism of the eastern Snake River Plain, Idaho: *in* Link, P.K., Kuntz, M.A., and Platt, L.B., eds., Regional Geology of Eastern Idaho and Western Wyoming: Geological Society of America Memoir 179, p. 227-267.

Lachenbruch, A.H. and Sass, J.H., 1978, Models of an extending lithosphere and heat flow in the Basin and Range Province: *in* Smith, R.B., and Eaton, G.P., eds., Cenozoic tectonics and regional geophysics of the western Cordillera: Geological Society of America Memoir 152, p. 209-250.

Lageson, D.R., 1987, Laramide uplift of the Gros Ventre Range and implications for the origin of the Teton Fault, Wyoming: Wyoming Geological Association Guidebook, 38th Annual Field Conference, p.79-89.

Lageson, D.R., 1992, Possible Laramide influence on the Teton normal fault, western Wyoming: *in* Link, P.K., Kuntz, M.A., and Platt, L.B., eds., Regional Geology of Eastern Idaho and Western Wyoming: Geological Society of America Memoir 179, p. 183-196.

Lamerson, P., 1983, Field trip guide: Rendezvous Peak and Jackson Hole: Structural Geology School, American Association of Petroleum Geologists, 1983, Jackson, Wyoming.

Leat, P.T., Thompson, R.N., Morrison, M.A., Hendry, G.L., and Dicken, A.P., 1991, Alkaline hybrid mafic magmas of the Yampa area, NW Colorado, and their relationship to the Yellowstone mantle plume and lithospheric mantle domains: Contributions to Mineralogy and Petrology, v. 107, p. 310-327.

LeBas, M.J., Le Maitre, R.W., Streckeisen, A., and Zanettin, B., 1986, A chemical classification of volcanic rocks based on the total alkali-silica diagram: Journal of Petrology, v. 27, p. 745-750.

Leeman, W.P., 1982a, Development of the Snake River Plain-Yellowstone Plateau province, Idaho and Wyoming: An overview and petrologic model: *in* Cenozoic Geology of Idaho, Bonnichsen, B., and Breckenridge, R.M., eds., Idaho Bureau of Mines and Geology Bulletin 26, p. 155-177.

Leeman, W.P., 1982b, Olivine tholeiitic basalts of the Snake River Plain, Idaho: *in* Cenozoic Geology of Idaho, Bonnichsen, B., and Breckenridge, R.M., eds., Idaho Bureau of Mines and Geology Bulletin 26, p. 181-191.

Leeman, W.P., 1982c, Rhyolites of the Snake River Plain-Yellowstone Plateau Province, Idaho and Wyoming: A Summary of Petrogenetic Models: *in* Cenozoic Geology of Idaho, Bonnichsen, B., and Breckenridge, R.M., eds., Idaho Bureau of Mines and Geology Bulletin 26, p. 203-212

Leeman, W.P., 1982d, Evolved and Hybrid Lavas from the Snake River Plain, Idaho: *in* Cenozoic Geology of Idaho, Bonnichsen, B., and Breckenridge, R.M., eds., Idaho Bureau of Mines and Geology Bulletin 26, p. 193-202.

Leeman, W.P., Menzies, M.A., Matty, D.J., and Embree, G.F., 1985, Strontium, neodymium, and lead isotopic compositions of deep crustal xenoliths from the Snake River Plain: Evidence for Archean basement: Earth and Planetary Science Letters, v. 75, p. 354-368.

Leeman, W.P., 1989, Origin and Development of the Snake River Plain - an Overview: *in* Field Guide to the Snake River Plain-Yellowstone Volcanic Province, International Geological Congress Field Trip T305, p.4 -12.

Leeman, W.P., Menzies, M.A., Matty, D.J., and Embree, G.F., 1985, Strontium, neodymium, and lead isotopic compositions of deep crustal xenoliths from the

Snake River Plain: Evidence for Archean basement: Earth and Planetary Science Letters, v. 75, p. 354-368.

Leeman, W.P., Smith, D.R., Hildreth, W., Palacz, Z., and Rogers, N., 1990, Compositional diversity of late Cenozoic basalts across the southern Washington Cascades: Implications for subduction zone magmatism: Journal of Geophysical Research, v. 95, no. B12, p. 19561-19582.

Lindsay, D.A., 1972, Sedimentary petrology and paleocurrents of the Harebell Formation, Pinyon Conglomerate, and associated coarse clastic deposits, northwest Wyoming: United States Geological Survey Professional Paper 734-B, 68p.

Lindsley, D.H., 1983, Pyroxene thermometry: American Mineralogist, v. 68, p. 477-493.

Lipman, P.W., 1992, Magmatism in the Cordilleran United States; Progress and problems: *in* Burchfiel, B.C., Lipman, P.W., and Zoback, M.L., eds., The Cordilleran Orogen: Conterminous U.S.: Boulder, Colorado, Geological Society of America, The Geology of North America, v. G-3, p. 481-514.

Lipman, P.W., Prostka, H.J., and Christiansen, R.L., 1972, Cenozoic volcanism and plate-tectonic evolution of the western United States: I. Early and middle Cenozoic: Philosophical Transactions of the Royal Society of London, Series A. 271, p. 217-248.

Lipman, P.W., Clague, D.A., Moore, J.G., and Holcomb, R.T., 1989, South Arch volcanic field - Newly identified young lava flows on the sea floor south of the Hawaiian Ridge: Geology, v. 17, p. 611-614.

Love, J.D., 1956a, Cretaceous and Tertiary stratigraphy of the Jackson Hole area, northwestern Wyoming: Wyoming Geological Association Guidebook, 11th Annual Field Conference, p.76-94.

Love, J.D., 1956b, Summary of Geologic History of Teton County, Wyoming, during Late Cretaceous, Tertiary, and Quaternary Times: Wyoming Geological Association Guidebook, 11th Annual Field Conference, p. 140-150.

Love, J.D., 1956c, New geologic formationn names in Jackson Hole, Teton County, northwestern Wyoming: American Association of Petroleum Geologists Bulletin, v.40, p. 1899-1914.

Love, J.D., 1960, Cenozoic sedimentation and crustal movement in Wyoming: American Journal of Science, v. 258-A, p. 204-214.

Love, J.D., 1973, Harebell Formation (Upper Cretaceous) and Pinyon Conglomerate (Uppermost Cretaceous and Paleocene), northwestern Wyoming: United States Geological Survey Professional Paper 734-A, 54p.

Love, J. D., 1977, Summary of Upper Cretaceous and Cenozoic stratigraphy, and of tectonic and glacial events in Jackson Hole, northwestern Wyoming: Wyoming Geological Association Guidebook, 29th Annual Field Conference, p.585-593.

Love, J.D. and Albee, H.F., 1972, Geologic map of the Jackson Quadrangle, Teton County, Wyoming: United States Geological Survey Map I-769-A.

Love, J.D., Leopold, E.B., and Love, D.W., 1978, Eocene rocks, fossils, and geologic history, Teton Range, northwestern Wyoming: United States Geological Survey Professional Paper 932-B, 40p.

Love, J.D. and Montagne, J., 1956, Pleistocene and recent tilting of Jackson Hole, Teton County, Wyoming: Wyoming Geological Association Guidebook, 11th Annual Field Conference, p. 169-178.

Love, J.D., and Reed, J.C., 1971, Creation of the Teton Landscape: Grand Teton Natural History Association, Moose, Wyoming, 120p.

Love, J.D., Reed, J.C., Christiansen, R.L., and Stacey, J.R., 1973, Geologic block diagram and tectonic history of the Teton region, Wyoming-Idaho: United States Geological Survey Map I-730.

Love, J.D., Reed, J.C., and Christiansen, A.C., 1992, Geologic map of Grand Teton National Park, Teton County, Wyoming: United States Geological Survey Map I-2031.

Love, J. D. and Taylor, D.W., 1962, Faulted Pleistocene strata near Jackson, northwestern Wyoming: United States Geological Survey Professional Paper 450-D, p.136-139.

Love, L.L., Kudo, A.M., and Love, D.W., 1976, Dacites of Bunsen Peak, the Birch Hills, and the Washakie Needles, northwestern Wyoming, and their relationship to the Absaroka volcanic field, Wyoming and Montana: Geological Society of America Bulletin, v. 87, p. 1455-1462.

Love, T.C., 1986, Geochemical correlation of Salt Lake-equivalent pyroclastic deposits in Idaho and Wyoming [M.S. Thesis]: University of New Orleans, 114p.

Luedke, R.G. and Smith, R.L., 1978a, Map showing distribution, composition, and age of late Cenozoic volcanic centers in Arizona and New Mexico: United States Geological Survey Map I-1091-A.

Luedke, R.G. and Smith, R.L., 1978b, Map showing distribution, composition, and age of late Cenozoic volcanic centers in Colorado, Utah, and southwestern Wyoming: United States Geological Survey Map I-1091-B.

Luedke, R.G. and Smith, R.L., 1978c, Map showing distribution, composition, and age of late Cenozoic volcanic centers in California and Nevada: United States Geological Survey Map I-1091-C.

Luedke, R.G. and Smith, R.L., 1978d, Map showing distribution, composition, and age of late Cenozoic volcanic centers in Oregon and Washington: United States Geological Survey Map I-1091-D.

Luedke, R.G. and Smith, R.L., 1978e, Map showing distribution, composition, and age of late Cenozoic volcanic centers in Idaho, Western Montana, west-central South Dakota, and northwestern Wyoming: United States Geological Survey Map I-1091-E.

Lum, C.C.L., Leeman, W.P., Foland, K.A., Kargel, J.A., and Fitton, J.G., 1989, Isotopic variations in continental basaltic lavas as indicators of mantle heterogeneity: Examples from the western U.S. Cordillera: Journal of Geophysical Research, v. 94, no. B6, p. 7871-7884.

Mabey, D.R., Zietz, I., Eaton, G.P., and Kleinkopf, M.D., 1978, Regional magnetic patterns in part of the Cordillera in the western United States: *in* Smith, R.B., and Eaton, G.P., eds., Cenozoic tectonics and regional geophysics of the western Cordillera: Geological Society of America Memoir 152, p. 93-106.

Mahaney, W.C., and Spence, J.R., 1990, Neoglacial chronology and floristics in the Middle Teton area, central Teton Range, western Wyoming: Journal of Quaternary Science, v. 5, p. 53-66.

McBirney, A.R., Sutter, J.F., Naslund, H.R., Sutton, K.G., and White, C.M., 1974, Episodic volcanism in the central Oregon Cascade Range: Geology, v. 2, p. 585-589.

McDowell, R.J. and Fritz, W.J., 1995, Geochemistry of the Tertiary Dillon volcanics of southwestern Montana: Transition from arc to extensional volcanism: Geological Society of America, Abstracts with Program, Rocky Mtn. Section, 1995, p. 46.

McKenzie, D. and Bickle, M.J., 1988, The volume and composition of melt generated by extension of the lithosphere: Joural of Petrology, v. 29, pt. 3, p. 625-679.

McMillan, N.J. and Dungan, M.A., 1988, Open system magmatic evolution of the Taos Plateau volcanic field, northern New Mexico: 3. Petrology and geochemistry of andesite and dacite: Journal of Petrology, v. 29, pt. 3, p.527-557.

Meen, J.K. and Eggler, D.H., 1987, Petrology and geochemistry of the Cretaceous Independence volcanic suite, Absaroka Mountains, Montana: Clues to the composition of the Archean sub-Montana mantle: Geological Society of America Bulletin, v. 98, p. 238-247.

Menzies, M.A., Leeman, W.P., and Hawkesworth, C.J., 1983, Isotope geochemistry of Cenozoic volcanic rocks reveals mantle heterogeneity below western U.S.A.: Nature, v. 303, p. 205-209.

Menzies, M.A., 1989, Cratonic, circumcratonic and oceanic mantle domains beneath the western United States: Journal of Geophysical Research, v. 94, p. 7899-7915.

Miller, S.H., Hildebrandt, P.K., Erslev, E.A., and Reed, J.C., 1986, Metamorphic and deformation history of the gneiss complex in the northern Teton Range, Wyoming: Montana Geological Society, Yellowstone-Bighorn Research Association Field Conference, p.91-105.

Morgan, L.A., 1992, Stratigraphic relations and paleomagnetic and geochemical correlations of ignimbrites of the Heise volcanic field, eastern Snake River Plain, eastern Idaho and western Wyoming: *in* Link, P.K., Kuntz, M.A., and Platt, L.B., eds., Regional Geology of Eastern Idaho and Western Wyoming: Geological Society of America Memoir 179, p. 215-226.

Morgan, L.A., Doherty, D.J., and Leeman, W.P., 1984, Ignimbrites of the eastern Snake River Plain: Evidence for major caldera-forming eruptions: Journal of Geophysical Research, v. 89, p. 8665-8678.

Morgan, L.A., and Hackett, W.R., 1989, Explosive basaltic and rhyolitic volcanism of the eastern Snake River Plain: *in* Field Guide to the Snake River Plain-Yellowstone Volcanic Province, International Geological Congress Field Trip T305, p. 39-47.

Myers, W.B., and Hamilton, W., 1964, Deformation accompanying the Hebgen Lake earthquake of August 17, 1959: United States Geological Survey Professional Paper 435, p. 55-98.

Naeser, C.W., Izett, G.A., and Obradovich, J.D., 1980, Fission-track and K-Ar ages of natural glasses: United States Geological Survey Bulletin 1489, 31p.

Nelson, S.T., and Montana, A., 1992, Sieve-textured plagioclase in volcanic rocks produced by rapid decompression: American Mineralogist, v. 77, p. 1242-1249.

Nixon, G.T., 1988, Petrology of the younger andesites and dacites of Iztaccihuatl Volcano, Mexico: I. Disequilibrium phenocryst assemblages as indicators of magma chamber processes: Journal of Petrology, v. 29, p. 213-264.

Norman, M.D., and Leeman, W.P., 1989, Geochemical evolution of Cenozoic-Cretaceous magmatism and its relation to tectonic setting, southwestern Idaho, U.S.A.: Earth and Planetary Science Letters, v. 94, p. 78-96.

Norman, M.D. and Mertzman, S.A., 1991, Petrogenesis of Challis Volcanics from central and southwestern Idaho: Trace element and Pb isotopic evidence: Journal of Geophysical Research, v. 96, no. B8, p. 13279-13293.

Olson, T.J. and Schmitt, J.G., 1987, Sedimentary evolution of the Miocene-Pliocene Camp Davis basin, northwestern Wyoming: Wyoming Geological Association Guidebook, 38th Annual Field Conference, p. 225-242.

Oriel, S.S. and Moore, D.W., 1985, Geologic Map of the West and East Palisades roadless areas, Idaho and Wyoming, United States Geological Survey Map MF-1619-B.

Pampeyan, E.H., Schroeder,M.L., Schell, E.M., and Cressman, E.R., 1967, Geologic map of the Driggs Quadrangle, Bonneville and Teton Counties, Idaho and Teton County, Wyoming: United States Geological Survey Map MF-300.

Pearce, J.A., 1982, Trace element characteristics of lavas from destructive plate boundaries: *in* R.S. Thorpe, ed., Andesites: Orogenic andesites and related rocks, John Wiley and Sons, New York.

Pearce, J.A., and Cann, J.R., 1973, Tectonic setting of basic volcanic rocks determined using trace element analyses: Earth and Planetary Science Letters, v. 19, p. 290-300.

Pearce, J.A., and Norry, M.J., 1979, Petrogenetic implications of Ti, Zr, Y, and Nb variations in volcanic rocks: Contributions to Mineralogy and Petrology, v. 69, p. 33-47.

Perkins, M.E. and Nash, W.P., 1994, Tephrochronology of the Teewinot Formation, Jackson Hole, Wyoming: Geological Society of America Abstracts with Programs, Rocky Mountain Section, p. 58.

Perry, F.V., Baldridge, W.S., and DePaolo, D.J., 1987, Role of asthenosphere and lithosphere in the genesis of late Cenozoic basaltic rocks from the Rio Grande Rift and adjacent regions of the southwestern United States: Journal of Geophysical Research, v. 92, no. B9, p. 9193-9213.

Pierce, K.L. and Good, J.D., 1992, Field Giude to the Quaternary Geology of Jackson Hole, Wyoming: United States Geological Survey Open File Report 92-504, 49p.

Pierce, K.L., and Morgan, L.A., 1992, The track of the Yellowstone hot spot: Volcanism, faulting, and uplift: *in* Link, P.K., Kuntz, M.A., and Platt, L.B., eds., Regional Geology of Eastern Idaho and Western Wyoming: Geological Society of America Memoir 179, p. 1-53.

Piety, L.A., Wood, C.K., Gilbert, J.D., Sullivan, J.T., and Anders, M.H., 1986, Seismotectonic study for Palisades dam and reservoir, Palisades Project: Seismotectonic Report 86-3, Bureau of Reclamation, Engineering and Research Center, Denver, Colorado, 198p.

Priest, G.R., 1990, Volcanic and tectonic evolution of the Cascade volcanic arc, central Oregon: Journal of Geophysical Research, v. 95, no. B12, p. 19583-19599.

Rasmussen, J., and Humphreys, E., 1988, Tomographic image of the Juan de Fuca Plate beneath Washington and western Oregon using teleseismic P-wave travel times: Geophysical Research Letters, v. 15, p. 1417-1420.

Reed, J.C. and Zartman, R.E., 1973, Geochronology of Precambrian rocks of the Teton Range, Wyoming: Geological Society of America Bulletin, v. 84, p. 561-582.

Ritchie, E.L., 1981, Geochemical correlation of Tertiary volcanic ash, Idaho and Wyoming [M.S. Thesis]: University of New Orleans, 60p.

Robyn, T.L., 1979, Miocene volcanism in eastern Oregon: An example of calc-clkaline volcanism unrelated to subduction: Journal of Volcanology and Geothermal Research, v. 5, p. 149-161.

Rodgers, D.W., Hackett, W.R., and Ore, H.T., 1990, Extension of the Yellowstone Plateau, eastern Snake River Plain, and Owyhee Plateau: Geology, v. 18, no. 11, p. 1138-1141.

Rowell, W.F., and Edgar, A.D., 1983, Cenozoic potassium-rich mafic volcanism in the western U.S.A.: Its relationship to deep subduction: Journal of Geology, v. 91, p. 338-34.

Royden, L.H., 1993, The tectonic expression of slab pull at continental convergent boundaries: Tectonics, v. 12, no. 2, p. 303-325.

Russell, J.K., and Nicholls, J., 1988, Analysis of petrologic hypotheses with Pearce element ratios: Contributions to Mineralogy and Petrology, v. 99, p. 25-35.

Ryerson, F.J., and Watson, E.B., 1987, Rutile saturation in magmas: Implications for Ti-Nb-Ta depletion in island arc basalts: Earth and Planetary Science Letters, v. 86, p. 225-239.

Sacks, I.S., 1983, The subduction of young lithosphere, Journal of Geophysical Research, v. 88, no. B4, p. 3355-3366.

Saunders, A.D., Tarney, J., and Weaver, S.D., 1980, Transverse geochemical variations across the Antarctic Peninsula: Implications for the genesis of calc-alkaline magmas: Earth and Planetary Science Letters, v. 46, p. 344-360.

Schmitt, J.G., 1987, Origin of Late Cretaceous to Early Tertiary quartzite conglomerates in northwestern Wyoming: Wyoming Geological Association Guidebook, 38th Annual Field Conference, p. 217-224.

Schroeder, M.L., 1969, Geologic map of the Teton Pass Quadrangle, Teton County, Wyoming: United States Geological Survey Map GQ-793.

Schroeder, M.L., 1972, Geologic map of the Rendezvous Peak Quadrangle, Teton County, Wyoming: United States Geological Survey Map GQ-980.

Schroeder, M.L., 1974, Geologic map of the Camp davis Quadrangle, Teton County, Wyoming: United States Geological Survey Map GQ-1160.

Schroeder, M.L., 1976, Geologic map of the Bull Lake Quadrangle, Teton and Sublette Counties, Wyoming: United States Geological Survey Map GQ-1300.

Scopel, L.J., 1949, The volcanic history of Jackson Hole, Wyoming [M.S. Thesis]: Detroit, Michigan, Wayne State University, 34p.

Scopel, L.J., 1956, The volcanic rocks of the Gros Ventre Buttes, Jackson Hole, Wyoming: Wyoming Geological Association Guidebook, 11th Annual Field Conference, p.126-128.

Simons, F.S., Love, J.D., Keefer, W.R., Harwood, D.S., Kulik, D.M., and Bieniewski, C.L., 1988, Mineral resources of the Gros Ventre Wilderness study area, Teton and Sublette Counties, Wyoming: United States Geological Survey Bulletin 1591, 65p.

Sleep, N.H., 1990, Hotspots and mantle plumes: some phenomenology: Journal of Geophysical Research, v. 95, no. B5, p. 6715-6736.

Smith, D.J., 1990, Structural analysis of the Buck Mountain Fault and related intra-range faults, Teton Range, Wyoming [M.S. Thesis]: Bozeman, Montana State University, 92p.

Smith, D.J., Lageson, D.R., and Smith, M.S., 1991, Influence of basement anisotropy on Laramide faults, Teton Range, Western Wyoming: Geological Society of America Abstracts with Program, South-central and Rocky Mountain Sections, p. 95.

Smith, R.B., Pelton, J.R., and Love, J.D., 1977, Seismicity and the possibility of earthquake related landslides in the Teton-GrosVentre-Jackson Hole area, Wyoming: Wyoming Geological Association Guidebook, 29th Annual Field Conference, p.603-610.

Smith, R.B., Pierce, K.L., and Wold, R.J., 1992, Seismic surveys and Quaternary history of Jackson Lake, Wyoming: *in* G. Glass, ed., Geology of Wyoming, Wyoming Geological Association.

Smith, R.B. and Braile, L.W., 1994, The Yellowstone hotspot: Journal of Volcanology and Geothermal Research, v. 61, p. 121-187.

Snyder, W.S., Dickinson, W.R., and Silberman, M.L., 1976, Tectonic implications of space-time patterns of Cenozoic magmatism in the western United States: Earth and Planetary Science Letters, v. 32, p. 91-106.

Sohn, I.G., 1956, Pliocene ostracodes from Jackson Hole, Wyoming: Wyoming Geological Association Guidebook, 11th Annual Field Conference, p. 120-122.

Stimac, J.A., and Pearce, T.H., 1992, Textural evidence of mafic-felsic magma interaction in dacite lavas, Clear Lake, California: American Mineralogist, v. 77, p. 795-809.

Stolz, A.J., Jochum, K.P., Spettel, B., and Hofman, A.W., 1996, Fluid- and melt-related enrichment in the subarc mantle: Evidence from Nb/Ta variations in island-arc basalts: Geology, v. 24, p. 587-590.

Suneson, N.H. and Lucchitta, I., 1983, Origin of bimodal volcanism, southern Basin and Range province, west-central Arizona: Geological Society of America Bulletin, v. 94, p.1005-1019.

Tatsumi, Y., Hamilton, D.L., and Nesbitt, R.W., 1986, Chemical characteristics of fluid phase released from a subducted lithosphere and origin of arc magmas: Evidence from high-pressure experiments and natural rocks: Journal of Volcanology and Geothermal Research, v. 29, p. 293-309.

Tatsumi, Y., 1989, Migration of fluid phases and genesis of basalt magmas in subduction zones: Journal of Geophysical Research, v. 94, no. B4, p. 4697-4707.

Taylor, D.W., 1956, Pliocene mollusks from Jackson Hole, Grand Valley, and Star Valley, Wyoming and Idaho: Wyoming Geological Association Guidebook, 11th Annual Field Conference, p. 123-125.

Vasko, A.M., 1982, Structural setting of Teton Pass with emphasis on fault breccia associated with the Jackson Thrust Fault: M.S.Thesis, Montana State University, 64p.

Vollmer, R., Ogden, P., Schilling, J. -G., Kingsley, R.H., and Waggoner, D.G., 1984, Nd and Sr isotopes in ultrapotassic volcanic rocks from the Leucite Hills, Wyoming: Contributions to Mineralogy and Petrology, v. 87, p. 359-368.

White, R., and McKenzie, D., 1989, Magmatism at rift zones: The generation of volcanic continental margins and flood basalts: Journal of Geophysical Research, v. 94, no. B6, p. 7685-7729.

Whitlock, C., 1992, Holocene vegetation and climate of Grand Teton National Park and vicinity: United States Geological Survey Open File Report 92-504, p. 50-54.

Wilcox, R.E., 1944, Rhyolite-basalt complex on Gardner River, Yellowstone National Park, Wyoming: Geological Society of America Bulletin, v. 55, p. 1047-1079.

Wooden, J.L., and Mueller, P.A., 1988, Pb, Sr, and Nd compositions of a suite of Late Archean, igneous rocks, eastern Beartooth Mountains: Implications for crust-mantle evolution: Earth and Planetary Science Letters, v. 87, p. 59-72.

Wright, J.E., and Snoke, A.W., 1993, Tertiary magmatism and mylonitization in the Ruby-East Humboldt metamorphic core complex, northeastern Nevada: U-Pb geochronology and Sr, Nd, and Pb isotope geochemistry: Geological Society of America Bulletin, v. 105, p. 935-952.

Wyllie, P.J., 1982, Subduction products according to experimental prediction: Geological Society of America Bulletin, v. 93, p. 468-476.

Zeller, C.G., 1982, Structural geology along Teton Pass, Wyoming: Rocky Mountain Association of Geologists Yearbook 1982, p. 831-843.

Zoback, M.L. and Zoback, M.D., 1989, Tectonic stress field of the continental United States: *in* Pakiser, L.C., and Mooney, W.D., eds., Geophysical framework of the continental United States: Boulder, Colorado, Geological Society of America Memoir 172, p. 523-539.

APPENDIX

Sample Locations

Sample JH1: Basaltic andesite, base of cliff, head of Middle Fork of Phillips Creek, 43°32'30" N, 110°56'50" W, Rendezvous Peak Quadrangle.

Sample JH2: Basaltic andesite, north end of road cut, Wyoming Hwy. 22 at Phillips Canyon on Teton Pass. 43°30'18" N, 110°55'20" W, Rendezvous Peak Quadrangle.

Sample JH3: Andesite, cutbank above parking lot of Jackson Hole Athletic Club, north side of US Hwy. 26-89-187. SW1/4 NW1/4 Sec.33 T41N R116W, Jackson Quadrangle.

Sample JH5: Basaltic andesite, outcrop on summit of south end of East Gros Ventre Butte, SW1/4 SW1/4 Sec28 T41N R116W, Jackson Quadrangle.

Sample JH6: Dacite, top of prominent outcrop northeast shoulder of West Gros Ventre Butte, NE1/4 SE1/4 Sec8 T41N R116W, Teton Village Quadrangle.

Sample JH7: Dacite, quarry at base of north end of West Gros Ventre Butte, NE1/4 SW1/4 Sec5 T41N R116W, Teton Village Quadrangle.

Sample JH9: Andesite, outcrop southwest of summit of Haystack Butte, SW1/4 SW1/4 Sec32 T41N R116W, Jackson Quadrangle.

Sample JH10: Andesite, outcrop summit of ridge north of Mosquito Creek, 43°27'35" N, 110°55'20"W, Teton Pass Quadrangle.

Sample JH11: Andesite, outcrop east of summit ridge of East Gros Ventre Butte east of Spring Creek Resort, NE1/4SE1/4 Sec21 T41N R116W, Jackson Quadrangle.

Sample JH12: Dacite, outcrop on west side of gully south of Hansen Peak, NE1/4 NE1/4 Sec18 T41N R116W, Teton Village Quadrangle.

Sample JH13: Rhyolite, roadcut on north side of Indian Paintbrush Subdivision access road, SE1/4 NE1/4 Sec33 T41N R117W, Teton Pass Quadrangle.

Sample JH14: Obsidian, surface concentration of clasts on ridge southeast of Teton Pass, 43°28'40"N 110°56'40"W, Teton Pass Quadrangle.

Sample JH15: Rhyolite, quarry on northwest side of West Gros Ventre Butte, NW1/4 NE1/4 Sec7 T41N R116W, Teton Village Quadrangle.

Sample JH17: Trachyandesite, quarry west of West Gros Ventre Butte, NE1/4 SE1/4 Sec24 T41N R117W, Teton Village Quadrangle.

Sample JH18: Rhyolitic tuff, south end of roadcut, Wyoming Hwy. 22 at Phillips Canyon on Teton Pass. 43°30'5" N, 110°55'20" W, Rendezvous Peak Quadrangle.

Sample 81: Basaltic andesite, south side of bluff-like outcrop at mouth of Flat Creek canyon, NW1/4 SW1/4 Sec36 T42N R115W, Blue Miner Lake Quadrangle.

Sample JH519: Andesite, outcrop on ridge southeast of Teton Pass. 43°28'20" N, 110°54'40"W, Teton Pass Quadrangle.

Sample JH617: Andesite, outcrop on west side of West Gros Ventre Butte. NW1/4 NE1/4 Sec19 T41N R116W, Teton Village Quadrangle.

Sample IPK2: Basaltic trachyandesite, outcrop northeast of Indian Peak. 43°16'20" N, 110°54'25" W, Observation Peak Quadrangle.

Sample IPK6: Basaltic trachyandesite, outcrop southwest of Indian Peak. 43°16' N, 110°55' W, Observation Peak Quadrangle.

Sample JH640: Andesite, outcrop southeast of east abutment of Palisades Dam. 43°19'40" N, 111°11'20"W, Palisades Dam Quadrangle.

Sample SM4: Dacite clast in block and ash flow, outcrop on hillside north of Ditch Creek. NW1/4 SW1/4 Sec33 T44N R114W, Shadow Mountain Quadrangle.

Sample 606: Trachyandesite, quarry west of West Gros Ventre Butte, NE1/4 SE1/4 Sec24 T41N R117W, Teton Village Quadrangle.

Sample 625: Andesite, outcrop on southwest flank of the southern end of East Gro Ventre Butte. SW1/4 SE1/4 Sec 29 T41N R116W, Jackson Quadrangle.

Sample 32: Dacite, outcrop on westside of East Gros Ventre Butte. NE1/4 SW1/4 Sec16 T41N R116W, Teton Village Quadrangle.

Sample 701: Welded rhyolitic tuff, outcrop on hillside north of mouth of Moose Creek west of Teton Pass. 43°34'N, 111°3'30" W, Victor Quadrangle.